



# The ribosome-inactivating protein gelonin and parts thereof to be employed for a potential treatment of cancer

Vom Fachbereich Chemie  
der Technischen Universität Kaiserslautern  
zur Verleihung des akademischen Grades  
“Doktor der Naturwissenschaften”  
genehmigte

DISSERTATION

(D 386)

Vorgelegt von

Mohamed Badr

Betreuer: Prof. Dr. Wolfgang E. Trommer

Department of Chemistry/Biochemistry  
Technical University Kaiserslautern

2012

This work was performed from June 2009 until April 2012 at the work group of Prof. Dr. Wolfgang E. Trommer, Department of Chemistry/Biochemistry, Technical University of Kaiserslautern, Germany.

Tag der wissenschaftlichen Aussprache: 12.07.2012

Promotionskommission:

Vorsitzender: Prof. Dr.-Ing. Stefan Ernst

1. Berichterstatter: Prof. Dr. W. E. Trommer

2. Berichterstatter: Prof. Dr. Dr. Gerd Klock

*For my Family*

*Für meine Familie*

اهداء الى اسرتي

---

## I. INDEX

I. INDEX .....	II
II. LIST OF ABBREVIATIONS .....	V
III. LIST OF FIGURES .....	VII
IV. LIST OF TABLES .....	IIIX
V. Summary .....	X
1. <b>Introduction</b> .....	1
1.1. Ribosome-inactivating proteins (RIPs).....	1
1.1.1. Classification of RIPs.....	1
1.1.2. Structure .....	1
1.1.3. Toxicity mechanism.....	2
1.1.4. <i>Gelonium multiflorum</i> .....	4
1.1.4.1. <i>Gelonium multiflorum</i> proteins .....	4
1.1.4.2. Gelonin.....	5
1.1.4.3. <i>Gelonium</i> Anti-HIV Protein (GAP31) .....	6
1.2. Immunotoxin (ITs).....	8
1.3. Methotrexate (MTX).....	8
1.4. Research goals .....	10
2. <b>Materials</b> .....	12
2.1. Cells .....	12
2.1.1. MCF-7 cell line .....	12
2.2. Bacterial strains.....	12
2.3. Plasmid constructs .....	13
2.4. Enzymes.....	13
2.5. Antibody .....	14
2.6. Chemicals.....	14
2.7. Detection, purification and synthesis kits .....	14
2.8. Instruments.....	15
2.9. Software .....	16
3. <b>Methods</b> .....	17
3.1. Molecular biological methods.....	17
3.1.1. Preparation of competent <i>E. coli</i> cells.....	17
3.1.2. Transformation of competent cells.....	17
3.1.3. LB-agar plate.....	17
3.1.4. Preparation of plasmid DNA.....	18
3.1.5. Determination of nucleic acid concentration .....	19
3.1.6. DNA sequencing .....	19
3.1.7. Restriction analysis .....	20

---

3.1.8.	Agarose gel electrophoresis .....	20
3.1.9.	Extraction and purification of DNA fragments from agarose gel .....	21
3.1.10.	Ligation reaction .....	21
3.1.11.	ELISA .....	22
3.2.	Cell biology methods .....	23
3.2.1.	Culture of MCF-7 cells .....	23
3.2.2.	Freezing of cells .....	23
3.2.3.	Treatment of MCF-7 with different compounds .....	23
3.3.	Protein isolation, purification and characterization methods .....	23
3.3.1.	Expression and purification of recombinant gelonin by Ni <sup>2+</sup> affinity chromatography .....	23
3.3.2.	Isolation of native gelonin (Gel) .....	25
3.3.3.	Isolation of GAP31 .....	25
3.3.4.	Determination of protein concentration .....	26
3.3.5.	Enzymatic deglycosylation of purified protein .....	26
3.3.5.1.	N-glycan release by PNGase F .....	26
3.3.5.2.	N-glycan release by Endo H .....	26
3.3.5.3.	Release and isolation N-glycan by Endo H and PNGase F .....	26
3.4.	Enzymatic digestion .....	27
3.4.1.	In-gel tryptic digestion .....	27
3.4.2.	In-gel Arg-C digestion .....	28
3.5.	Mass spectrometry .....	29
3.5.1.	MALDI-TOF-MS analysis .....	29
3.5.2.	ESI-MS analysis .....	30
3.6.	Preparation of MTX-gelonin conjugate .....	30
3.7.	Toxicity measurements .....	30
3.7.1.	MTT cell proliferation assay .....	30
3.7.2.	DNase activity assay .....	32
3.7.3.	The inhibition of protein synthesis <i>in-vitro</i> .....	32
3.7.4.	Dihydrofolate reductase assay .....	34
3.7.5.	Comet assay and evaluation of (oxidative) DNA breakage .....	34
<b>4.</b>	<b>Results &amp; Discussion</b> .....	<b>38</b>
4.1.	Part A .....	38
4.1.1.	Recombinant gelonin (rGel) .....	38
4.1.2.	Truncated gelonins .....	40
4.1.2.1.	Cloning of recombinant C-terminally truncated gelonin (rC3-gelonin) .....	40
4.1.2.2.	Cloning of recombinant N- and C-terminally truncated gelonin (rN34C3-gelonin) .....	43
4.1.3.	Characterization and toxicity of gelonins .....	48
4.1.3.1.	Characterization of His-proteins by ELISA .....	48
4.1.3.2.	<i>In-vitro</i> cytotoxicity .....	48
4.1.3.3.	DNase-like activity test .....	49
4.1.3.4.	<i>In-vitro</i> translation assay .....	50
4.1.4.	Discussion .....	51
4.1.4.1.	Gelonin and its truncated forms did not induce MCF-7 cell death .....	52
4.1.4.2.	N-terminal amino acid residues are involved in regulation of gelonin DNase activity ..	52

---

4.1.4.3. C-and N-terminal amino acid residues are involved in regulation of gelonin N-glycosidase activity .....	52
4.1.5. Conclusion .....	53
4.2. Part B .....	54
4.2.1. Chemistry .....	54
4.2.1.1. Synthesis of MTX-NHS active ester.....	54
4.2.1.2. Synthesis and characterizations of MTX-gelonin conjugate .....	55
4.2.1.3. Characterizations of MTX-binding sites by MALDI.....	57
4.2.2. Biology.....	60
4.2.2.1. Inhibitions of cell proliferation by MTX-gelonin conjugate.....	60
4.2.2.2. DNA Fragmentation Induced by MTX-gelonin.....	61
4.2.2.3. <i>In-vitro</i> translation test .....	62
4.2.2.4. DNase-like activity assay .....	62
4.2.2.5. DHFR Inhibition Activities of MTX and the Conjugates .....	63
4.2.3. Discussions.....	64
4.2.3.1. MTX-conjugate is toxic to intact cells .....	64
4.2.3.2. Genotoxic effects of MTX-gelonin in MCF-7 cells.....	66
4.2.3.3. Amino groups are involved in regulation of Gel DNase and N-glycosidase activities... ..	66
4.2.3.4. The MTX $\alpha$ - and $\gamma$ -carboxyl groups are involved in MTX anti-folate activity .....	67
4.2.4. Conclusion .....	67
4.3. Part C .....	68
4.3.1. Protein isolation and toxicity .....	68
4.3.1.1. Gelonin isolation and purification.....	68
4.3.1.2. GAP31 isolation and purification.....	68
4.3.1.3. Protein synthesis inhibitory activity .....	70
4.3.2. Peptide mapping.....	70
4.3.2.1. In-gel tryptic gelonin digestion .....	70
4.3.2.2. In-gel tryptic GAP31 digestion .....	73
4.3.2.3. In-gel Arg-C digestion of gelonin .....	77
4.3.2.4. In-gel Arg-C digestion of GAP31 .....	79
4.3.3. ESI-MS characterization of proteins .....	81
4.3.4. Enzymatic deglycosylation .....	86
4.3.4.1. Enzymatic gelonin deglycosylation .....	87
4.3.4.2. Enzymatic GAP31 deglycosylation .....	89
4.3.5. Discussion .....	91
4.3.5.1. Characterization of the glycosylation sites .....	91
4.3.5.2. Structures of N-linked glycan .....	91
4.3.6. Conclusion .....	92
5. <b>References</b> .....	93
6. <b>Appendix</b> .....	102
7. <b>Acknowledgements</b> .....	105
8. <b>Curriculum Vitae</b> .....	106

## II. LIST OF ABBREVIATIONS

ACN	Acetonitril
Amp	Ampicillin
APS	Ammonium persulfate
BSA	Bovine serum albumin
DCC	<i>N,N</i> -dicyclohexylcarbodiimide
DHB	2,5-Dihydroxybenzoic acid
DHFR	Dihydrofolate reductase
DMF	Dimethyl formamide
DMSO	Dimethyl sulfoxide
DTT	Dithiothreitol
<i>E. coli</i>	Escherichia coli
EF	Elongation factor
Endo H	Endoglycosidase H
ESI	Electrospray-ionization
ER	Endoplasmic reticulum
EtBr	Ethidium bromide
FBS	Fetal bovine serum
FH <sub>4</sub>	Tetrahydrofolate
Fuc	Fucose
GAP31	Gelonium Anti-HIV Protein 31 kDa
GlcNAc	N-acetyl-D-glucosamine
IAA	Iodoacetamide
IPTG	Isopropyl- $\beta$ -thiogalactopyranoside
Kb	Kilo base
KDa	Kilo dalton
LB	Luria Bertani
MALDI	Matrix-assisted laser desorption/ionization
Man	Mannose
MEM	Minimal essential medium
MFR	Membrane-associated folate receptor
MTX	Methotrexate
MW	Molecular weight
NHS	N-hydroxysuccinimide
OD	Optical density
PBS	Phosphate buffered saline
PMSF	Phenylmethanesulfonyl fluoride
RNase	Ribonuclease
RIPs	Ribosome inactivating proteins
PNGase F	Peptide <i>N</i> -glycosidase F
RFC	Reduced folate carrier
RT	Room temperature

## ABBREVIATIONS

---

rpm	Revolutions per minute
SDS	Sodium dodecyl sulfate
SDS-PAGE	SDS-Polyacrylamide gel electrophoresis
SEM	Standard error of the mean
TAE	Tris acetate EDTA buffer
TEMED	N,N,N',N'-Tetramethylethylene diamine
TFA	Trifluoroacetic acid
THF	Tetrahydrofuran
TOF	Time-of-flight
Tris	Tris-(hydroxymethyl)-aminomethane
UV	Ultraviolet
Xyl	Xylose



### III. LIST OF FIGURES

Figure 1: Schematic representation of the mature forms of RIPs type I, type II and type III. ...	3
Figure 2: Schematic representation of the depurination of the $\alpha$ -sacrin/ricin loop by RIPs. ....	3
Figure 3: Alignment of gelonin sequence published by Rosenblum et al. 1995 and GAP31 sequence published by Huang et al., 1999. ....	4
Figure 4: The gelonin primary structure. ....	6
Figure 5: Structure of GAP31 with adenine at its binding pocket . ....	7
Figure 6: Chemical structure of Methotrexate. ....	8
Figure 7: Mechanism of action of MTX ..... 9	9
Figure 8: MCF-7 cells in monolayer culture. ....	12
Figure 9: Scheme showing the cleavage sites of PNGase F and Endo H enzymes. ....	27
Figure 10: Conversion of MTT to formazan by NADH-dependent reductases. ....	31
Figure 11: Construction of the plasmid pET-gel ..... 38	38
Figure 12: A; SDS-PAGE of recombinant gelonin was obtained by affinity chromatography on a nickel chelating column. ....	39
Figure 13: The amino acid sequence of His-tag fusion recombinant gelonin. ....	39
Figure 14: Agarose gel electrophoresis of pET-gel and pET-28a(+) plasmids. ....	41
Figure 15: Diagram of the coding strand of the 5310 bps (F1) and 742 bps (F2) fragments obtained after double enzymatic restriction ( <i>Sall</i> and <i>Ndel</i> ) of the pET-28a(+) and pET-gel, respectively. ....	41
Figure 16: Construction of plasmid pET-C3-gel. ....	42
Figure 17: SDS-PAGE showing the purification of recombinant gelonin ..... 43	43
Figure 18: The amino acid sequence of rC3-gelonin. ....	43
Figure 19: Agarose gel electrophoresis of pET-gel and pET-28a(+) plasmids. ....	44
Figure 20: Diagram of the coding strand of the 5252 bps (F1) and 634 bps (F2) fragments... 44	44
Figure 21: Construction of plasmid pET-N34C3-gel. ....	45
Figure 22: SDS-PAGE of rN34C3-gelonin purified by affinity chromatography on a Ni <sup>2+</sup> chelating column. ....	46
Figure 23: The amino acid sequence of rN34C3-gelonin. ....	46
Figure 24: Diagram illustrating the strategy used for cloning of different gelonin genes. ....	47
Figure 25: Characterization of the fusion proteins using an ELISA against the anti-His-tag.. 48	48
Figure 26: Cytotoxicity of rGel, rC3-gel, and rN34C3-gel against MCF-7 cells. ....	49
Figure 27: DNase activity of truncated gelonins. ....	50
Figure 28: Inhibition of <i>in-vitro</i> translation by gelonin and the fusion protein. ....	51

Figure 29: Synthesis of the MTX-gelonin conjugate. ....	55
Figure 30: ESI-MS analysis spectra display molecular charge of MTX-mono-methyl ester	56
Figure 31: Characterization of gelonin and conjugate. ....	57
Figure 32: MALDI-MS TOF spectra display molecular ions of peptides obtained after in-gel trypsin digestion of gelonin (top) and MTX-gelonin conjugate (down).....	58
Figure 33: Cytotoxicity of native gelonin, MTX-gelonin, and MTX against MCF-7 cells. ...	60
Figure 34: DNA damage (TI %) in MCF-7 cells exposed to gelonin and MTX-gelonin. ....	61
Figure 35: Inhibition of protein synthesis in the cell-free translational system. ....	62
Figure 36: DNase activity of gelonin, MTX-gelonin, and MTX.. ....	63
Figure 37: DHFR inhibition by free MTX and conjugates. ....	63
Figure 38: The expected mechanism of the growth inhibition activity of MTX-gelonin.. ....	65
Figure 39: Sephadex G-75 column chromatography of <i>Gelonium</i> seed proteins. ....	69
Figure 40: SDS-PAGE of the <i>Gelonium multiflorum</i> homogenate.....	69
Figure 41: Inhibition of <i>in-vitro</i> translation by gelonin and GAP31.....	70
Figure 42: MALDI-MS TOF spectra display molecular ions of peptides obtained. after in-gel trypsin digestion of gelonin. ....	71
Figure 43: ESI-MS spectrum of gelonin peptides obtained by in-gel tryptic digestion.....	73
Figure 44: MALDI-MS TOF spectra of peptides obtained after in-gel trypsin digestion of GAP31.....	74
Figure 45: ESI-MS spectrum of GAP31 peptide obtained by in-gel tryptic digestion. ....	75
Figure 46: Overview of peptides generated by in-gel tryptic cleavage of gelonin. ....	76
Figure 47: MALDI-MS TOF spectra of peptides obtained after in-gel Arg-C digestion of Gel .....	78
Figure 48: Overview of peptides generated by in-gel digestion of gelonin with Arg-C.....	78
Figure 49: MALDI-MS TOF spectra display molecular ions [M] of peptides obtained after in- gel Arg-C digestion of GAP31 (A) glycosylation, and (B) following deglycosylation. ..	80
Figure 50: Overview of peptides generated by in-gel digestion of GAP31 with Arg-C.....	80
Figure 51: ESI-MS of gelonin (51A) and Enlargement of charge state 28 <sup>+</sup> (51B). ....	81
Figure 52: Deconvolution spectrum of Gelonin.....	83
Figure 53: ESI-MS of GAP31 (concentrated and dialyzed).....	84
Figure 54: Deconvoluted spectrum of GAP31 .....	85
Figure 55: SDS-PAGE of purified and deglycosylated gelonin and GAP31.....	86
Figure 56: ESI-MS spectrum of released N-glycan from gelonin by.....	88
Figure 57: ESI-MS spectrum, in positive mode, of N-glycan from GAP31 .....	90

**IV. LIST OF TABLES**

Table 1: List of various RIPs dependent on their origin. .... 2

Table 2: A summary of different pET plasmids and different truncated gelonins..... 51

Table 3: Assignment of peaks from Trypsin cleavage of MTX-gelonin conjugates. .... 58

Table 4: Determination of sites modified with MTX..... 59

Table 5: Assignment of peaks from Trypsin cleavage of gelonin (MALDI analysis)..... 72

Table 6: Assignment of peaks from in-gel tryptic cleavage of gelonin (ESI analysis)..... 73

Table 7: Assignment of peaks from trypsin cleavage of GAP3 (MALDI-MS analysis). .... 75

Table 8: Assignment of peaks from in-gel tryptic cleavage of GAP31 (ESI analysis)..... 76

Table 9: Assignment of peaks from Arg-C cleavage of gelonin..... 77

Table 10: Assignment of peaks from Arg-C cleavage of GAP31 ..... 79

Table 11: The most abundant masses of gelonin species A..... 82

Table 12: The most abundant masses of gelonin species B ..... 82

Table 13: The most abundant masses of gelonin species C ..... 82

Table 14: Composition and molecular masses of gelonin species ..... 83

Table 15: The most abundant masses of GAP31 species A ..... 84

Table 16: The most abundant masses of GAP31 species B ..... 84

Table 17: The most abundant masses of GAP31 species C ..... 85

Table 18: Composition and molecular masses of GAP31 species (ESI-MS spectra)..... 85

## V. Summary

Due to their N-glycosidase activity, ribosome-inactivating proteins (RIPs) are attractive candidates as antitumor and antiviral agents in medical and biological research. In the first part, we have successfully cloned two different truncated gelonins into pET-28a(+) vectors and expressed intact recombinant gelonin (rGel), recombinant C-terminally truncated gelonin (rC3-gelonin) and recombinant N- and C-terminally truncated gelonin (rN34C3-gelonin). Biological experiments showed that:

- The recombinant truncated-gelonins are still having a specific structure that does not allow for internalization into cells.
- Truncation of gelonin leads to partial or complete loss of N-glycosidase as well as DNase activity compared to intact recombinant gelonin (rGel).
- C- and N-terminal amino acid residues are involved in the catalytic and cytotoxic activities of recombinant gelonin.

In the second part, an immunotoxin composed of gelonin and methotrexate (MTX) has been studied as a potential tool of gelonin delivery into the cytoplasm of cells. Results of many experiments showed that:

- The methotrexate-gelonin conjugate is able to reduce the viability of MCF-7 cell in a dose-dependent manner (ID<sub>50</sub>, 10 nM) as shown by MTT and significantly induce direct and oxidative DNA damage as shown by the alkaline comet assay.
- The positive charge plays an important role in the DNase activity as well as the N-glycosidase activity of gelonin.
- Conjugation of methotrexate to gelonin permits delivery of the conjugate into the cytoplasm of cancer cells and exerts a measurable toxic effect.

In the third part, we have isolated and characterized two ribosome-inactivating proteins (RIPs) type I, gelonin and GAP31, from seeds of *Gelonium multiflorum*. Results of many experiments showed that:

- Both RIPs inhibit protein synthesis by a rabbit reticulocyte lysate with 50% inhibition at 4.6 and 2 ng/ml for gelonin and GAP31, respectively.
- The amino acid sequence of gelonin and GAP31 peptides - obtained by proteolytic digestion - are consistent with the amino acid sequence published by Rosenblum et al and Huang et al, respectively.
- Gelonin and GAP31- isolated from the seeds of *Gelonium multiflorum*- consists of at least three different post-translationally modified forms.
- The N-glycan core of gelonin is N-acetyl-D-glucosamine. While, the N-glycan core of GAP31 is fucose- $\alpha$ (1-6)-N-acetyl-D-glucosamine.
- Standard plant paucimannosidic N-glycosylation patterns (GlcNAc<sub>2</sub>Man<sub>2-5</sub>Xyl<sub>0-1</sub> and GlcNAc<sub>2</sub>Man<sub>6-12</sub>Fuc<sub>1-2</sub>Xyl<sub>0-2</sub>) were identified using electrospray ionization MS for gelonin (making up 4.5% of the total molecular mass) and GAP31 (making up 9.4% of the total molecular mass), respectively.

## 1. Introduction

### 1.1. Ribosome-inactivating proteins (RIPs)

Ribosome-inactivating proteins (RIPs) are toxins able to specifically and irreversibly inhibit protein synthesis in eukaryotic cells. RIPs are widely distributed in nature but are found predominantly in plants, bacteria and fungi (Table 1). Most plant and bacterial RIPs, such as gelonin and Shiga toxins, exert their toxic effects through binding to the large 60S ribosomal subunit on which they act as N-glycosidases by specifically cleaving the adenine base A4324 in the 28S ribosomal rRNA subunit (Olsnes & Pihl, 1973; Endo et al., 1987; Stirpe et al., 1992; Barbieri et al., 1997; Peumans et al., 2001; Begam et al., 2006). The simple removal of one adenine base renders the 60S ribosome unable to bind elongation factor 2, with consequent arrest of protein synthesis (Montanaro et al., 1975). Besides their activity on rRNA, certain RIPs display a variety of anti-microbial activities *in-vitro*, such as anti-fungal, anti-bacterial, and broad-spectrum anti-viral activities against both human and animal viruses, including the human immunodeficiency virus, HIV (Zarling et al., 1990).

#### 1.1.1. Classification of RIPs

RIPs are classified into three groups based on their physical properties (Fig. 1). Type I RIPs, such as saporin (from soapwort, *Saponaria officinalis*), is composed of a single polypeptide chain of approximately 30 kDa (Barbieri et al., 1993). Type II RIPs, like ricin and abrin, are highly toxic heterodimeric proteins with enzymatic and lectin properties in separate polypeptide subunits, each of approximate MW of 30 kDa. One polypeptide with RIP activity (A-chain) is linked to a galactose binding lectin (B-chain) through a disulfide bond (Olsnes & Pihl 1973; 1982; Barbieri et al., 2004). The lectin chain can bind to galactosyl moieties of glycoproteins and/or glycolipids found on the surface of eukaryotic cells (Olsnes & Sandvig 1988; Steeves et al., 1999) and mediate retrograde transport of the A-chain to the cytosol. Once it reaches the cytosol, the RIP has access to the translational machinery and readily disrupts protein synthesis. On the other hand, type III RIPs, such as maize proRIPs, are synthesized as inactive precursors (ProRIPs) that require proteolytic processing events to form an active RIP (Walsh et al., 1991).

#### 1.1.2. Structure

More than 15 type II RIPs and 50 type I RIPs have been sequenced and/or cloned. A comparison between the type I RIPs and the A-chain of type II RIPs reveals high sequence similarity between the amino-terminal and core sequences of RIPs. While, the difference in carboxyl-terminal sequences explains why some RIPs activities are conserved whereas other activities are not. Although, the B-chains of different type II RIPs share high sequence similarity and virtually identical 3-dimensional structures, there are pronounced differences in sugar binding specificity. These differences in lectin activity and specificity are important

because the toxicity and cytotoxicity of type II RIPs is determined by the binding of the B-chain to a sugar-containing receptor on the cell surface (Battelli et al., 1997).

**Table 1:** List of various RIPs dependent on their origin.

Source	scientific name	RIP	Type	MW (kDa)	Glycosylated
<b>Plant</b>					
	<i>Abrus precatorius</i>	abrin	II	65	Yes
	<i>Ricinus communis</i>	ricin	II	65	Yes
	<i>Gelonium multiflorum</i>	gelonin	I	30	Yes
	<i>Saponaria officinalis</i>	saporin	I	29.5	No
<b>Bacteria</b>					
	<i>C. diphtheriae</i>	diphtheria toxin	II	62	No
	<i>E. coli O157:H7</i>	Shiga toxin	II	68	Yes
<b>Fungi</b>					
	<i>Aspergillus giganteus</i>	$\alpha$ -sarcin	I	17	No
	<i>Aspergillus restrictus</i>	restrictocin	I	17	No

### 1.1.3. Toxicity mechanism

Ribosome-inactivating proteins (RIPs) interfere with protein biosynthesis by catalyzing the depurination of a specific nucleotide in a ribosomal RNA sequence called the  $\alpha$ -sarcin/ricin loop (Fig. 2). Depurination occurs when a nucleotide loses its nucleobase, becoming an abasic site that is incapable of participating in base pairing. The first identified RIPs, ricin and abrin, are potent toxic heterodimeric proteins. Endo and co-workers in 1987 described how ricin recognizes a highly conserved region in the large 28S rRNA and hydrolytically cleaves a specific N-C glycosidic bond between an adenine and the nucleotide on the RNA.

The B-chain binds to galactosyl moieties of glycoproteins and/or glycolipids on the cell surface and facilitates the internalization of the enzymatic chain. Entry occurs by receptor mediated endocytosis. From there, the protein moves by retrograde trafficking to the endoplasmic reticulum (ER) via the trans-Golgi network and Golgi apparatus. In the ER, the disulfide bond between the two chains can be reduced by protein disulfide isomerase. The separated A-chain can inactivate ribosomes, thus arresting protein synthesis and killing the cell (Sandvig & van Deurs, 2000; Sandvig & van Deurs, 2002).

In contrast, type I ribosome-inactivating proteins (RIP-I), which lack a B subunit, are much less toxic than type II because of poor ability to enter cells, and internalized much less efficiently by cells, mainly by non-specific fluid phase pinocytosis and mannose receptor-

mediated endocytosis (Madan & Ghosh, 1992; Colaco et al., 2002), or through the  $\alpha$ 2-macroglobulin receptor (Cavallaro, 1995) and consequently have relatively low toxicity.

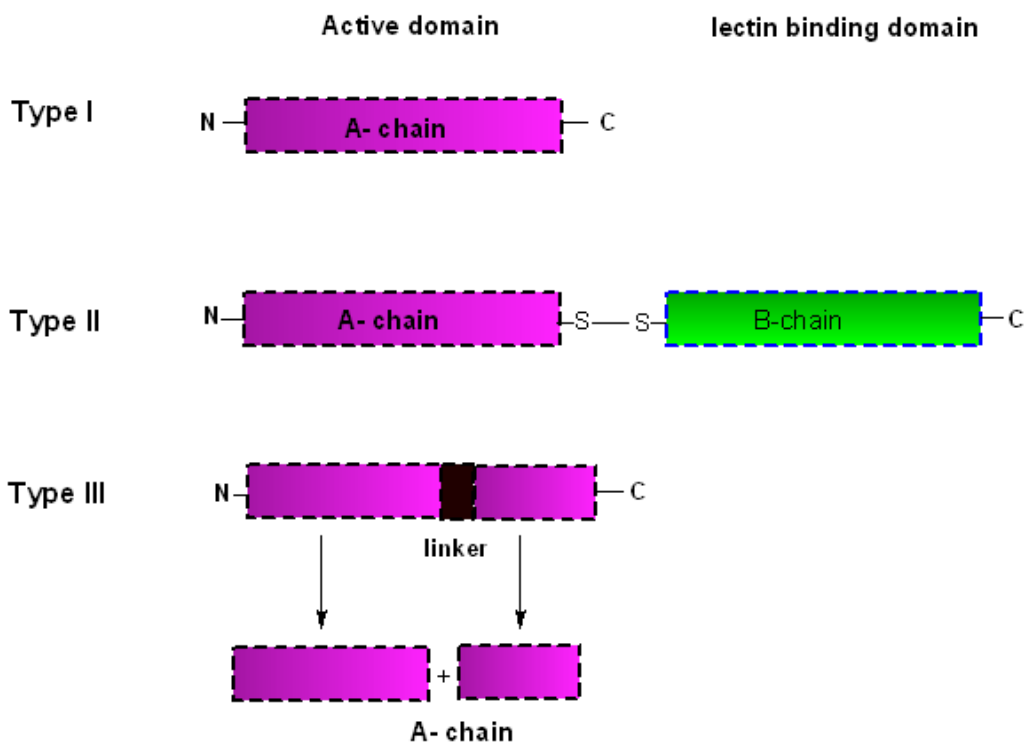


**Figure 1:** Schematic representation of the mature forms of RIPs type I, type II and type III.

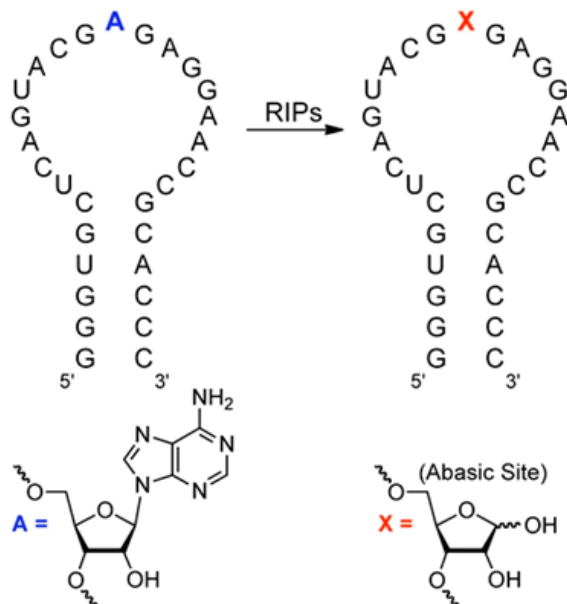


**Figure 2:** Schematic representation of the depurination of the  $\alpha$ -sacrin/ricin loop by RIPs.

### 1.1.4. *Gelonium multiflorum*

*Gelonium multiflorum* is a plant in the Euphorbiaceae family. It grows widely throughout tropical and subtropical areas especially in Asia and Africa. This plant has been reported to possess different medicinal applications like skin infection and lymphatic disorders, treatment of hepatic and gum diseases, and treatment of inflammatory-related diseases (Tewtrakul et al., 2011). Some phytochemical components of *G. multiflorum* can be applied in many areas of medicine, like anti-cancer (Rosenblum et al., 1992; Lee et al., 2008), anti-parasitic (Surolia & Misquith, 1996), anti-viral (Foa-Tomasi et al., 1982), anti-allergic (Cheenpracha et al., 2006), anti-fungal, and anti-bacterial activities. Also, this plant has been reported to provide various chemical compounds as alkaloids, cardiac glycosides, flavonoids (Das & Chakravarty, 1993), lactones and proteins (Stirpe et al., 1980; Bourinbaiar & Lee-Huang, 1996).

#### 1.1.4.1. *Gelonium multiflorum* proteins

There are two different RIP (type I) sequences from *Gelonium multiflorum* reported in the literature. A comparison of the two amino acid sequences is shown in Fig. 3. The first reported full-length sequence will be referred as gelonin (Rosenblum et al., 1995). The protein contains 258 amino acids and is based upon Edman sequence analysis of the native protein. The protein has a MW of 28.8 kDa, and has a pI of pH 8.9, as calculated using online “MS-digest”.

Gelonin	1	GLDTSVFSSTKGATYITYVNFNLNLRVCLKPEGNSHGIPLLRK--GDDPGKCFVLVALSNDN	59
GAP31	1	GLDTSVFSSTKGATYITYVNFNLNLRVCLKPEGNSHGIPLLRKCDDPGKCFVLVALSNDN	60
Gelonin	60	GQLAEIAIDVTSVYVVGQVRNRSYFFKDAPDAAAYEGLFKNTIKNPLLFGGKTRLHFGGS	119
GAP31	61	GQLAEIAIDVTSVYVVGQVRNRSYFFKDAPDAAAYEGLFKNTIK-----TRLHFGGS	112
Gelonin	120	YPSLEGEKAYRETTDLGIEPLRIGIKLDENAIDNYKPTIEASSLLVVIQMVSEARFTF	179
GAP31	113	YPSLEGEKAYRETTDLGIEPLRIGIKLDENAIDNYKPTIEASSLLVVIQMVSEARFTF	172
Gelonin	180	IENQIRNNFQQRIRPANNTISLENKWGKLSFQIRTSGANGMFSEAVELERANGKYYVTA	239
GAP31	173	IENQIRNNFQQRIRPANNTISLENKWGKLSFQIRTSGANGMFSEAVELERANGKYYVTA	232
Gelonin	240	VDQVKPKIALLKFVDKDPE	258
GAP31	233	VDQVKPKIALLKFVDKDPK	251

**Figure 3:** Alignment of gelonin sequence published by Rosenblum et al. 1995 (top) and GAP31 sequence published by Huang et al., 1999(down).

The second protein sequence (Fig. 3), referred as GAP31 (Huang et al., 1999). The protein consists of 251 amino acids and is based upon Edman sequence analysis of the native protein. The protein has a MW of 28.2 kDa and a pI of pH 9.1, as calculated using online “MS-



digest". However, the gelonin sequence differs from the GAP31 sequence in three positions as is illustrated in Fig. 3. First, there is one additional lysine and one additional cysteine residue (Lys43 and Cys44) in the GAP31 sequence, which are not found in the gelonin sequence. Secondly, there is a stretch of 8 amino acids (NPLLFGGK) between Lys103 and Thr112 in the gelonin sequence, which is not present in the GAP31 sequence. Finally, the last amino acid differs between the two molecules. Also, both proteins were reported to be glycosylated (Rosenblum et al. 1995; Li et al., 2010).

### 1.1.4.2. Gelonin

Gelonin is a 30 kDa single-chain ribosome-inactivating protein (type I) and was originally isolated from the seeds of *Gelonium multiflorum* (Stirpe et al., 1980). Gelonin is highly effective in cell free systems but relatively non-toxic to intact cells because it is not able to cross the plasma membrane at levels that are therapeutically useful due to lack of a carbohydrate-binding domain (B-chain). However, the cytotoxicity of gelonin can be enhanced if entry into the cell cytoplasm is facilitated. This can be achieved by conjugating gelonin to the acetylcholine receptor in order to treat autoimmune Myasthenia Gravis in rats (Urbatsch et al., 1993; Hossann et al., 2006), to humanized anti-CD33 monoclonal antibody in order to treat leukemia (Pagliaro et al., 1998), or to luteinizing hormone in order to design an hormonotoxin (Singh, 1991; Singh & Curtiss, 1993; Singh & Curtiss, 1994). Entry of gelonin into cells can be facilitated by electrical pulses (Mir et al., 1988), shock waves (Delius et al., 1999; Kodama et al., 2003), or photochemical internalization (Selbo et al., 2002).

Gelonin consists of 258 amino acid residues, contains 21 lysine residues and approximately 23% sequence homology with other scRIPs such as trichosanthin, ricin D and abrin A (Rosenblum et al., 1995). The primary sequence and structure of the gelonin precursor is shown in Figs. 3 and 4.

Falasca et al., 1982 reported that gelonin is a glycoprotein with sugar residues making up to 4.5% of the total molecular mass. The glycosylation motif is mainly composed of mannose, glycosamine and xylose.

**Recombinant gelonin (rGel):** A recombinant, de-glycosylated version of gelonin (rGel) has been expressed in bacteria and is biologically equi-potent to the natural substance (Nolan et al., 1993; Hossann et al., 2006). The rGel consists of 251 amino acid residues (Hossann et al., 2006). Structurally, gelonin belongs to the alpha helix + beta sheet class of proteins (Fig. 4). The N-terminal region (1–100 residues) has a predominantly beta secondary structure (Levitt & Chothia, 1976; Richardson, 1981). Six strands,  $\beta$ 1,  $\beta$ 4,  $\beta$ 5,  $\beta$ 6,  $\beta$ 7 and  $\beta$ 8, form a mixed beta sheet, in which the central four strands are antiparallel; and the two outer pairs are parallel (Richardson, 1981). The C-terminal region (101–247 aa) has a predominantly alpha-helical structure. The helical regions, except for short segments of type  $3_{10}$  (123–125 and 237–239 aa), are all of the alpha-helix type (Barlow & Thornton, 1988). There are two

distinct structural domains, one large (domain 1) and one small (domain 2). Domain one consists of residues 3–32 and 40–187, while domain two consists of residues 33–39 and 188–247. The residues Tyr74, Arg169, Gly111, Glu166, Tyr113, Trp198 form the active site of gelonin, and are located at the cleft between domains one and two (Hosur et al., 1995; Kim & Robertus, 1992).



**Figure 4:** The gelonin primary structure.

### **1.1.4.3. *Gelonium* Anti-HIV Protein (GAP31)**

GAP31 is a member of the type I ribosome-inactivating plant toxin family and has been also isolated from the seeds of *Gelonium multiflorum* (Lee-Huang et al., 1991). It is a 31 kDa single-chain ribosome-inactivating protein that inactivates the ribosomal 60S subunit by cleaving rRNA and inhibiting protein synthesis. Similar in action to other plant toxins such as gelonin, GAP31 has the powerful N-glycosidase activity and induces cell death by the same mechanism as gelonin. GAP31 is not toxic to intact cells, human spermatocytes or intact animals (Schreiber et al., 1999; Lee-Huang et al., 2000).

GAP31 has been reported to exhibit various medical actions such as inhibition of de novo HIV-1 infection, cell-to-cell transmission of the virus, viral replication in already infected cells, affecting multiple targets of HIV-1 including viral entry, viral genome integration and topology of viral DNA (Lee-Huang et al., 1991; Lee-Huang et al., 1995; Arazi et al., 2002; Lee-Huang et al., 2003). In addition to HIV-1, it is effective against herpes simplex viruses (HSV) (Bourinbaïar & Lee-Huang, 1996) and human herpes virus 8 (HHV8) (Sun et al., 2001). Moreover, GAP31 exerts a powerful anti-tumor activity against melanoma, brain and breast cancer cell lines (Rybak et al., 1994) and prevents tumor development in SCID mice xenografted with human breast tumor (Lee-Huang et al., 2000). In addition to tumor and viral

targets, GAP31 modulates the expression of host genes related to tumorigenesis, signal transduction, apoptosis, proliferation, stress and infection (Lee-Huang et al., 2003).

**Structure:** GAP31 consists of 251 amino acid residues (Fig. 3) and two cysteine residues (Cys44 and Cys50) are well positioned to form a disulfide bond (Huang et al., 1999). The structure of GAP31 is highly homologous to other type I RIPs and the A-chain of type II RIPs. Also, the GAP31 molecule contains eight major helices and three beta sheets, one of six strands and two of two strands (Li et al., 2010) (Fig. 5).



**Figure 5:** Structure of GAP31 with adenine at its binding pocket (Li et al., 2010).

**Catalytic mechanism:** Li et al., 2010 reported the active site of GAP31 to be located in a cleft of the molecule formed largely by residues highly conserved for RIPs (Fig. 3). Where, the active site including Tyr74, Arg169, Gly111, Gln166, Tyr113 and Trp198. There is a number of hydrogen bonding interactions between these residues, such as Arg169/Glu166. In addition, water molecules participate in the catalytic reaction. Arg169, Gly111 and Val75 at the active center are involved in hydrogen bonding with adenine. The guanidinium group of Arg169 is at a hydrogen-bonding distance from N3 of the adenine. The carbonyl oxygens of Gly111 and Val75 are capable of forming hydrogen bonds with the N7 and N1 of the adenine, respectively. In addition, Arg169 plays an important role in the RNA glycosidase mechanism of RIPs, either to protonate N3 of adenine, or to act as a strong electrostatic stabilizing group to promote electron withdrawal from C1' to N9 of adenine.

## 1.2. Immunotoxin (ITs)

Immunotoxins are protein-based drugs combining a target-specific binding domain with a cytotoxic domain. The target-domain binds to a surface antigen on a cell, enters it by endocytosis, and the cytotoxic domain kills it. Plants and fungi produce a number of molecules with defensive functions, to protect themselves against pathogens and predators. These defense proteins include ribosome-inactivating proteins. Also, these proteins have a broad spectrum of activities, encompassing anti-proliferative, anti-tumor, immunomodulatory, anti-viral, anti-fungal and anti-insect activities (Kreitman, 2006). Many efforts have been made in research into ITs as anticancer agents, dependent on the observation that a single molecule of toxin in the cytosol is sufficient to kill the cell.

## 1.3. Methotrexate (MTX)

The MTX is an anti-metabolite and anti-folate drug (Fig. 6). It is used in treatment of acute leukemia, osteogenic sarcoma (Garnett et al., 1985; Mir et al., 2008), rheumatoid arthritis (Cronstein, 2005; Zuo et al., 2009), and for the induction of medical abortions (Mol et al., 2008).

- **Mechanism of action**

MTX inhibits dihydrofolate reductase (DHFR), an enzyme that catalyzes the conversion of dihydrofolate to the active tetrahydrofolate (Tian & Cronstein, 2007). After entering the cell, MTX is polyglutamated (Glu) by the the enzyme folylpolyglutamate synthase. MTX and its polyglutamates inhibit the enzyme dihydrofolate reductase, thereby blocking the conversion of dihydrofolate (FH<sub>2</sub>) to tetrahydrofolate (FH<sub>4</sub>). Folic acid is needed for the de novo synthesis of the nucleoside thymidine, required for DNA synthesis. Also, folate is needed for purine base synthesis, so all purine synthesis will be inhibited (Aggarwal et al., 2006). MTX, therefore, inhibits the synthesis of DNA, RNA, thymidylates, and proteins (Kobayashi et al., 2002) (Fig. 7).

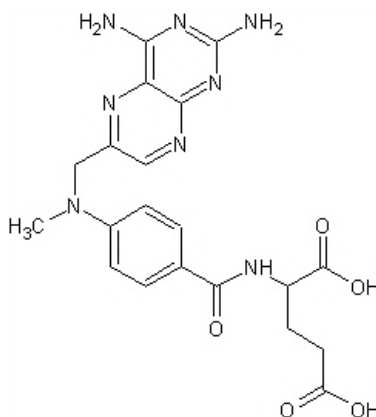


**Figure 6:** Chemical structure of Methotrexate.

- **MTX uptake**

The first step in the cellular action of MTX is its entry into the cell, which can be mediated by three different routes (Fig. 7): the reduced folate carrier (Kaufman et al., 2004), membrane-associated folate receptors (MFRs), or a proton-coupled (low pH) folate transporter (PCFT). PCFT is mainly involved in intestinal uptake of folate. The membrane-associated folate receptor (MFR) is rarely expressed or inaccessible in most normal cells (Da & Rothenberg, 1996; Weitman et al., 1994). However, it is up-regulated in select cancers of epithelial origin (Parker et al., 2005), and in more than 90% of non-mucinous ovarian carcinomas. Also, MFR is expressed at high to moderate levels in malignant tissues of epithelial origin, particularly the ovary (Toffoli et al., 1997), uterus, kidney, head and neck (Ross et al., 1994), endometrium (Wu et al., 1999), brain (Weitman et al., 1994), breast cancer (Hartmann et al., 2007), and mesothelium (Bueno et al., 2001).

The reduced folate carrier (RFC) is expressed in human normal and cancer cells (Gruner & Weitman, 1998; Weitman et al., 1992; Kaufman et al., 2004).

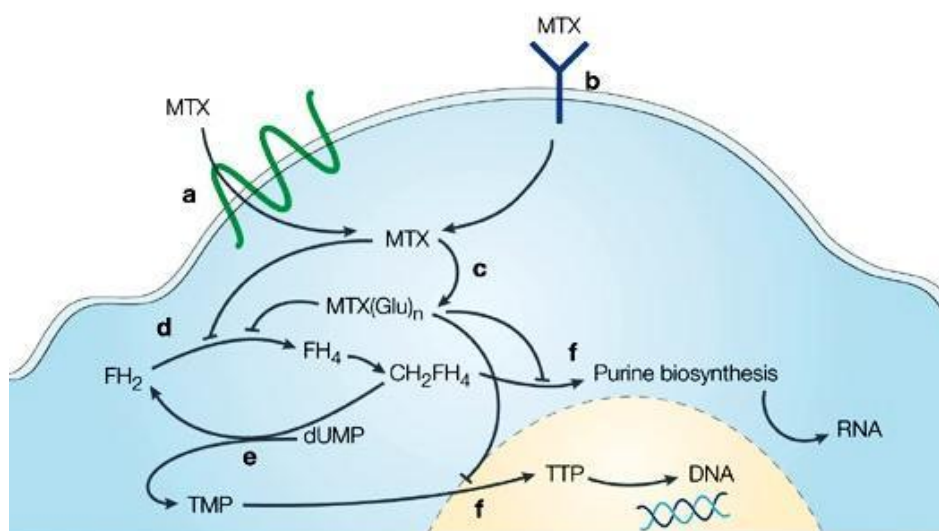


**Figure 7:** Mechanism of action of MTX

Transport of MTX across the membrane occurs through the reduced folate carrier (a) or folate receptor (b). Inside the cell the conversion to polyglutamated (Glu) MTX is catalyzed by folyl polyglutamate synthase (c). Both free and polyglutamated MTX inhibit DHFR (d) preventing the reduction of dihydrofolate (FH<sub>2</sub>) to FH<sub>4</sub>. Subsequently, thymidylate (TMP) synthesis (e) is reduced, which ultimately inhibits DNA synthesis (f). Polyglutamated MTX has an increased inhibitory effect on purine biosynthesis (f) required for RNA production (Chabner & Roberts, 2005).

## 1.4. Research goals

Actually, this work is divided into three parts.

- A- Biological activity of truncated mutants of the ribosome-inactivating protein gelonin**
- B- Synthesis and characterization of an anti-cancer candidate, MTX-gelonin conjugate**
- C- Isolation and characterization of two RIPs, gelonin and GAP31, from the seeds of *Gelonium multiflorum***

### **Part A.**

Ribosome-inactivating proteins (RIP) are a class of plant proteins, which inhibit protein synthesis via the catalytic cleavage of an N-glycosidic bond in the 28S rRNA from 60S subunit of eukaryotic ribosomes (Begam et al., 2006).

Recombinant gelonin has no active mechanism of cell entry and hence, it is relatively non-toxic to intact cells (Nolan et al., 1993). It cannot get into cells in significant concentrations (Stirpe et al., 1980). This gives gelonin very low systemic toxicity alone.

In the first part, we have cloned and expressed two truncated gelonins in order

- To investigate the relationship between the conformational structure of recombinant gelonin and its possibility to pass through the cell membrane as well as its function.
- To measure the cytotoxicity of recombinant gelonin and truncated gelonin.

Finally, this work may be useful in understanding the role of C- and N-terminal amino acid residues in gelonin activity as well as cellular intoxication. With a better understanding of these roles, we can engineer more effective agents with more therapeutic uses.

### **Part B.**

The treatment and cure of cancer is an important field of medical research. This part is focused on synthesis and characterization of an anti-cancer candidate, MTX-gelonin conjugate. In our study, we tried to generate a highly potent immunotoxin with a potential application in tumor-targeted drug delivery. In order to realize this aim, we chose a plant toxin, gelonin, as the main compound of the planned therapeutic agent. This protein is a type I RIP that is unable to bind to the cell surface and therefore is non-toxic to intact cells. To achieve the desired toxicity effect on target cells, we chemically joined gelonin to MTX. The anti-folate MTX displays significant tumoricidal activity against a variety of human malignancies (Frei, 1985; Gurdag et al., 2006). MTX contains carboxyl as well as amino groups which make the chosen molecule an optimal binding partner for proteins. We decided to use MTX because of its ability to interact with reduced folate receptors which are highly expressed in cancer cells (Parker et al., 2005). Thus, MTX may be useful to improve protein target delivery and cytotoxicity inside the cancer cell.

**Part C.**

For many years researchers believed that there is only one protein isolated from *Gelonium multiflorum* seeds. Many previous studies reported the isolation of gelonin (30 kDa) alone (Stirpe et al., 1992; Rosenblum et al. 1995), whereas another studies reported the isolation of GAP31 alone (Lee-Huang et al., 1991; Huang et al., 1999; Li et al., 2010), and another studies confused gelonin with GAP31 (Brigotti et al., 1995; Katiyar et al., 2011).

In order to decide whether one or two proteins are isolated from *Gelonium multiflorum* seeds, we performed in-gel tryptic and Arg-C digest for 30 and 31-kDa bands followed by MALDI-TOF MS (positive mode) and ESI ion-trap MS. Data achieved by this analysis were compared with calculated values obtained from online “MS digest” of gelonin and GAP31 sequences. The present study also was aimed to determine the composition and structures of the N-glycans profile of a given glycoprotein. For this purpose; the N-glycan pattern was released by enzymatic deglycosylation endo- $\beta$ -*N*-acetylglucosaminidase H (Endo H) and/or peptidyl-N-glycosidase F (PNGase F) followed by MS detection.

## 2. Materials

### 2.1. Cells

#### 2.1.1. MCF-7 cell line

The human (*Homo sapiens*) breast adenocarcinoma cell line MCF-7 was established in 1973 by Herbert Soule and isolated from a 69-year-old Caucasian woman. The cells express the estrogen receptor. The epithelial-like, adherent cells grow in monolayer cultures as small aggregates (Fig. 8). The cell line was kindly provided by Prof. Dr. Elke Richling (toxicology, chemistry department, TU Kaiserslautern).

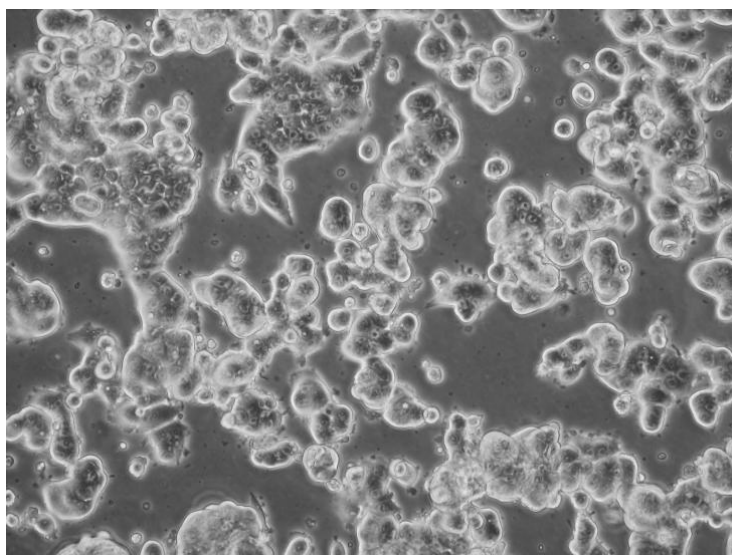


**Figure 8:** MCF-7 cells in monolayer culture.

### 2.2. Bacterial strains

<i>E. coli</i> strains	Genotype	Reference
BL21 (DE3)	F <sup>+</sup> ompT gal [dcm] [lon] hsdS <sub>B</sub> (r <sub>B</sub> <sup>-</sup> , m <sub>B</sub> <sup>-</sup> ) λ(DE3)	Novagen
XL-1 blue	recA1, endA1, gyrA96, thi-1, hsdR17, supE44, relA1, lac [F'proAB lacIqZΔM15 Tn10 (Tet <sup>R</sup> )]	Stratagene



### 2.3. Plasmid constructs

All plasmids described below have already been used in the laboratory.

**pET-28a-(+) vectors:** The pET-28a-(+) vectors carry an N-terminal His-Tag/thrombin/T7•Tag configuration plus an optional C-terminal His-Tag sequence. In addition, the vector contains a multiple cloning site (MCS158-203), kanamycin resistance gene (813bp), f1 origin, T7 promoter, Lac operator, LacI and pBR322 origin (Novagen).

**pET-gel plasmid:** The pET-gel expression plasmid was constructed in the work group of Prof. Dr. Wolfgang E. Trommer and published by Hossann et al., 2006.

**pUC18 plasmid:** The pUC18 plasmid was obtained from MBI Fermentas and used as a substrate in DNase like activity tests.

### 2.4. Enzymes

**Restriction endonucleases:** Type II restriction endonucleases were obtained from MBI Fermentas. The enzymes were used with optimized buffers supplied by the company.

**Lysozyme:** Lysozyme is a single chain polypeptide of 129 amino acids cross-linked with four disulfide bridges. It hydrolyzes the glycosidic bond of the bacterial mureine.

**Thrombin:** Thrombin is an endoprotease that specifically cleaves the sequence LeuValProArg GlySer (Novagen, Darmstadt).

**Trypsin:** Trypsin is a serine protease that specifically cleaves at the carboxylic side of lysine and arginine residues of protein and yields peptides of molecular weights that can be analyzed by mass spectrometry. The enzyme was purchased from Sigma (Aldrich) and (Promega).

**Arg-C:** Endoproteinase Arg-C - isolated from *Clostridium histolyticum* - is a cysteine proteinase and cleaves peptide bonds at the carboxyl side of arginine residues. The enzyme was purchased from Roche Applied Science.

**PNGase F:** PNGaseF (peptide: N-glycosidase F) -purified from *Flavobacterium meningosepticum*- is an amidase that cleaves between the innermost GlcNAc and asparagine residues of high mannose, hybrid, and complex oligosaccharides from N-linked glycoproteins. The enzyme was purchased from New England Biolabs (NEB).

**Endo H:** Endoglycosidase H is a glycosidase which cleaves the bond in the diacetylchitobiose core of oligosaccharides between two N-acetylglucosamine (GlcNAc) subunits directly proximal to the asparagine residue to which the sugar is attached, generating a truncated sugar molecule with one N-acetylglucosamine residue remaining on the asparagine. The enzyme was purchased from New England Biolabs (NEB).

## 2.5. Antibody

Antibody	Dilution	Properties	Manufacturer
Anti-poly-Histidine antibody	1:1000	Mouse monoclonal	Sigma-Aldrich
Anti-Mouse IgG (Fc specific)– Alkaline phosphatase	1:1000	peroxidase conjugate	Sigma-Aldrich

## 2.6. Chemicals

Amersham Pharmacia Biotech	L-[U- <sup>14</sup> C]-valine
AppliChem (Darmstadt)	Agar, glycerol, glycine, TEMED, Tris (hydroxymethyl) aminomethane, Tween® 20.
Merck (Darmstadt)	Ethanol, Nickel sulfate.
PAA (Cölbe)	RPMI 1640, RPMI without phenol red, Trypsin-ETDA, non-essential amino acids.
Promega (USA)	Rabbit reticulocyte lysate system, Untreated.
Roth (Karlsruhe)	acrylamide, agarose, rotiszint ecoplus, LB-Medium
Serva (Heidelberg)	Ammonium persulfate (APS), ampicillin (Amp), bromophenol blue, creatine phosphate, CM52-cellulose, Coomassie Brilliant Blue R 250, ethidium bromide (EtBr), hemin, penicillin G potassium salt, sodium dodecyl sulfate.
Sigma (Aldrich)	Dicyclohexylcarbodiimide (DCC), dihydrofolic acid, imidazole; iodoacetamide, L-valine, methotrexate, NADPH tetrasodium salt, N-hydroxysuccinimide, sephadex G75.
Sigma (Taufkirchen)	Dimethylsulfoxide (DMSO), dithiothreitol (DTT), isopropanol, phenylmethanesulfonyl fluoride (PMSF).

## 2.7. Detection, purification and synthesis kits

Kit name	Manufacturer
BCA Protein Assay Kit	Pierce
GeneJet™ Gel Extraction Kit	MBI Fermentas

QIAprep Spin <sup>®</sup> Miniprep Kit	Qiagen
HiTrap Chelating Column	Amersham Pharmacia Biotech
Jet star Plasmid Purification Kit	Genomed (Löhne)
Thrombin Cleavage Capture Kit	Novagen (Darmstadt)

## **2.8. Instruments**

Autoclave	Systec V65
Automatic pipettes	Eppendorf Research (10-1000)
Bi-Distiller apparatus	QCS Bi 18E
Centrifuges	Beckman J2-21 Centrifuge (Rotors JA-14, JA-20) Eppendorf Table Centrifuge 5415C and 5414 Eppendorf Table-top cooling centrifuge 5810R VWR Galaxy 16DH
Incubator	New Brunswick Scientific CO <sub>2</sub> Innova <sup>®</sup> CO-17 Heraeus Cytoperm 8080 (with gas flow) Thermo Scientific SHKA4000 (with shaking)
Concentrator	Sartorius Vivaspin6 and 20
Electric power apparatus	Biometra P 25/30
Electroporator	BioRad Gene Pulser II
ESI ion-trap mass	Bruker Daltonics Esquire 3000 <sup>+</sup>
MALDI- Ultraflex-TOF-TOF	Bruker Daltonics
Peristaltic pump	Pharmacia P-1 and P-3
PH meter	Schütt Labortechnik 535 Multi Cal
Sterile syringe	Sartorius (Göttingen)
Spectrophotometer	Beckman DU 640 Thermo Scientific Genesys 10UV

Thermomixer	Eppendorf 5355
Tissue culture plastic ware	Greiner
Ultra-Sound sonicator	Branson Sonorex RK 106

## **2.9. Software**

<b>Program Name</b>	<b>Company / Organization</b>
BLAST	NCBI
ChemSketch Freeware (Free)	Advanced Chemistry Development
Clone Manger 6	Sci Ed Central
Comet Assay IV	Perceptive Instruments
Corel Draw	Corel
Data analysis™ 3.4	Bruker Daltonics
Doc It	UVP
Esquire control 6.2	Bruker Daltonics
MS Office	Microsoft
MS-Digest	<a href="http://prospector.ucsf.edu/prospector">http://prospector.ucsf.edu/prospector</a>
NEBcutter V2.0	<a href="http://tools.neb.com/NEBcutter2/index.php">http://tools.neb.com/NEBcutter2/index.php</a>

### 3. Methods

#### 3.1. Molecular biological methods

##### 3.1.1. Preparation of competent *E. coli* cells

One clone of *E. coli* strain BL21 (DE3) was grown at 37°C overnight in 5 ml LB medium. Two ml of this culture were added to 200 ml LB medium and incubated at 37°C for 3-5 h until OD<sub>600</sub> reached 0.4-0.5. The culture was incubated for 20 min on ice and centrifuged at 1000 g for 15 min (Eppendorf 5415C rotor). Cells must remain cold for the rest of the procedure: The pellet was resuspended in 30 ml of cold 0.1 M CaCl<sub>2</sub>. The resuspended cells were transferred into 50 ml polypropylene falcon tubes, and incubated on ice for 30 mins. The culture was centrifuged at 4°C for 10 min at 3000 g (2500 rpm). The media were removed and the pellet was resuspended in 8 ml cold 0.1M CaCl<sub>2</sub> containing 15% glycerol. The cells were stored in aliquots of 100 µl, frozen in liquid N<sub>2</sub>, and stored at -80°C.

##### 3.1.2. Transformation of competent cells

Approximately 1 ng of plasmid DNA was mixed with competent *E. coli* and incubated for 30 min on ice, and then heat shocked for 2 min at 42°C and incubated on ice for 2 min. 500 µl LB medium was added to the bacteria and incubated for 60 min at 37°C on a thermomixer. 20-30 µl of the bacterial suspension was plated on LB agar plates containing ampicillin or kanamycin. The plates were incubated overnight at 37°C.

**LB medium:** (pH 7.0, autoclaved and stored at 4°C):

Tryptone	10	g
Yeast extract	5	g
NaCl	10	g
H <sub>2</sub> O bidest	1	l

##### 3.1.3. LB-agar plate

500 ml of LB medium containing 7.5 g of bactoagar were autoclaved. After cooling to 40-50°C, the antibiotic stock solutions were added (60 µg/ml). After mixing the solution (10 ml) was poured to sterile Petri dishes of 10 cm diameter. The dishes were dried in a sterile atmosphere and finally stored at 4°C in the dark room.

### 3.1.4. Preparation of plasmid DNA

- **Small-scale preparation of plasmid DNA**

The QIAprep™ Spin Miniprep Kit was used if DNA of high purity was necessary. 2 -10 ml of LB medium with a proper antibiotic was inoculated with a single colony and incubated at 37°C and 300 rpm for 10-12 h. 2-5 ml of the overnight culture was divided in 2.5 ml micro-centrifuge tubes and centrifuged at 13000 rpm for 10 min. The media were removed and the pellets were resuspended in 250 µl of resuspension buffer P1 until no cell clumps were visible. 250 µl of lysis buffer P2 was added and mixed by inverting 4-6 times. After addition of 350 µl of neutralization buffer N3, the mixture was inverted and centrifuged at 13000 rpm for 10 min. The supernatants were applied from the tube to a QIAprep™ spin column placed in a 2 ml collection tube. The columns were centrifuged at 13000 rpm for 1 min and the flow-through was discarded. Each column was washed by adding 0.75 ml of washing buffer PE and centrifuging for 1 min at 13000 rpm. The flow-through was discarded again and the residual washing buffer was removed by centrifuging as before. The spin column was placed in a fresh 1.5 ml micro-centrifuge tube, and 50 µl of elution buffer EB (10 mM Tris, pH 7.5) was added. After 1 min, the tube was centrifuged as before. The plasmid preparations were stored at –20°C.

- **Large-scale preparation of plasmid DNA (Maxi preparation)**

The preparation of plasmid DNA in the µg range (maxi prep) was carried out by using the manufacturer protocol of the *JETStar* Plasmid MaxiPrep Kit (Genomed, Löhne).

A single colony of *E. coli* XL-1 blue was inoculated into 3 ml LB medium containing 7.5 µl ampicillin (60 mg/ml) and grown for 6-8 h at 37°C with shaking. Then, 200 µl of the starter bacterial culture was used to inoculate 200 ml LB and cultured overnight with shaking at 37°C. Cells were harvested by centrifugation for 20 min at 4°C and 5000 rpm (Beckman Centrifuge, JA-14 Rotor) and all traces of medium were removed carefully. The pellet was re-suspended in 10 ml solution E1. Then, 10 ml of solution E2 were added and mixed gently and incubated at RT for 5 min. Thereafter, 10 ml solution E3 were added for neutralization, mixed immediately by inverting the tube 5 times and centrifuged for 20 min at 20°C and 15000 rpm (Beckman Centrifuge, JA-14 Rotor). The supernatant was applied to a column, which was equilibrated by adding 30 ml of solution E4. Then, the lysate was allowed to run through the column by gravity flow. The column was then washed with 60 ml of solution E5 and allowed to empty by gravity flow. The column was eluted with 15 ml of solution E6 and the eluted DNA was precipitated by adding 10.5 ml of isopropanol after incubation overnight at -20°C. The samples were centrifuged at 4°C for 40 min and 9500 rpm (Beckman Centrifuge, JA-14 Rotor), all isopropanol was removed and the pellet was washed with 5 ml of 70% ethanol and centrifuged for 40 min at 4°C and 9500 rpm (Beckman Centrifuge, JA-14 Rotor). The pellet was air-dried for 10-20 min, dissolved in 1 ml of sterile H<sub>2</sub>O and stored at –20°C.

## METHODS

---

<b><u>Solution E1:</u></b>	<b>Final concentration</b>		<b><u>Solution E2:</u></b>	<b>F. concentration</b>	
Tris	50	mM	NaOH	200	mM
EDTA	10	mM	SDS	1	% (w/v)
RNase (final concentration 100 µg/ml E1)			stored at RT.		
pH 8.0, adjusted with HCl, stored at 4°C					
<b><u>Solution E3:</u></b>			<b><u>Solution E4:</u></b>		
Potassium acetate	3.1	M	NaCl	600	mM
			Sodium acetate	100	mM
			TritonX-100	0.15	%
pH 5.5, adjusted with acetic acid, stored at RT.			pH 5.0, adjusted with acetic acid, stored at RT.		
<b><u>Solution E5:</u></b>			<b><u>Solution E6:</u></b>		
NaCl	800	mM	NaCl	1250	mM
Sodium acetate	100	mM	Tris	100	mM
PH 5.0, adjusted with acetic acid, RT			pH 8.5, adjusted with HCl, stored at RT		

### 3.1.5. Determination of nucleic acid concentration

The concentration of nucleic acids was determined by measuring the absorption at 260 nm (Beckman DU640 Spectrophotometer). The optical density at 260 nm of 1 (OD<sub>260</sub>=1) is equivalent to 50 µg/ml of double-stranded DNA, 40 µg/ml RNA, 37 µg/ml single-stranded DNA, or 30 µg/ml oligonucleotides in a 1 cm cuvette (Sambrook et al., 1989).

### 3.1.6. DNA sequencing

DNA sequencing was done at the immunology and genetic center at the TU Kaiserslautern.

### 3.1.7. Restriction analysis

Digestion of DNA with restriction enzymes was performed using type II restriction endonucleases. The sample volume and the amount of enzyme were adjusted according to the amount of DNA. For the analysis of mini-preparations approximately 1000 ng plasmid DNA was digested with 5 U of restriction enzyme in a final volume of 20  $\mu$ l.

The restriction digestions were performed for 1 hour at 37°C. DNA fragments obtained from the restriction digestions were directly analyzed by agarose gel electrophoresis.

#### Restriction mixture:

Plasmid DNA	1	$\mu$ g
10X Buffer (enzyme specific)	2	$\mu$ l
Restriction enzyme (10 U/ $\mu$ l)	0.5	$\mu$ l
H <sub>2</sub> O bidest to	20	$\mu$ l

### 3.1.8. Agarose gel electrophoresis

DNA fragments were separated electrophoretically on horizontal agarose gels in 1X TAE buffer. The DNA samples were mixed with 10X DNA loading buffer and run at 7.5 V/cm<sup>2</sup>. When the DNA samples or dye had migrated a sufficient distance through the gel, the fragments were visualized by staining the gel in 1X TAE buffer or H<sub>2</sub>O containing 10  $\mu$ l of 10 mg/ml ethidium bromide for 20-30 min at RT. The gel was washed with H<sub>2</sub>O to remove the background staining and the DNA fragments were visualized under UV light (254 nm) and photographed. The estimation of the sizes of the DNA fragments was done by comparison with a size standard marker 1 kb DNA ladder (MBI Fermentas GmbH).

#### TAE (50X):

	Final concentration	
Tris	121	g/l
EDTA	18.6	g/l
Acetic acid	28.6	ml

Adjusted pH 8.0 with acetic acid, autoclaved and stored at RT



**DNA loading buffer:**

Ficoll ® 400	10%	(w/v)
Orange G	0.01%	(w/v)
H <sub>2</sub> O and stored at -20°C		

**3.1.9. Extraction and purification of DNA fragments from agarose gel**

The extraction and purification of DNA fragments from agarose gels was carried out by using the manufacturer's protocol of the GeneJET™ Gel Extraction Kit (Fermentas GmbH). The DNA fragment of interest is excised from an agarose gel using a clean scalpel or razor blade, placed in a 1.5 ml micro-centrifuge tube. The gel was mixed with binding buffer (1:1 v/w) and incubated at 50-60°C for 10 min until the gel slice is completely dissolved. An 800 µl of the solubilized gel solution was transferred to the GeneJET™ purification column and centrifuged for 1 min and 13000 rpm. The flow-through was discarded. The column was washed by adding 0.7 ml of washing buffer and centrifuging for 1 min at 13000 rpm. The flow-through was discarded again and the residual washing buffer was removed by centrifuging as before. The spin column was placed in a fresh 1.5 ml micro centrifuge tube and 50 µl of elution buffer was added to the centre of the column. After 1 min, the tube was centrifuged as before. The DNA fragment was stored at - 20°C.

**3.1.10. Ligation reaction**

The ligation reaction was performed by using the enzyme T4 ligase, which catalyzes the formation of a phosphodiester bond between 3'-OH and free 5'-phosphate of double-stranded DNA fragments.

**Ligation reaction:**

Vector DNA	150	ng
Insert DNA	X	ng
Ligase 10X buffer	2	µl
T4 DNA ligase	2	µl
Nuclease-free H <sub>2</sub> O to	20	µl

The components were mixed and incubated at 16°C for 20 h prior to transformation.

### 3.1.11. ELISA

The basic principle of an ELISA is to use an enzyme (connected to a secondary antibody) to detect the binding of antigen (Ag) to the primary antibody (Ab). The enzyme converts a colorless substrate (chromogen) to a colored product, indicating the presence of Ag:Ab binding, which can be detected spectro-photometrically. The plate's wells were coated with protein (2 µg) in 100 µl of coating buffer and incubated at 4°C overnight. The wells were saturated with 200 µl of blocking solution (1% BSA in PBS) for 90 min at room temperature. After blocking, the wells were washed with PBS-Tween three times (200 µl/well). The first antibody was added and incubated for 1 h at room temperature (100 µl/per well). The wells were washed three times with PBS-Tween. After washing, the secondary antibody was added and incubated for 1 h at room temperature (100 µl/well). The wells were continuously washed with PBS-Tween four times. The substrate buffer was added and incubated for 30 min at room temperature (100 µl/well) and the color developed in 30 min was measured at 405 nm using a microtiter plate reader.

**Coating buffer:** A: 100 ml 0.2 M Na<sub>2</sub>CO<sub>3</sub> (2.12 g ad 100 ml)

B: 100 ml 0.2 M NaHCO<sub>3</sub> (1.68 g ad 100 ml)

Working solution: 8.5 ml A + 4 ml B /pH 10.6/ H<sub>2</sub>O<sub>bidest</sub> to 50 ml

**PBS buffer (pH7.2):**

Na<sub>2</sub>HPO<sub>4</sub> 0.92 g

NaH<sub>2</sub>PO<sub>4</sub> 8.18 g

NaCl 0.35 g

H<sub>2</sub>O<sub>bidest</sub> to 1 l

**PBS-Tween:**

PBS 100 ml

Tween 20 0.45 ml

H<sub>2</sub>O<sub>bidest</sub> to 1 l

**Block solution:**

1% BSA in PBS buffer (250 mg BSA in 25 ml PBS)

**Substrate buffer (pH 9.8):**

NaN<sub>3</sub> 0.2 g

MgCl<sub>2</sub>\*6H<sub>2</sub>O 0.1 g

DEA 97 ml

H<sub>2</sub>O<sub>bidest</sub> to 1 l

**Substrate solution:**

15 mg p-nitrophenyl phoshate + 15 ml substrate buffer

## **3.2. Cell biology methods**

### **3.2.1. Culture of MCF-7 cells**

MCF-7 cells cultured in an 175 cm<sup>2</sup> cell-culture flask were maintained in RPMI 1640 supplemented with 10% (w/v) fetal bovine serum, 1% non-essential amino acids and 0.5% (w/v) antibiotic. For sub-culturing, 80-90% confluent flask was rinsed twice with 10-15 ml 1 × PBS, treated with 3 ml trypsin-EDTA for approximately 2-3 min and the reaction was stopped by adding 5 ml of growth medium with 10% FBS which contains trypsin inhibitors. For treatment, cells were plated in 2.5 ml of medium on culture dishes of 60 mm diameter. After 24 h the medium was changed. A volume of 2.5 ml medium per 60 mm culture dish was added. The incubation of MCF-7 cells was performed in CO<sub>2</sub> incubators.

### **3.2.2. Freezing of cells**

The cells from a 175 cm<sup>2</sup> culture flask grown to 90-95% confluency were washed with 15 ml 1X PBS. Then 3 ml of Trypsin/EDTA was applied to detach the cells. After suspension in 7 ml complete RPMI 1640 (to a total volume of 10 ml) and centrifugation at room temperature and 1000 rpm for 5 min (Heraeus Labofuge A), the cell pellet was resuspended in 800 µl complete RPMI 1640 and filled in a 1.5 ml eppendorf cup. Then, 200 µl DMSO was added dropwise. The cells were cooled down to 4°C and then to -20°C before they were finally stored at -80°C.

### **3.2.3. Treatment of MCF-7 with different compounds**

Freshly isolated MCF-7 was allowed to attach for 24 h and culture medium was changed. After 24 h the MCF-7 was treated with different concentrations of the tested protein or drug. For MTT test the cells were treated for 72 h, for comet assay the cells were treated for 24 h before harvesting without changing the medium.

## **3.3. Protein isolation, purification and characterization methods**

### **3.3.1. Expression and purification of recombinant gelonin (rGel) by Ni<sup>2+</sup> affinity chromatography**

One single colony of BL21 (DE3)/pET-gel that was grown on an LB plate (80 µg/ml kanamycin) was picked and inoculated into 20 ml of LB medium at 37°C and 225 rpm overnight. This culture was used to inoculate 1l of the same medium. The culture was incubated at 37 °C at 220 rpm until an optical density at 600 nm of 0.7 was reached. IPTG was added to give a final concentration of 1 mM, and the culture was incubated overnight at

## METHODS

---

identical conditions. The cells were harvested by centrifugation at 6400 g for 30 min at 4°C. The pellets were suspended in 50 ml of suspension buffer. The suspension was sonified 15 times for 8 s each in an ice-water bath. The non-soluble parts were removed by centrifugation (30000 g for 30 min at 4°C). The supernatant was loaded on a HiTrap Chelating HP column that had been loaded with nickel ions (1 M NiSO<sub>4</sub>) and equilibrated with loading buffer (Suspension buffer). After removal of impurities by washing buffer (20 mM phosphate buffer containing 100 mM imidazole, 500 mM sodium chloride, and 1.5 mM PMSF, pH 7.2), gelonin was eluted with 500 mM imidazole in 20 mM phosphate buffer containing 500 mM sodium chloride and 1.5 mM PMSF, pH 7.2. The fractions containing gelonin were finally subjected to dialysis against 20 mM phosphate, pH 7.2, at 4°C overnight.

For removal of the His-tag in solution, recombinant gelonin was diluted to a concentration of 0.2 mg/ml using the buffers supplied with the thrombin kit from Novagen (Darmstadt, Germany) and incubated with 1 of mU thrombin per µg of protein for 16 h at RT.

### **Pellet washing buffer:**

			<b>Final concentration</b>
Tris	1.2114	g	20 mM
H <sub>2</sub> O	500	ml	
pH 7.2 /RT			

### **Suspension buffer:**

NaH <sub>2</sub> PO <sub>4</sub>	2.7598	g	20 mM
Imidazol	1.3616	g	20 mM
NaCl	29.22	g	500 mM
H <sub>2</sub> O	1	l	
pH 7.2 /RT, before use add 1 ml PMSF/l			

### **PMSF stock solution:**

PMSF	0.31	g
2-Propanol	2.36	ml

**Lysozyme stock solution:** Lysozyme 10 mg/ml of 100 mM Tris, pH 8

**IPTG stock solution:** IPTG 1 M sterile by filtration, store at -20 C

### 3.3.2. Isolation of native gelonin (Gel)

Gelonin was isolated from the seeds of *Gelonium multiflorum* using the method established in the research group of Prof. Dr. Trommer in modification of the original method as described by Stirpe et al., 1980.

23 g of the peeled seeds were transferred to 400 ml of 5 mM NaH<sub>2</sub>PO<sub>4</sub> buffer, containing 0.14 M NaCl, pH 7.4 (bidistilled water, 4°C) and crushed with a mixer 10 times for 30 s at 4°C. The result was a milky homogenate which was stirred overnight at 4°C. The next day the homogenate was filtered with a cloth made of mull and the suspension was centrifuged 30 min at 30000 g (4°C). After the centrifugation the fat was decanted with a plastic spoon. The supernatant was dialyzed 6 x 50 minutes against 5 l of 5 mM NaH<sub>2</sub>PO<sub>4</sub> buffer, containing 5 mM EDTA pH 6.5. After dialysis the precipitate was removed, and the remaining solution was applied to an ion exchange column (IEC, Fractogel TSK CM 650 M) with a flow rate of 3.3 ml/min. The column itself had been prepared as follows: 40 ml of the carrier material was suspended in 500 ml of 1 M NaCl and equilibrated for 30 minutes while temporarily slurring. Then it was washed with 2 l of bidistilled water using a suction filter (pore size 2). The gel was resuspended in 2 l of 0.5 M NaOH and after 30 min it was washed with bidistilled water until it was neutral. The same procedure was carried out with 0.5 M HCl. Afterwards the gel was washed with 500-1000 ml of 5 mM NaH<sub>2</sub>PO<sub>4</sub> buffer, containing 5 mM EDTA pH 6.5 (until the pH of the washing solution was 6.5) and filled into an appropriate column. After application of the gelonin, the column was washed with buffer overnight until no protein absorption could be measured with a photometer. The next day the protein on the column was eluted using a gradient of 0-0.3 M NaCl in the same buffer (2 x 500 ml). The protein fractions eluted at 0.12 M NaCl were collected and concentrated using a centrifugal filter device (Centriprep-10, cutoff: 10 kDa). The purity of the sample was determined by means of sodium dodecyl sulfate polyacrylamide gel electrophoresis and the concentration by means of BCA assay.

### 3.3.3. Isolation of GAP31

Homogeneous GAP31 was isolated from mature seeds of *Gelonium multiflorum*.

- **Initial extraction**

Shelled seeds were extracted with PBS -10 mM sodium phosphate buffer, pH 9.2, containing 0.15 M NaCl- (4 gm : 25 ml) using a mixer 10 times for 30 s at 4°C. The extract was stirred gently overnight followed by centrifugation at 16000 g for 30 min to remove cell debris.

- **Size fractionation by sephadex G75 column chromatography**

The homogenate (4 ml) was applied to a sephadex G75 column (1.5x70 cm) with flow rate 2 ml/min with 10 mM Tris, 50 mM NaCl pH 7.2. The solution was fractionated to 3 fractions.

Fraction 1 contained GAP31 and a protein of about 22 kDa, fraction 2 contained gelonin and fraction 3 contained non protein compounds. The fraction containing GAP31 was concentrated by ammonium sulfate precipitation (80% saturation) at 4°C overnight. The precipitate was dissolved in and dialyzed against 5 mM Na phosphate, pH 6.4.

- **Cationic exchange by CM 52 cellulose column chromatography**

The dialyzed sample was applied to a CM 52 cellulose column with a flow rate of 2 ml/min and washed by the same buffer overnight. The protein was eluted using a gradient of 0-0.3 M NaCl in the same buffer (2x500 ml). The eluted protein was dialyzed against 5 mM Na phosphate, 5 mM EDTA, pH 6.5. The purity of the sample was determined by means of SDS-PAGE and the concentration by means of the BCA assay.

### **3.3.4. Determination of protein concentration**

Protein concentration was determined by the methods of Bradford (Bradford et al., 1976) or BCA assay (Smith et al., 1985) using bovine serum albumin as a standard.

### **3.3.5. Enzymatic deglycosylation of purified protein**

#### **3.3.5.1. N-glycan release by PNGase F**

10 µg of proteins were heated with denaturing buffer (1 µl) in a 10 µl total reaction volume at 100°C for 10 minutes. After protein denaturation a 2 µl of 10XG7 reaction buffer, 2 µl 10% of NP40, 1-2 µl of PNGase F (500000 units/ml) and H<sub>2</sub>O was added to make the final volume 20 µl. The reaction mixture was incubated at 37 °C overnight. The reaction buffer, denaturing buffer and NP40 were obtained from New England Biolabs (Frankfurt am Main, Germany).

#### **3.3.5.2. N-glycan release by Endo H**

20 µg of proteins were heated with 1 µl of 10X denaturing buffer in a 10 µl total reaction volume at 100°C for 10 minutes. After protein denaturation, 2 µl of 10XG5 reaction buffer, 1-5 µl of Endo H (500000 U/ml) and H<sub>2</sub>O was added to make the final volume 20 µl. The reaction mixture was incubated at 37 °C overnight. The reaction buffer and denaturing buffer were obtained from New England Biolabs (Frankfurt am Main, Germany).

#### **3.3.5.3. Release and isolation N-glycan by Endo H and PNGase F**

N-glycans were released from gelonin and GAP31 by treatment with Endo H followed by PNGase F according to the protocol described above. Proteins and oligosaccharides were precipitated by adding 4 volume of -20°C acetone, and the mixtures were incubated at -20°C

for 1 h. Samples were centrifuged at 13,000g at 4°C for 10 min, and the salt containing 80% acetone supernatant was discarded. The pellet was extracted twice by trituration in small volumes of ice-cold 60% aqueous methanol. Pooled methanol supernatants contained the Endo H-released oligosaccharides and were concentrated by evaporation. The glycoprotein pellet was dissolved with 0.05 M NaOH, and immediately adjusted to pH 8.5. PNGase F was added, and the mixture was incubated overnight at 37°C. N-linked oligosaccharides were isolated by solvent precipitation/extraction exactly as described above. The released N-glycan was dissolved in H<sub>2</sub>O/MeOH/acetic acid (49:49:2), and analyzed by ESI-MS.

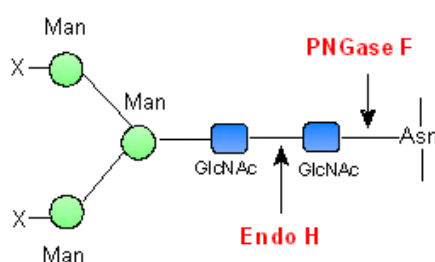


**Figure 9:** Scheme showing the cleavage sites of PNGase F and Endo H enzymes.

### 3.4. Enzymatic digestion

#### 3.4.1. In-gel tryptic digestion

Purified proteins were subjected to electrophoresis on a 12% SDS-polyacrylamide gel and visualized by staining with Coomassie Blue. Purified bands were excised, and gel slices were washed three times with 50% acetonitrile in 25 mM NH<sub>4</sub>HCO<sub>3</sub>, soaked in 100% acetonitrile, and dehydrated by speed-vac for 10 min. 150 µl of 10 mM DTT in 100 mM NH<sub>4</sub>HCO<sub>3</sub> was added to the dried gel pieces, and incubated at 56°C for 1 hr. The supernatant was removed and 150 µl of 55 mM iodoacetamide in 100mM NH<sub>4</sub>HCO<sub>3</sub> was added to the gel pieces, which were then vortexed. These suspensions were allowed to stand at RT in the dark for 45 min. The supernatant was removed and discarded. The gel pieces were washed with aqueous NH<sub>4</sub>HCO<sub>3</sub> (150 µl, 100 mM) for 10 min. The supernatant was discarded, and the gel pieces were dehydrated by treatment with acetonitrile (0.1 ml, 50% 25 mM NH<sub>4</sub>HCO<sub>3</sub>) twice. The gel pieces were dried as described above. To each gel, 0.1 ml of trypsin solution (12.5 ng/µl, 50 mM NH<sub>4</sub>HCO<sub>3</sub>) was added and incubated at 37°C for 19 hr. The supernatant was separated in a new tube, extracted twice, with 50µl of 50% acetonitrile/0.1% TFA (with mixing) for 30 minutes each time, at RT. Tryptic peptides were desalted with C18 ZipTip™ (OMIX), eluted with 0.6 µl of 10 mg/ml 2,5-dihydroxybenzoic acid (DHB) in 50% acetonitrile, 0.1% (v/v) TFA, applied onto the target plate and allowed to air dry. The peptide masses were measured by MALDI-TOF/TOF mass spectrometer (Ultraflex MALDI-TOF-TOF, Bruker Daltonics)

using positive reflector mode. The peptide calibration standard II (Bruker Daltonics, Germany) was used as the close external calibration.

### 3.4.2. In-gel Arg-C digestion

Endoproteinase Arg-C - isolated from *Clostridium histolyticum* - is a cysteine proteinase that cleaves peptide bonds at the carboxyl side of arginine residues. Protein bands were subjected to electrophoresis and visualized by staining with Coomassie Blue and reduced by DTT but not subjected to iodoacetamide. The gel pieces were rehydrated in 85 µl of incubation buffer (100 mM Tris-HCl, 10 mM CaCl<sub>2</sub>, pH 7.6). To each sample, 5 µl of Arg-C (0.5 µg, 50 mM Tris-HCl, 10 mM CaCl<sub>2</sub>, 5 mM EDTA, pH 8), 10 µl of activation solution (50 mM DTT, 5 mM EDTA) and 100 µl of incubation buffer were added and the gel pieces were incubated at 37°C overnight for digestion. The supernatant was separated in a new tube, extracted twice, with incubation buffer containing 1% acetic acid.

<u>Solution Name:</u>	<u>Composition</u>		
<b>100 mM ammonium bicarbonate</b>	ammonium bicarbonate	395.3	mg
	HPLC water up to	50	ml
<b>100 mM ammonium bicarbonate in 50% acetonitrile</b>	ammonium bicarbonate	395.3	mg
	HPLC acetonitrile	25	ml
	HPLC water up to	50	ml
	Store at RT		
<b>10 mM DTT</b>	dithiothreitol (DTT)	7.71	mg
	100 mM ammonium bicarbonate up to	5	ml
	(MAKE FRESH)		
<b>50 mM IAA</b>	iodoacetamide	56	mg
	ammonium bicarbonate	6.06	ml
	(MAKE FRESH)		
<b>20 mM ammonium bicarbonate in 50% acetonitrile</b>	100mM ammonium bicarbonate	10	ml
	HPLC water	15	ml



	HPLC acetonitrile	25	ml
	Store at RT		
<b>40 mM ammonium bicarbonate in 10% acetonitrile</b>	100 mM ammonium bicarbonate	20	ml
	HPLC acetonitrile	5	ml
	HPLC water	25	ml
	Store at RT		
<b>50 mM acetic acid</b>	Acetic acid (100%)	144	μl
	HPLC water up to	50	ml
	Store at RT		
<b>Trypsin solution</b>	trypsin (Promega)	100	μg
	50 mM acetic acid	100	μl
	40 mM ammonium bicarbonate in 10% acetonitrile up to	5	ml
	aliquot into 100 μl, store at -80C		
<b>50% acetonitrile/1% TFA</b>	HPLC acetonitrile	25	ml
	TFA	0.5	ml
	HPLC water up to	50	ml

### 3.5. Mass spectrometry

#### 3.5.1. MALDI-TOF-MS analysis

Matrix-assisted laser desorption/ionization time-of-flight mass spectrometry (MALDI-TOF-MS) is a soft ionization technique used in mass spectrometry and based on an ultraviolet absorbing matrix. This analytical tool allows the detection of compounds by separating the ions by their mass-to-charge ratios using a mass spectrometer.

### 3.5.2. ESI-MS analysis

Electrospray ionization (ESI) is a technique used in mass spectrometry to produce ions. The liquid containing the analyte of interest is dispersed by electrospray into a fine aerosol. The aerosol is sampled into the first vacuum stage of a mass spectrometer through a capillary, which can be heated to aid further solvent evaporation from the charged droplets. The solvent evaporates from a charged droplet until it becomes unstable upon reaching its Rayleigh limit. At this point, the droplet deforms and emits charged jets in a process known as Coulomb fission. During the fission, the droplet loses a small percentage of its mass (1.0-2.3%) along with a relatively large percentage of its charge (10-18%).

### 3.6. Preparation of MTX-gelonin conjugate

- **Activation process of MTX with DCC and NHS**

The activation process of MTX with DCC and NHS is an established technique already used to generate the first macromolecular prodrug of MTX that has reached the clinic (Stehle et al. 1997; Riebeseel et al. 2002). The coupling reaction between MTX-NHS active ester and gelonin was carried out as described previously (Garnett et al., 1985). Briefly, MTX (30 mg) was dissolved in DMF (0.4 ml) and activated by NHS (15.2 mg/0.1 ml of DMF) and DCC (27.26 mg/0.1 ml of DMF) at RT for 1 h and then 18 h at 4°C in the dark. The precipitate of the reaction product was removed by centrifugation, and the supernatant containing the active ester derivative was concentrated under reduced pressure at 37°C and stored in the dark at -20°C.

- **Preparation of MTX-linked gelonin**

The conjugate was prepared by incubating the active ester of MTX with gelonin in PBS, pH 8.5 (6:1 molar ratio of MTX and gelonin) under stirring at 4°C overnight. MTX-gelonin conjugate was dialyzed with PBS, pH 8.5; overnight. The concentration of MTX in the conjugate was determined by its absorbance at 370 nm using a molar absorbance coefficient of  $6.5 \times 10^3 \text{ M}^{-1} \text{ cm}^{-1}$ . The conjugate was stored at -20°C.

### 3.7. Toxicity measurements

#### 3.7.1. MTT cell proliferation assay

The MTT proliferation assay measures the activity of the mitochondrial and cytosolic dehydrogenases of living cells. Thereby the faintly yellow tetrazolium MTT (3-(4,5-dimethylthiazol-2-yl)-2,5-diphenyl-tetrazolium bromide) penetrates into the cell and there its tetrazolium ring is opened by the succinate-reductase system in the cytosol and active

mitochondria resulting in the water insoluble purple formazan (Mosmann, 1983; Scudiero et al., 1988). The generated intracellular formazan can be solubilized with acidic isopropanol and the absorbance of this colored solution can be quantified by a spectrophotometer at a wavelength of 570 nm (Fig. 10). In general, the MCF-7 cells were seeded at a density of 100000 cells/well in the 6-well, microassay plate and incubated for 24 h. The different proteins or PBS, as a control, were then added in varying concentrations to the culture media, and the mixture was incubated for another 72 h at 37°C. At the end of the experiment, the cells were washed once with 1 ml of warm RPMI without phenol red and thereafter 1 ml of 1X MTT solution was added to each well. Then, the plates were returned to the cell culture incubator for 2 to 4 hours. When the purple precipitate was clearly visible under the microscope the MTT solution was removed and 1 ml of acidic isopropanol was added, resuspended and carried over into cups. After a centrifugation at 13000 rpm for 3 min the absorbance was measured at 570 nm and a background of 650 nm (Beckman, UV DU<sup>®</sup> 640 spectrophotometer).

The cell viability (%) was calculated according to the following equation:

$$\text{Cell viability (\%)} = [\text{OD}_{570} (\text{sample})] / [\text{OD}_{570} (\text{control})] \times 100$$

Where the optical density OD<sub>570</sub> (sample) and OD<sub>570</sub> (control) represented measurements from wells treated with each sample and that with PBS treatment, respectively

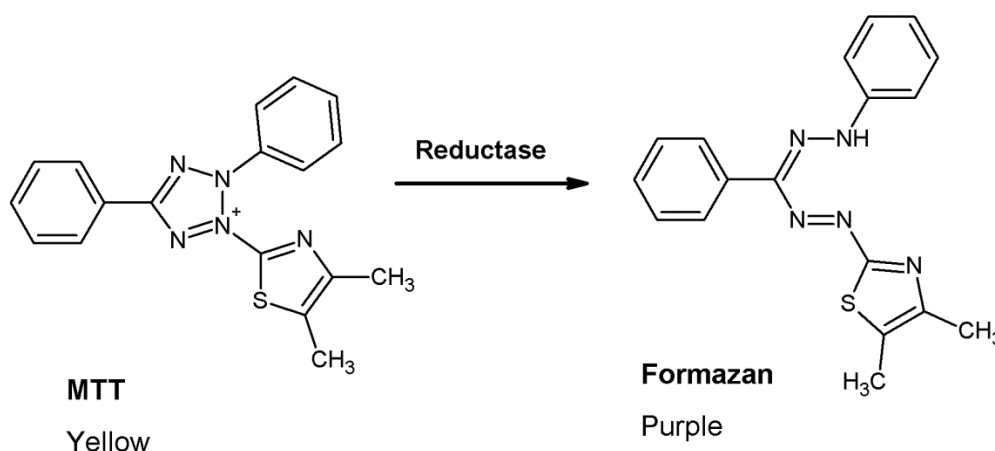


**Figure 10:** Conversion of MTT to formazan by NADH-dependent reductases.

**10x MTT Solution:**

MTT	5	mg
RPMI without phenol red	1	ml

The solution was sterilized by filtration and stored at 4°C protected from light.

**Acidic Isopropanol:**

		<b>Final concentration</b>
HCl (37%)	1.66 $\mu$ l	0.04 mM
absolute isopropanol up to	500 ml	

**3.7.2. DNase activity assay**

One microgram of pUC18 was incubated with different concentrations of gelonin, MTX-gelonin and MTX in 20  $\mu$ l of reaction buffer at 37°C for 2 h. The samples were analyzed in a 1% agarose gel and visualized by staining with 0.05% ethidium bromide.

**Reaction buffer (pH 7.5):**

Tris-HCl	50 mM
KCl	50 mM
MgCl <sub>2</sub>	10 mM

**3.7.3. The inhibition of protein synthesis *in-vitro***

The rabbit reticulocyte lysate translation system plays an important role in the investigation of transcriptional and translational regulation. The procedure was performed in 96 well micro-titer plates. To examine the toxicity of the fusion protein, a series of samples were diluted as follows  $1 \times 10^{-7.5}$  M,  $1 \times 10^{-8.5}$  M,  $1 \times 10^{-9.5}$  M,  $1 \times 10^{-10.5}$  M,  $1 \times 10^{-11.5}$  M to  $1 \times 10^{-12.5}$  M. 5  $\mu$ l solution taken out from each diluted sample was added into a well of the test plate and mixed with 40  $\mu$ l complement lysate, incubated at 37°C for 5 min. Then 10  $\mu$ l of master mixture containing L-(U-<sup>14</sup>C)-valine, 100  $\mu$ Ci was added into each well and incubated 10 min again. After that, two parallel 5  $\mu$ l culture from each well were added into 1 ml of pre-cooled distilled water, mixed with 500  $\mu$ l valine (1mg/ml) at 37°C for 15 min (each sample should be repeated). Finally, the protein precipitated by 4 ml 25% TCA (two times) was dried on glass microfiber filters under vacuum. The microfiber was incubated with 3 ml scintillations cocktail of B-counter (Beckman LS1701) for 2 h at RT. It was then assayed for the radioactivity.

**Solution A:**

H <sub>2</sub> O bidest	250 $\mu$ l
Glycerol	250 $\mu$ l
Creatin kinase	2.5 mg

**Solution B:**

Tris	242 mg
KCl	373 mg
Ethylene glycol	90 ml

## METHODS

---

H<sub>2</sub>O<sub>bidest</sub> 10 ml

pH 8.2

Hemin 65.2 mg

### **Solution C:**

Creatine phosphate 6.7 mg

H<sub>2</sub>O<sub>bidest</sub> 100 µl

### **Solution D:**

MgCl\*6H<sub>2</sub>O 9.5 mg

KCl 1.45 g

H<sub>2</sub>O<sub>bidest</sub> 10 ml

### **Solution E:**

L-(U-<sup>14</sup>C)-valine (100 µCi/ml) was purchased from Amersham

### **Solution F:** Amino acid solution

alanine; leucine 7.5 mM

aspartate; glutamate; glycine; histidine; lysine; serine 5 mM

arginine; asparagine; glutamine; isoleucine; phenylalanine; proline; threonine; tryptophan; tyrosine 3.75 mM

cysteine; methionine 2.5 mM

### **Complement Lysate:**

Lysate (Promega) 970 µl

Solution A 10 µl

Solution B 20 µl

### **MasterMix:**

Solution C 50 µl

Solution D 50 µl

Solution E 40 µl

Solution PBS 40 µl

Solution F 20 µl

### **Valine solution:**

NaOH 1 M

H<sub>2</sub>O<sub>2</sub> 0.5 M

Valine 100 mg

### **8% TCA solution:**

80 g TCA / 1 l H<sub>2</sub>O<sub>bidest</sub>

### **25% TCA solution:**

50 g TCA / 200 ml H<sub>2</sub>O<sub>bidest</sub>

H<sub>2</sub>O<sub>bidest</sub> up to 100 ml **Scintillations cocktail:** Rotiszint ecoplus

#### 3.7.4. Dihydrofolate reductase assay

The inhibitory effect of gelonin, MTX–gelonin conjugates and MTX on the target enzyme DHFR was evaluated in a cell-free dihydrofolate reductase (DHFR) assay. The assay is based on the ability of dihydrofolate reductase to catalyze the reversible NADPH-dependent reduction of dihydrofolic acid to tetrahydrofolic acid.



At pH 7.5, the equilibrium of the reaction lies relatively far to the right, and the reaction goes essentially to completion in the forward direction. The reaction progress was monitored by the decrease in absorbance at 340 nm.

$$\% \text{ of inhibition} = \frac{\text{DHFR activity (control)} - \text{DHFR activity (MTX or conjugate)}}{\text{DHFR activity (control)}} \times 100$$

Briefly, the reaction mixture contained PBS buffer, pH 7.5, 60  $\mu\text{M}$  NADPH, 50  $\mu\text{M}$  dihydrofolate, and  $1.5 \times 10^{-3}$  U DHFR was incubated for 5 min at 37°C with various concentrations of MTX, its conjugates, or control PBS. The reaction was then initiated by the addition of dihydrofolic acid, and the enzyme activity was determined spectrophotometrically at 340 nm.

#### 3.7.5. Comet assay and evaluation of (oxidative) DNA breakage

The comet assay, also known as single-cell gel electrophoresis assay (SCGE assay), is a simple method for measuring deoxyribonucleic acid (DNA) strand damage and other DNA alterations at the level of a single cell (Singh et al. 1988). Cells embedded in agarose on a microscope slide are lysed with detergent and high salt to form nucleoids containing supercoiled loops of DNA linked to the nuclear matrix. Electrophoresis at high pH results in structures resembling comets, observed by fluorescence microscopy; the intensity of the comet tail relative to the head reflects the number of DNA breaks.

As an additional step the repair enzyme, formamidopyrimidine glycosylase (FPG), was employed for the detection of oxidative DNA base damage, in particular 8-OH guanine, but also of other damaged purines. Strictly taken, the difference of DNA fragmentation introduced following FPG treatment of the cells and the damage that occurred without applying the repair enzyme represents the amount of a specific class of DNA damage which is due to the enzyme's action.

### **Procedure:**

DNA strand breaks were analyzed by the comet assay as described by Valentin-Severin and co-workers (2003). The inclusion of the digestion step with the bacterial enzyme FPG was performed according to Schaefer et al. (2006).

- **Agarose preparation**

0.5% LMPA (low melting point agarose) and 1.0% NMA (normal melting point agarose) were heated in the microwave until the agarose dissolved. NMP agarose was kept hot at 80°C in a water bath. While, LMP agarose was equilibrated at 40°C in a water bath.

- **Slide precoating**

Agarose-precoated slides were prepared by adding 40 µl 1.0% NMA to each slide and allow the agarose to air-dry to a thin film. In the middle of each slide, 2X65 µl of 1.0% NMA was added, covered with a cover slip and kept at 4°C to allow solidification of agarose.

- **Sample preparation**

MCF-7 was treated with different concentration of gelonin, MTX-gelonin or MTX for 24 h. The cells were rinsed twice with PBS and trypsinated. The cells were gently removed. Using a hemocytometer, cell density was adjusted to about  $7 \times 10^4$  cells per gel and the adequate volume of cell suspension was transferred to a 2.0 ml microtube in a total volume of 1 ml serum-containing DMEM. Cells were centrifuged (10 min, 2000 rpm, 4°C) and the pellet was rapidly mixed with 65 µl of LMA (40°C), distributed onto a glass microscope slide pre-coated with a layer of normal melting point agarose, covered with a coverslip and kept at 4°C for 5 min until the agarose layer hardened.

- **Cell Lysis, FPG enzyme treatment and electrophoresis**

The coverslips were removed and the slides submerged in a (horizontal) staining jar containing freshly prepared lysis solution (pH 10) and the cells were lysed overnight at 4°C to liberate DNA. Subsequently, the slides were washed three times for 5 min in cold FPG enzyme buffer (1X) at 4°C. After the last washing step the slides were put on a slide porter on ice, and FPG solution (300x diluted) or enzyme buffer (1X) alone as the control (50 µl/gel and two gels per treatment) was gently pipetted on the slides, covered with a coverslip and incubated for 30 min at 37°C on a water bath (Collins et al., 1996). Following FPG treatment, the coverslips were gently removed and the slides were placed horizontally in an electrophoresis chamber that was put on ice. Directly, the slides were exposed to alkaline denaturation buffer (pH 13). The high pH allows unwinding of the DNA (20 min). Electrophoresis was conducted keeping the electrophoresis solution in the chamber for 20 min at 300 mA (25 mV constant). The slides were removed from the electrophoresis chamber and neutralized by washing 3 times for 5 min with cold neutralization buffer. DNA was stained

## METHODS

---

with ethidium bromide (40  $\mu$ l, 10  $\mu$ g/ml) and viewed microscopically with a Zeiss Axioskop 20, equipped with filter set 15 (excitation, BP 546/12; emission, LP 590).

Fifty individual comets per slide and two slides per concentration were evaluated under a fluorescence microscope and analyzed using computerized image analysis system Comet IV (Perceptive Instruments). DNA migration is directly expressed as mean tail intensity (TI %) from one slide.

### **Comet assay solutions:**

If not indicated otherwise, all solutions for comet assay were prepared with autoclaved bidistilled water.

### **Lysing stock solution (pH 10):**

			<b>Final Concentration</b>	
NaCl	146.1	g	2.5	M
Titriplex III	37.2	g	100	mM
Tris	1.2	g	10	mM
H <sub>2</sub> O <sub>bidest</sub>	1	l		
N-laurylsarcosin	10	g		
Store at 4 °C				

### **Lysing working solution:**

Prepare freshly on the day of the experiment.

Lysing stock solution	89	ml
DMSO	10	ml
Triton X-100	1	ml

### **Denaturation and electrophoresis stock solutions:**

NaOH	40 g/ 100ml	10	N
Na <sub>2</sub> EDTA	7.4 g/ 100ml	200	mM
Store at room temperature			

### **Denaturation and electrophoresis Buffer, pH13:**

NaOH (10N)	30	ml	300	mM
Na <sub>2</sub> EDTA (200 mM)	5	ml	1	mM
H <sub>2</sub> O <sub>bidest</sub>	1	l		

Prepare freshly on the day of the experiment with cold H<sub>2</sub>O<sub>bidest</sub>.

### **PBS for agarose (pH 7.4):**

NaCl	8	g
KCl	0,2	g
KH <sub>2</sub> PO <sub>4</sub>	0,2	g
Na <sub>2</sub> HPO <sub>4</sub>	1,15	g



## METHODS

---

H <sub>2</sub> O bidest	1	l
-------------------------	---	---

### **Neutralisation buffer:**

Tris	48,5	g
------	------	---

H <sub>2</sub> O bidest	1	l
-------------------------	---	---

PH 7.5 with HCl, store at 4 °C.

### **NMA:**

0.5% in PBS

Heat in microwave, maintain at

80 °C in a water bath

### **LMA:**

0.7% in PBS

Heat in microwave, maintain at 37°C

in a water bath

### **FPG enzyme buffer stock solution (10x):**

HEPES	95	g
-------	----	---

KCl	74.6	g
-----	------	---

EDTA	1.96	g
------	------	---

BSA	2	g
-----	---	---

H <sub>2</sub> O	1	l
------------------	---	---

Adjust to pH 8 with KOH store at -20 °C

### **FPG enzyme stock solution (100x):**

FPG enzyme 1x	10	µl
---------------	----	----

Glycerol	100	µl
----------	-----	----

FPG enzyme buffer 1x	1	ml
----------------------	---	----

Prepare aliquots of 25 µl or 40 µl (-80°C)

### **FPG enzyme working solution (3000x):**

FPG aliquot (100x) 1: 30 of enzyme

Buffer 1x

Keep on ice

## 4. Results & Discussion

### 4.1. Part A

#### 4.1.1. Recombinant gelonin (rGel)

The pET-gel plasmid had been constructed in the work group of Prof. Dr. Wolfgang E. Trommer and was published by Hossann et al. (2006) (for complete DNA sequence see “appendix”). The gene encoding the gelonin sequence has been inserted in the pET-28a vector, whereas the gelonin gene was attached to N-terminal His-tag gene via a thrombin cleavage site. Also, the pET-gel plasmid (6089 bps) is under the control of the strong bacteriophage T7 transcription promoter. The target gelonin gene is expressed when the T7 RNA polymerase promoter is induced by inducers like IPTG (Fig. 11).

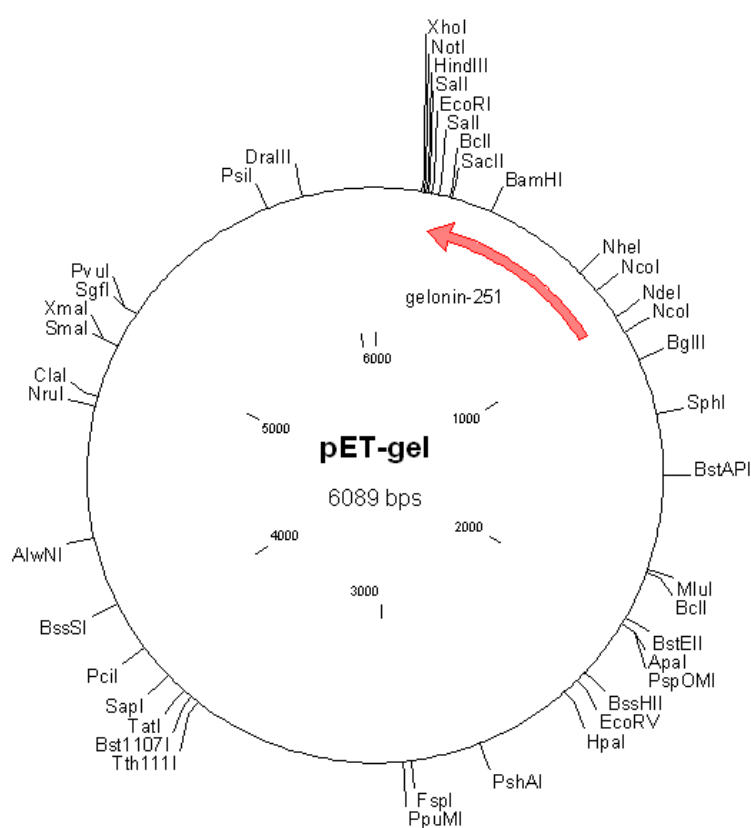


**Figure 11:** Construction of the plasmid pET-gel (Hossann et al., 2006).

- **Expression of pET-gel in *E. coli* BL21**

The pET-gel plasmid containing the fusion gene was transformed into *E. coli* BL-21 competent cells and then plated overnight on an LB-agar plate containing kanamycin. Many colonies were growing on the plate. Only one colony was allowed to grow in LB media containing kanamycin overnight. 20  $\mu$ l of the *E. coli* BL-21/pET-gel was inoculated in fresh

LB medium (1 l) containing kanamycin, and incubated in a shaking incubator at 37°C until the OD<sub>600</sub> reached approximately 0.6~0.7 and was immediately induced by IPTG (final conc. 1 mM) for another 4 h growing at the same temperature. Recombinant bacterial cells were collected by centrifugation and lysed by sonication. The supernatants were collected and loaded on a HiTrap Chelating HP column. Elution was performed with increasing imidazole concentrations. From 1 l expression cultures about 2.6±0.2 mg of pure gelonin was routinely obtained (Fig. 12).

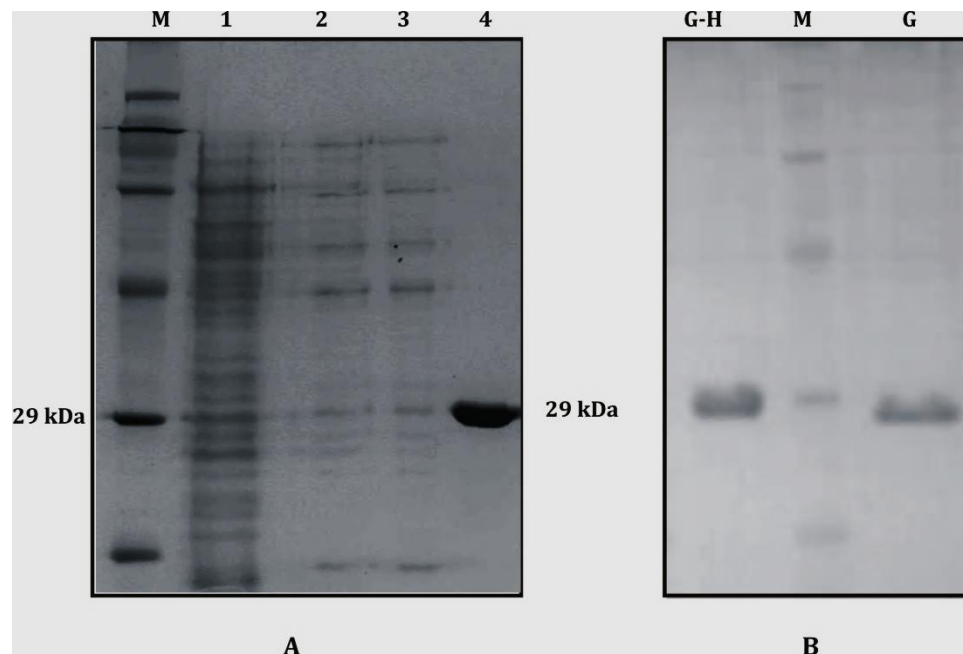


**Figure 12:** A; SDS-PAGE of recombinant gelonin was obtained by affinity chromatography on a nickel chelating column. Lane M, protein standard; lane 1, supernatant of cell lysate; lane 2, flow-through with 20 mM imidazole; lane 3, washing step with 100 mM imidazole; lane 4, elution step with 500 mM imidazole (rGel).B; SDS-PAGE of native rGel with His-tag (G-H) and rGel without His-tag (G) obtained after thrombin treatment.

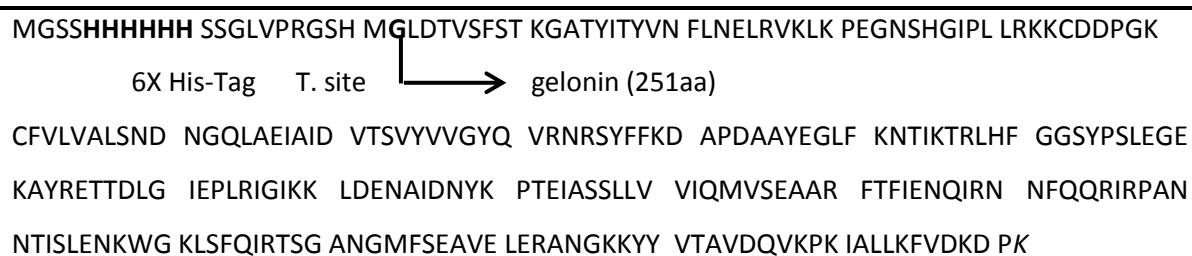


**Figure 13:** The amino acid sequence of His-tag fusion recombinant gelonin.

The expressed protein contains 251 amino acids (aa) of rGel and an extra 21-aa sequence containing an His-tag and a thrombin-cleavable peptide (LVPRGS) at the N-terminus (MGSSHHHHHSSGLVPRGSHM) (Fig. 13). The expressed rGel constitutes  $\approx$ 2–3% of the total *E. coli* cellular proteins. The calculated MW of the rGel is 30.47 or 28.74 kDa for native or thrombin-treated rGel, respectively.

## 4.1.2. Truncated gelonins

### 4.1.2.1. Cloning of recombinant C-terminally truncated gelonin (rC3-gelonin)

The pET-28a(+) and pET-gel were digested with *Sall* and *NdeI*. After restriction enzyme digestion, the linearized plasmid DNA was predicted to be 5310 bps and the insert was predicted to be 742 bps. Fig. 14 lane 2 shows two intense bands of the pET-gel product after digestion with *Sall* and *NdeI*. The smaller band corresponds to 742 bps of the truncated C3-gelonin gene. Fig. 14, lane 3 shows one intense band of the pET-28a(+)-5310bps-product after digestion with *Sall* and *NdeI*. The difference between a 5369 bps pET-28a plasmid and pET-28a(+)-5310bps-product was 59 bps-fragments which are not readily detectable by agarose gel electrophoresis.

Both the plasmid product band and insert DNA-product band were extracted by Gene JET™ Gel extraction Kit (Fermentas GmbH). The DNA concentrations were detected by measuring the absorption at 260 nm (Beckman DU640 Spectrophotometer).

- **Ligation of insert into plasmid**

Ligation of the C3-gelonin DNA insert into linearized pET-28a plasmid involved the formation of four new phosphodiester bonds between adjacent 5'-phosphate and 3'-hydroxy groups. Bacteriophage T4-DNA ligase was used to catalyze the formation of these phosphodiester bonds. The ligation reaction was performed according to the protocol described in the materials chapter. 20  $\mu$ l ligation reaction mixture, 150 ng of the restriction enzyme digest pET-28a(+) plasmid, 125 ng of insert (742 bps) and T4-DNA ligase were used (Fig.15). The reaction product was transformed into *E. coli* BL-21 competent cells and then plated overnight on an LB-agar plate containing kanamycin.

Many colonies were growing on the plate. Only one colony was allowed to grow in LB media containing kanamycin and the circular plasmid was isolated and purified by QIAprep™ Spin Miniprep Kit (Qiagen).

• DNA Sequencing

The isolated plasmid was sequenced at the Nano-Bio-Center at the TU Kaiserslautern. It was confirmed that the C3-gelonin DNA was correctly inserted into the pET-28a plasmid in frame. The new plasmid chart is shown in Fig. 16. The resulting plasmid was named pET-C3-gelonin, encoding a fusion protein composed of mature gelonin with three amino acid residues less. (For complete DNA sequence see “appendix”).

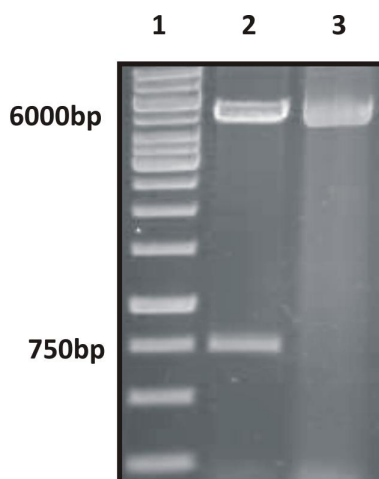


**Figure 14:** Agarose gel electrophoresis of pET-gel and pET-28a(+) plasmids cleaved by double enzymatic hydrolysis. (1) DNA marker; (2) pET-gel digested with both *Sall* and *NdeI*; (3) Vector pET28a digested with both *Sall* and *NdeI*.

<i>NdeI</i>	F1	<i>Sall</i>
5'-TATGGCTGCC-----	5310 bps-----	AGCTTG -3'
3'- ACCGACGG-----		TCGAACAGCT -5'
<i>Sall</i>	F2	<i>NdeI</i>
5'-TCGACGAATT-----	742 bps-----	CAGGCCCA -3'
3'- GCTTAA-----		GTCCGGGTAT -5'

**Figure 15:** Diagram of the coding strand of the 5310 bps (F1) and 742 bps (F2) fragments obtained after double enzymatic restriction (*Sall* and *NdeI*) of the pET-28a(+) and pET-gel, respectively.

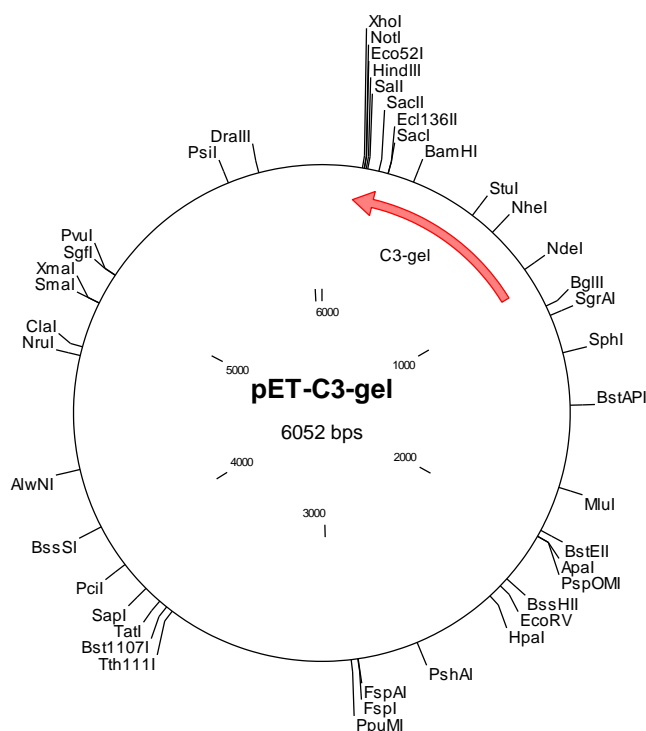


**Figure 16:** Construction of plasmid pET-C3-gel. The expression plasmid pET-C3-gel was prepared by inserting the *Sall* and *NdeI*-digested pET-gel plasmid into pET-28a(+) that also had been digested with *Sall* and *NdeI*.

- **Expression and purification of rC3-gelonin in *E. coli***

The rC3-gel was expressed and purified by the same protocol which was used in expression and purification of rGel. From 1 l expression cultures about  $3.6 \pm 0.2$  mg of pure rC3-gelonin was routinely obtained (Fig. 17). Fig. 16 shows the construct of the expression vector pET-C3-gel. The expressed protein contains 248 amino acids of C3-gel plus an extra 21-aa sequence containing a His-tag and a thrombin-cleavable peptide (LVPRGS) at the N-terminus (MGSSHHHHHSSGLVPRGSHM). In addition, an extra 12- aa sequence containing a His-tag (LAAALEHHHHH) at the C-terminus (Fig. 18). The expressed recombinant C3-gel constitutes  $\approx 3\text{--}5\%$  of the total *E. coli* cellular proteins. The calculated MW of the recombinant C3-gel is 31.38 or 29.636 kDa for native or thrombin treated C3-gel, respectively.

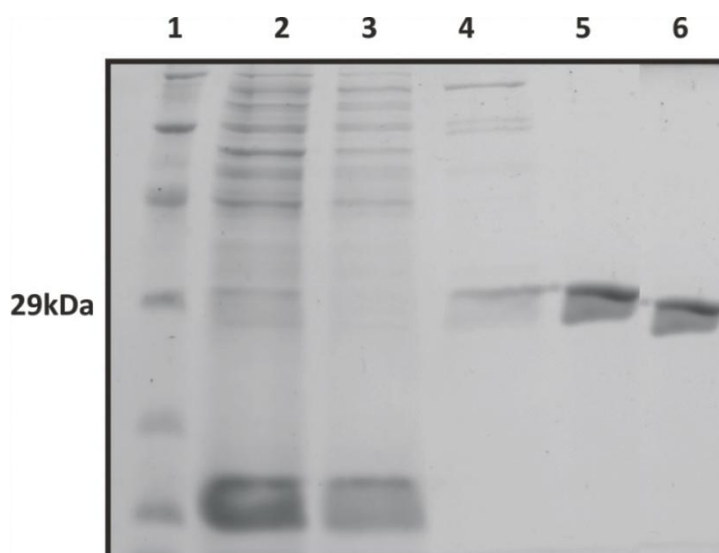


**Figure 17:** SDS-PAGE showing the purification of recombinant gelonin by affinity chromatography on a nickel chelating column. Lane 1 and 7, protein marker; lane 2, supernatant of cell lysate; lane 3, flow-through with 20 mM imidazole; lane 4, washing step with 100 mM imidazole; lane 5, elution with 500 mM imidazole (recombinant C3-gelonin) and lane 6, recombinant C3-gelonin (5 µg) after thrombin cleavage.

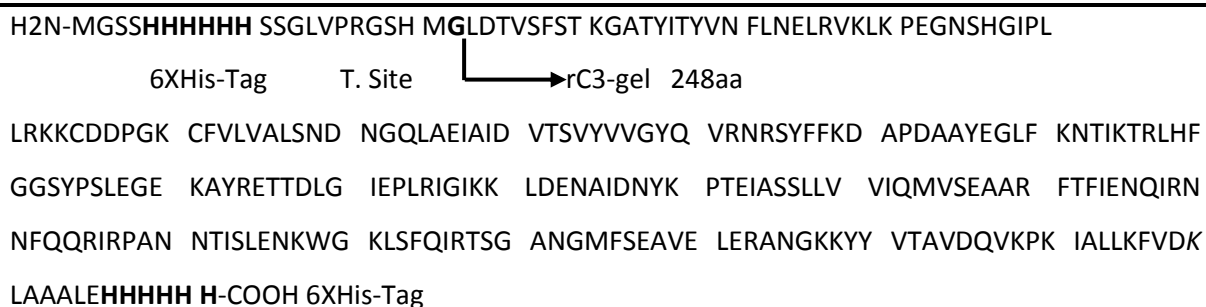


**Figure 18:** The amino acid sequence of rC3-gelonin.

#### 4.1.2.2 Cloning of recombinant N- and C-terminally truncated gelonin (rN34C3-gelonin)

The pET-28a(+) and pET-gel were digested with *Sall* and *NcoI*. After restriction enzyme digestion, the linearized plasmid DNA was predicted to be 5252 bps and the insert was predicted to be 634 bps. Fig. 19 lane 2 shows two intense bands of pET-gel product after digestion with *Sall* and *NcoI*. The smaller band revealed a 634 bps of truncated gelonin gene. Fig. 19 lane 3 shows one intense band of pET-28a(+)-5252 bps-product after digestion with *Sall* and *NcoI*. The difference between a 5369 bps pET-28a plasmid and pET-28a(+)-5252 bps-product was a 117 bps-fragment which are not readily detectable by agarose gel electrophoresis.

Both the plasmid product band and insert DNA-product band were extracted by Gene JET™ Gel extraction Kit (Fermentas GmbH). The DNA concentrations were detected by measuring the absorption at 260 nm (Sambrook et al, 1989).

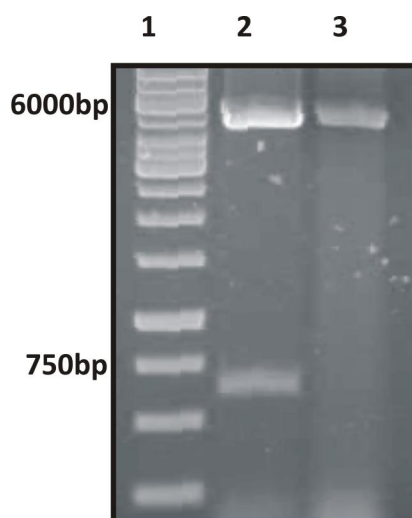


**Figure 19:** Agarose gel electrophoresis of pET-gel and pET-28a(+) plasmids cleaved by double enzymatic hydrolysis. (1) DNA marker; (2) pET-gel digested with both *Sall* and *NcoI*; (3) Vector pET28a digested with *Sall* and *NcoI*.

For the 20 µl ligation reaction mixture, 150 ng of the 5252 bps, restriction enzyme digest pET-28a(+) plasmid and 108 ng of insert (634 bps) were used (Fig. 20). The ligation reaction was performed by T4-DNA ligase as described above. The reaction product was transformed into *E. coli* BL-21 competent cells and then plated overnight on an agar plate containing kanamycin. Many colonies were growing on the plate. Only one colony was grown in LB media containing kanamycin, and the circular plasmid was isolated and purified by QIAprep™ Spin Miniprep Kit (Qiagen).

<i>NcoI</i>	F1	<i>Sall</i>
5-CATGGTATAT-----	5252 bps-----	AGCTTG -3
3- CATATA-----		TCGAACAGCT -5
<i>Sall</i>	F2	<i>NcoI</i>
5-TCGACGAATT-----	634 bps-----	GAATGC -3
3- GCTTAA-----		CTTACGGTAC -5

**Figure 20:** Diagram of the coding strand of the 5252 bps (F1) and 634 bps (F2) fragments obtained after double enzymatic restriction (*Sall* and *NcoI*) of the pET-28a(+) and pET-gel, respectively.



- **DNA Sequencing**

The new isolated plasmid was sequenced at the Nano-Bio-Center at the TU Kaiserslautern. It was confirmed that the N34C3-gelonin DNA was correctly inserted into the pET-28a plasmid in frame. The new plasmid is shown in Fig. 21 and was named pET-N34C3-gelonin. (For complete DNA sequence see “appendix“)

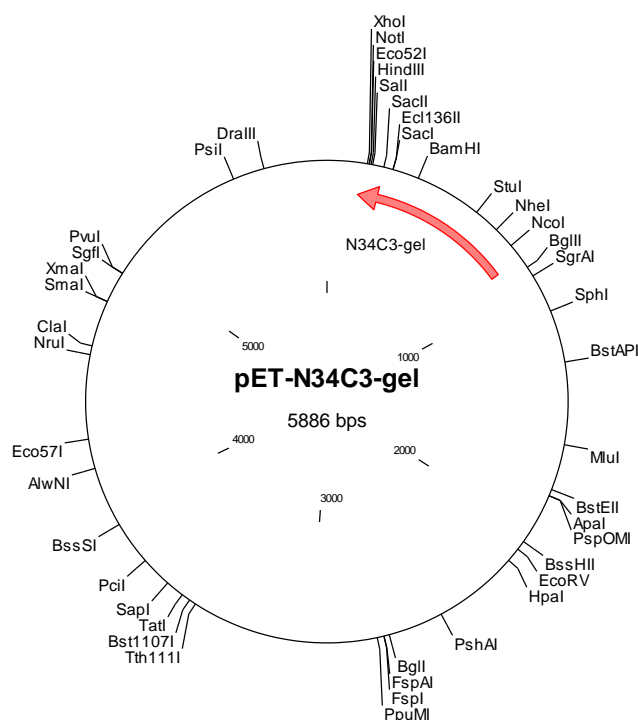


**Figure 21:** Construction of plasmid pET-N34C3-gel.

- **Expression and purification of rN34C3-gelonin in *E. coli***

The rN34C3-gel was expressed and purified by the same protocol which was used for expression and purification of rGel. From 1 l expression cultures about  $1.2 \pm 0.1$  mg of pure rN34C3-gelonin was routinely obtained (Fig. 22). The expressed protein contains 214 amino acid residues of rN34C3-gel and an extra 12-aa sequence containing a His-tag (LAAALEHHHHHH) at the C-terminus (Fig. 23). The expressed recombinant N34C3-gel constitutes  $\approx 1$ – $2\%$  of the total *E. coli* cellular proteins. The calculated MW of the recombinant N34C3-gel is 26.906 kDa.

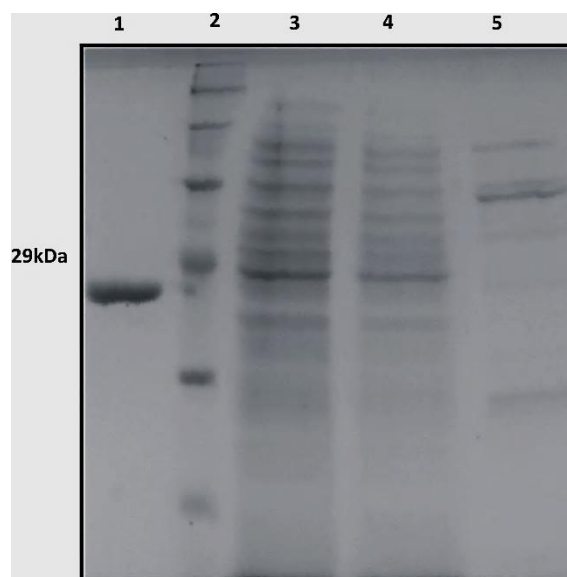


**Figure 22:** SDS-PAGE of rN34C3-gelonin purified by affinity chromatography on a Ni<sup>2+</sup> chelating column. Lane 2, protein marker; lane 3, supernatant of cell lysate; lane 4, flow-through with 20 mM imidazole; lane 5, washing step with 100 mM imidazole; lane 1, elution step with 500 mM imidazole (rN34C3-gelonin).

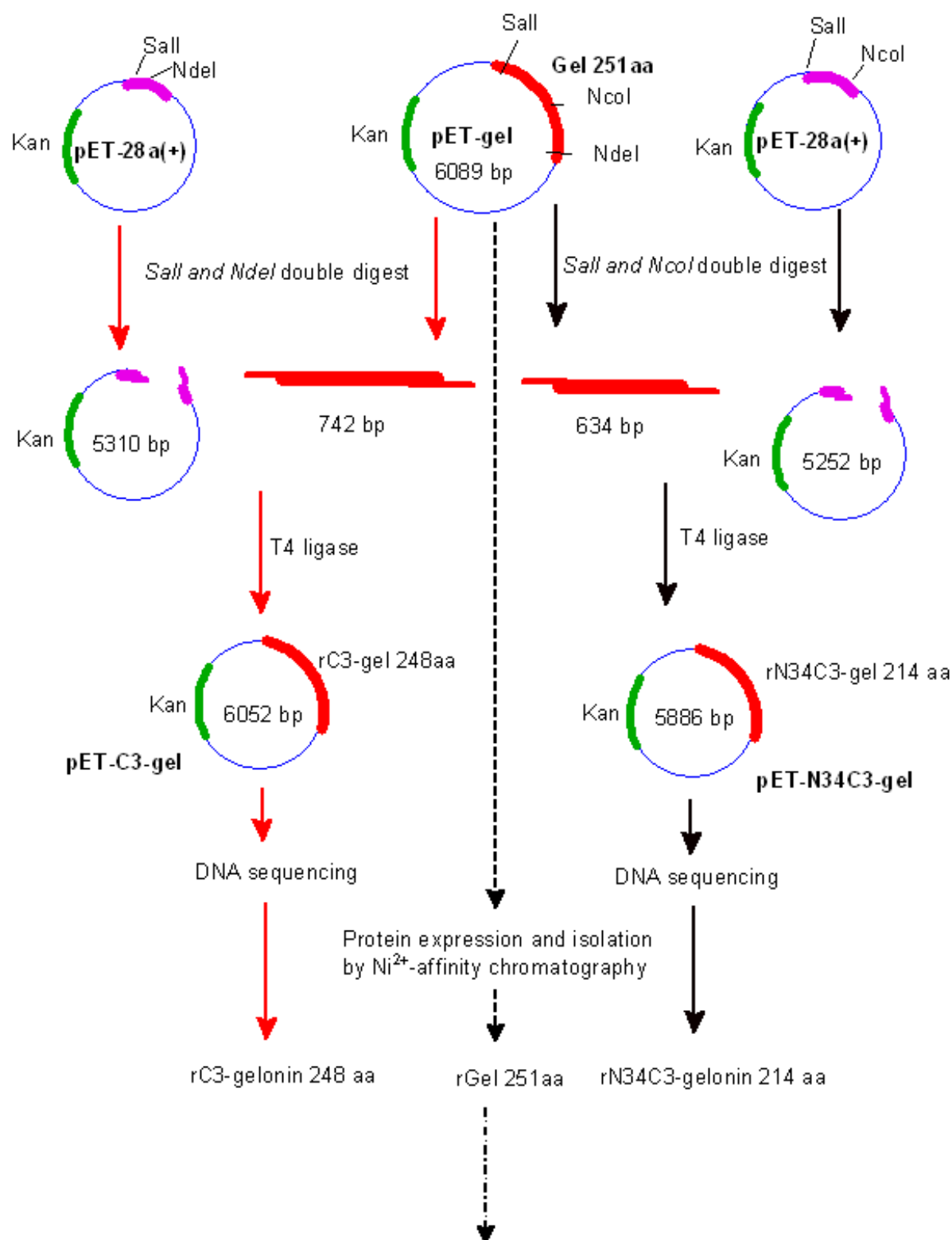
---

MGIPLLRKK CDDPGKCFVL VALSNDNGQL AEIAIDVTSV YVVG YQVRNR SYFFKDAPDA AYEGLFKNTI  
 ↓  
 N34C3-gel

KTRLHFGGSY PSLEGEKAYR ETDDLIEPL RIGIKLDEN AIDNYKPTI ASSLLVVIQM VSEARFTFI  
 ENQIRNNFQQ RIRPANNTIS LENKWGKLSF QIRTSGANGM FSEAVELERA NGKKYYVTAV DQVKPKIALL  
 KFVDKLAAL EHHHHHH 6XHis-Tag

---

**Figure 23:** The amino acid sequence of rN34C3-gelonin.



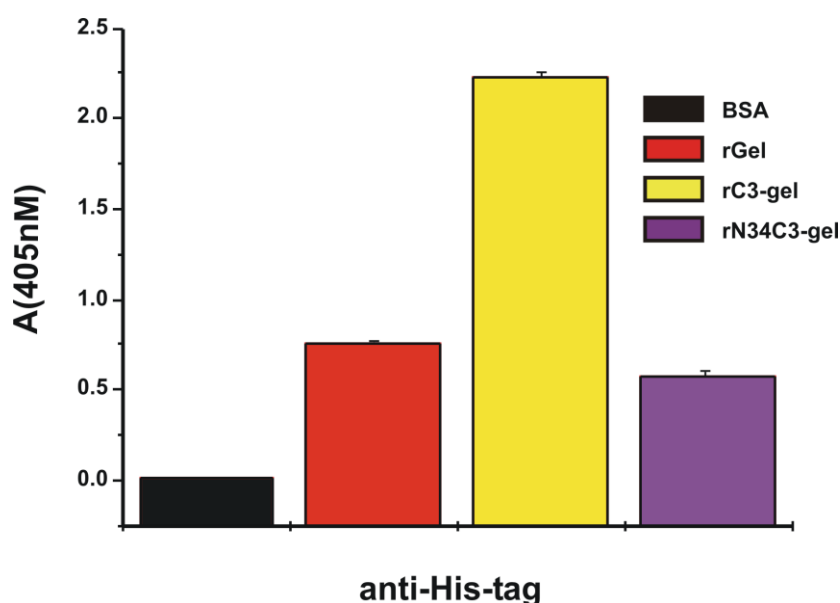
- A-Characterization of fusion proteins by SDS-PAGE and ELISA with anti-His
- B-Cytotoxicity of proteins with intact cells (MTT test)
- C- In vitro translation assay
- D- DNase like activity test

**Figure 24:** Diagram illustrating the strategy used for cloning of different gelonin genes.

### 4.1.3. Characterization and toxicity of gelonins

#### 4.1.3.1. Characterization of His-proteins by ELISA

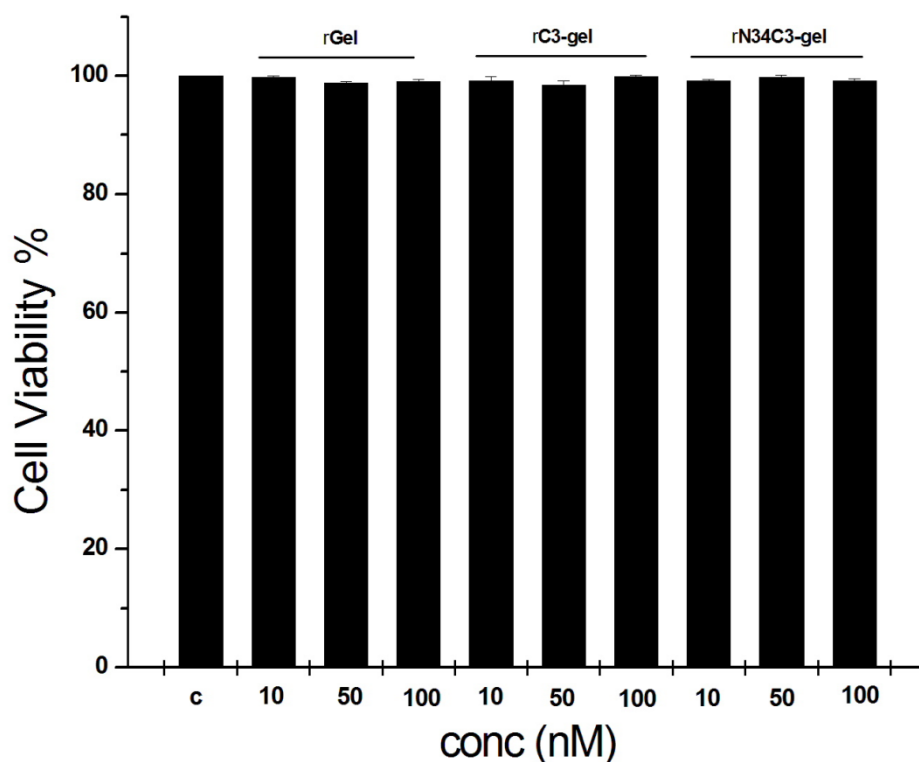
The isolated proteins were characterized by ELISA (see methods). As shown in Fig. 25 all the gelonin forms exert positive reaction with anti-His-tag antibody but with different intensity. The rC3-gelonin was about 3.5 or 4-fold more intense than that of rGel or rN34C3-gelonin, respectively. Also, the response of N-terminal His-tag protein was 1.5 fold more intense than that of the C-terminal His-tag protein.



**Figure 25:** Characterization of the fusion proteins using an ELISA against the anti-His-tag.

#### 4.1.3.2. *In-vitro* cytotoxicity

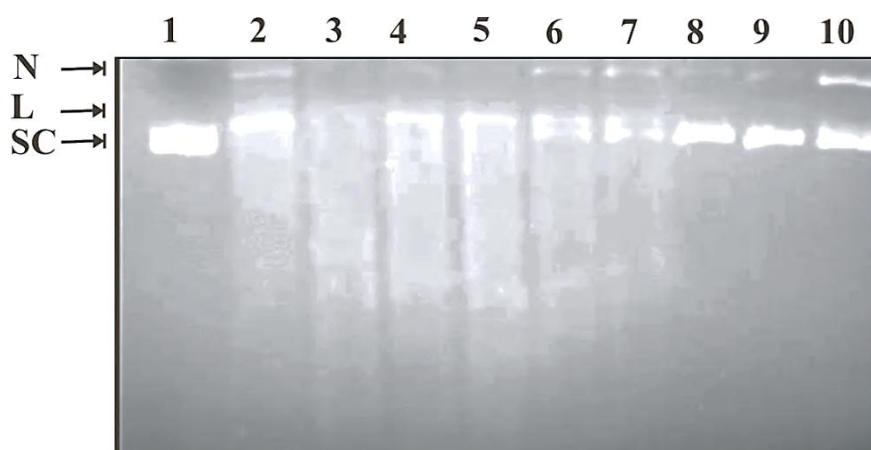
The previous data indicated that gelonin is relatively non-toxic to intact cell, due to an incapability to penetrate cell membranes. Therefore we tested whether rGel, rC3-gel and rN34C3-gel are able to inhibit proliferation of MCF-7 cells through measurement of the mitochondrial and cytosolic dehydrogenases activities of living cells by the MTT assay. The MCF-7 cells were incubated for 72 h at 37 °C with different concentration (10, 50, 100 nM) of full length or truncated gelonins. As shown in Fig. 26, the rGel and its truncated forms did not cause any detectable inhibition of cell growth at concentrations up to 100 nM.



**Figure 26:** Cytotoxicity of rGel, rC3-gel, and rN34C3-gel against MCF-7 cells. Various doses of each protein were added to the culture plates containing ~100 000 cells/plate. The plates were incubated for 72 h at 37 °C under an atmosphere of 5 % CO<sub>2</sub> in humidified air in an incubator. The amount of remaining cells in the wells was assessed by MTT assay and then compared with those of untreated cells in the control plates. Values were represented as mean  $\pm$  SD. Each experiment was performed in triplicate.

#### 4.1.3.3. DNase-like activity test

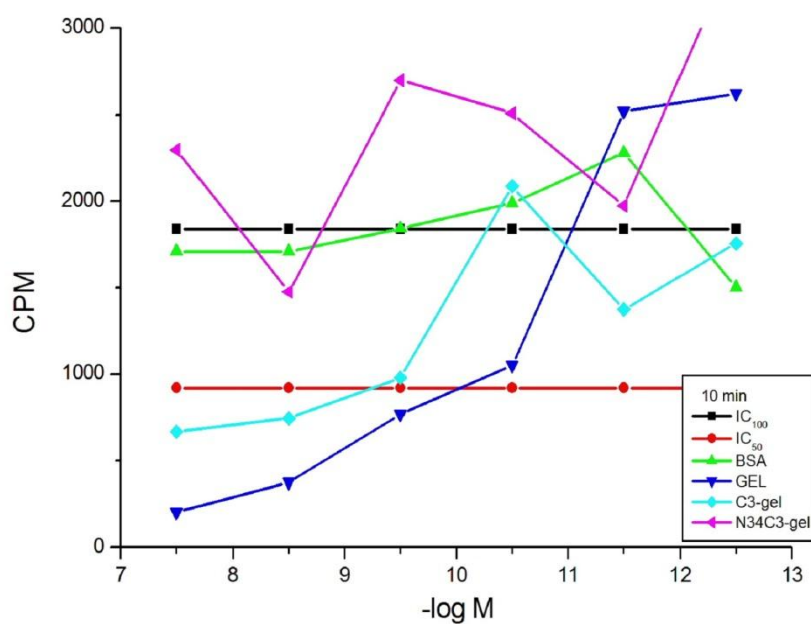
The DNase-like activity of gelonin and its truncated forms was tested on the supercoiled plasmid pUC18 DNA as a substrate. As shown in Fig. 27 both the gelonin and rC3-gelonin exert a powerful DNase activity via DNA degradation into fragments of different sizes as evidenced by the appearance of a smear, the disappearance of the supercoiled form and the appearance of the linearized and nicked forms of plasmid DNA. Interestingly, the N- and C-terminally truncated gelonin (rN34C3-gelonin) exerts a weak DNase activity against DNA plasmid through conversion of supercoiled DNA into linear and nicked forms, but no small DNA fragment was observed.



**Figure 27:** DNase activity of truncated gelonins. Lane 1, control; lanes 2–4, rGel; Lanes 5–7, rC3-gel; lanes 8–10, rN34C3-gel. A concentration series of proteins (100, 200, 400 ng) in the presence of 1000 ng dsDNA, SC, supercoiled form; L linearized; N, nicked forms.

#### 4.1.3.4. *In-vitro* translation assay

The ability of gelonin and its truncated forms to inhibit protein synthesis was tested in a rabbit reticulocyte lysate-based *in-vitro* translation assay. The decrease in the incorporation of [<sup>14</sup>C]-valine in the nascent peptides was taken as a measure of protein synthesis inhibition by the toxin. As shown in Fig. 28 both rGel and rC3-gelonin caused a dose-dependent inhibition of protein synthesis with an IC<sub>50</sub> of 2.4 and 9 ng/ml, respectively. Most notably, the N- and C-terminally truncated gelonin (rN34C3-gelonin) had no effect on protein synthesis.



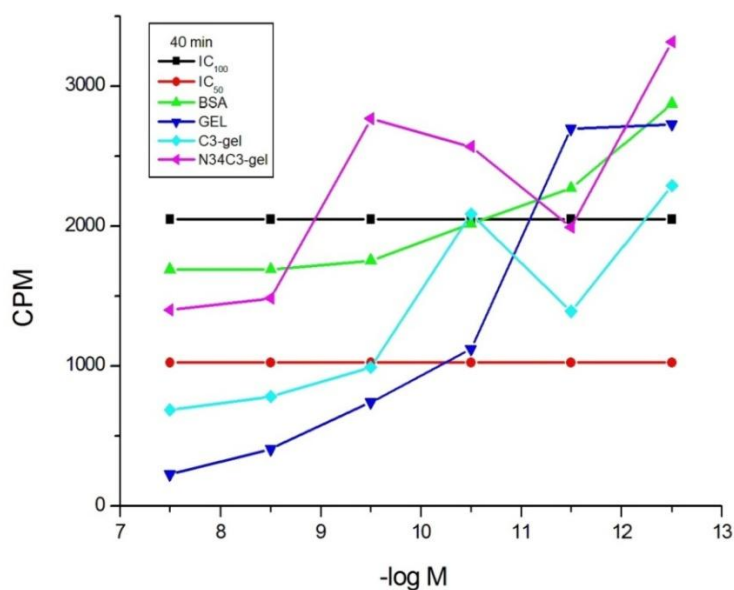


**Figure 28:** Inhibition of *in-vitro* translation by gelonin and the fusion protein. The incorporation of [<sup>14</sup>C]-valine into the nascent peptides was followed in a cell-free translation assay at various concentrations of gelonin and the fusion protein with BSA as standard after 10 min incubation and 40 min incubation.

#### 4.1.4. Discussion

The pET-gel plasmid containing the gelonin gene was constructed by molecular cloning in the work group of Prof. Dr. Wolfgang E. Trommer and published by Hossann et al. (2006). The recombinant gelonin was isolated by Ni<sup>2+</sup> affinity chromatography and characterized by SDS-PAGE (Fig. 13).

In this work, we have successfully cloned two truncated gelonins into pET-28a(+) vectors and produced two new recombinant plasmids called pET-C3-gel and pET-N34C3-gel (Figs. 17 and 22). Also, both recombinant proteins can be expressed and isolated by the method used for rGel. Further, it was found that the three recombinant proteins can be also characterized by ELISA using anti-His-tag antibody (Fig. 25). Interestingly, the protein containing His-tag at N- and C-terminus has more intensity than that of the protein containing one His-tag.

Table 2 shows a summary of different pET plasmids and their size. In addition, three recombinant gelonins were expressed and purified: intact rGel, C-terminally truncated (rC3-gelonin) and N- and C-terminally truncated gelonin (rN34C3-gelonin).

**Table 2:** A summary of different pET plasmids and different truncated gelonins

Plasmid name	Size in bps	Protein expressed	MW kDa + His-tag	MW kDa -His-tag	Yield (mg) (from 1 l culture)
pET-gel	6089	rGel	30.47	28.58	2.6±0.2
pET-C3-gel	6052	rC3-gelonin	31.381	29.49	3.6±0.2
pET-N34C3-gel	5886	rN34C3-gelonin	26.90	26.90	1.2±0.1

#### **4.1.4.1. Gelonin and its truncated forms did not induce MCF-7 cell death**

Gelonin is an N-glycosidase that cleaves a specific adenine from mammalian ribosomal RNA thereby ablating protein synthesis and resulting in cell death. As with many toxins of this class, rGel does not bind to or become internalized into cells at levels that are toxic unless it is conjugated or fused to a targeting moiety (Rosenblum et al., 1991). Our results are in line with previous studies (Rosenblum et al., 1992) showing that the rGel is non-toxic to intact cell because it is not able to cross the cell membrane at levels that are therapeutically useful due to lack of a carbohydrate-binding domain (B-chain). However, previous studies (Li et al., 2007) show that rGel inhibits cell growth of K562 tumour cells. This may be due to different cell lines used.

Also, it was found that neither rC3-gelonin nor rN34C3-gelonin has any inhibiting effect on MCF-7 cell lines (Fig. 26).

#### **4.1.4.2. N-terminal amino acid residues are involved in regulation of gelonin DNase activity**

DNase activities of purified rGel and truncated mutant gelonins were determined using pUC18 as substrate (Fig. 27). Experiments with rGel and rC3-gelonin indicated that these type I RIPs exhibit nuclease activity toward double-stranded DNA. On the other hand, N-terminal truncated gelonin has a weak DNase activity. Many previous studies (Roncuzzi & Gasperi-Campani, 1996; Nicolas et al., 1997A; Nicolas et al., 1998; Nicolas et al., 2000) reported that gelonin exerts single- and double-stranded oligonucleotide degradation by the removal of adenines, followed by generation of unstable products with several abasic sites and resulting in strand breakage and duplex melting, respectively.

A missing of thirty four amino acid residues leads to loss of proper gelonin folding and the DNase activity is decreased (Fig. 27) which is in line with Li et al., 2007. Our data together with other previous data shows that the intact rGel has higher DNase activity than truncated forms.

#### **4.1.4.3. C-and N-terminal amino acid residues are involved in regulation of gelonin N-glycosidase activity**

Biological activities of purified rGel and truncated mutant gelonins were determined in a cell-free *in-vitro* translation system of non-treated rabbit reticulocyte lysate. The relationship between the percentage of the protein synthesis inhibition at different doses of rGel and its truncated forms was determined (Fig. 28). The IC<sub>50</sub> of rGel was found to be 2.4 ng which is in line with (Hossann et al., 2006). The IC<sub>50</sub> of rC3-gelonin was 9.0 ng. But, the rN34C3-gelonin has no effect on protein synthesis.

However, six amino acid residues (Tyr74, Arg169, Gly111, Glu166, Tyr113 and Trp198) build up the active site of the adenine binding pocket (Hosur et al., 1995) are conserved in rN34C3-gelonin sequence. But, this protein has lost the N-glycosidase activity because the



amino acid residues in the N-terminal domain may be important to stabilize the interactions between the bases of the RNA and RIP. Also, three C-terminal amino acid residues are not involved in forming the active site pocket but may lead to a partial change in the conformational structure of the gelonin active site and reduce the N-glycosidase activity. Together, these data suggest that C-and N-terminal amino acid residues are involved in gelonin N-glycosidase activity.

#### **4.1.5. Conclusion**

In the present study, we have successfully cloned two different truncated gelonins into pET-28a(+) vectors and expressed intact rGel, rC3-gelonin and rN34C3-gelonin. Biological experiments showed that all these recombinant gelonins have no inhibiting effect on MCF-7 cell lines. This data suggests that the truncated-gelonins are still having a specific structure that does not allow for internalization into cells. Further, truncation of gelonin leads to partial or complete loss of N-glycosidase as well as DNase activity compared to intact rGel. Our data suggest that C-and N-terminal amino acid residues are involved in the catalytic and cytotoxic activities of rGel. In addition, the intact gelonin should be selected as a toxin in the immunoconjugate rather than truncated gelonin.

## 4.2. Part B

### 4.2.1. Chemistry

The methotrexate-gelonin (MTX-gelonin) conjugate was prepared in two steps: (1) activation of MTX with *N,N*-dicyclohexylcarbodiimide (DCC) and *N*-hydroxysuccinimide (NHS), and (2) coupling of MTX to gelonin.

Activation of the carboxyl groups of MTX with DCC and NHS for coupling the drug covalently to molecules amino groups, such as peptides or proteins, is an established technique (Rosowsky & Yu, 1978; Kulkarni et al., 1981). The activated MTX-NHS esters were reacted further with amino groups of gelonin. The reaction products were characterized by MALDI-TOF (Ultraflex MALDI-TOF-TOF, Bruker Daltonics) after in-gel tryptic digestion.

The active ester method not only yields the desired MTX  $\alpha$ - and  $\gamma$ -isomers but also bis-derivatives and several byproducts (Riebeseel et al. 2002). In order to find out more details about the structure of the MTX-gelonin conjugates we isolated intermediates of the synthesis, namely esters of MTX. The  $\alpha$ - and  $\gamma$ -MTX-NHS active esters are very unstable due to their high reactivity. To generate a stable intermediate without changing its structure an excess of methanol was added to the activation reaction. The stable methyl ester mix was separated by column chromatography and subsequently analyzed by electrospray-ionization (ESI).

#### 4.2.1.1. Synthesis of MTX-NHS active ester

The formation of active MTX ester was performed in this work according to the protocol described in methods. The carboxyl groups of nonreactive MTX were activated by DCC to react directly with NHS and to yield activated NHS esters (Fig. 29). The product mixture contained  $\alpha$ -,  $\gamma$ -MTX-NHS monoesters, MTX-NHS bis-ester ( $\alpha$  and  $\gamma$ ), and several by-products (e.g. *N*-acylisourea derivatives) (Rosowsky & Yu, 1978). The white precipitate (*N,N*-dicyclohexyl-urea) was removed, and the activated MTX-NHS ester was concentrated by evaporation.

To find out more details about the components present in the MTX-methyl ester mix, the mixture was subjected to column chromatography and analyzed by ESI. To perform column chromatography, we used silica gel as the stationary phase and 95:5 THF/H<sub>2</sub>O (V/V) as the mobile phase. Five fractions were collected and subsequently analyzed by ESI under positive ionization conditions. We found two fractions of high purity, No. 1 and 5, containing MTX-dimethyl ester and MTX-mono-methyl ester respectively. MTX-dimethyl ester with the molecular formula C<sub>18</sub>H<sub>20</sub>N<sub>8</sub>O (COOCH<sub>3</sub>)<sub>2</sub> has the calculated mono-isotopic MW of 482.2

Da. The  $m/z$  spectrum in Fig. 30B shows dominant ions at  $m/z$  483.2, which are consistent with the expected protonated molecular ions,  $(482.2+H^+)$ . MTX-mono-methyl ester,  $C_{19}H_{21}N_8O_3(COOCH_3)$ , with MW 468.2 Da was also suggested by the program in  $M+nH^+$  mode to achieve a value identical to the experimental one (Fig. 30A).

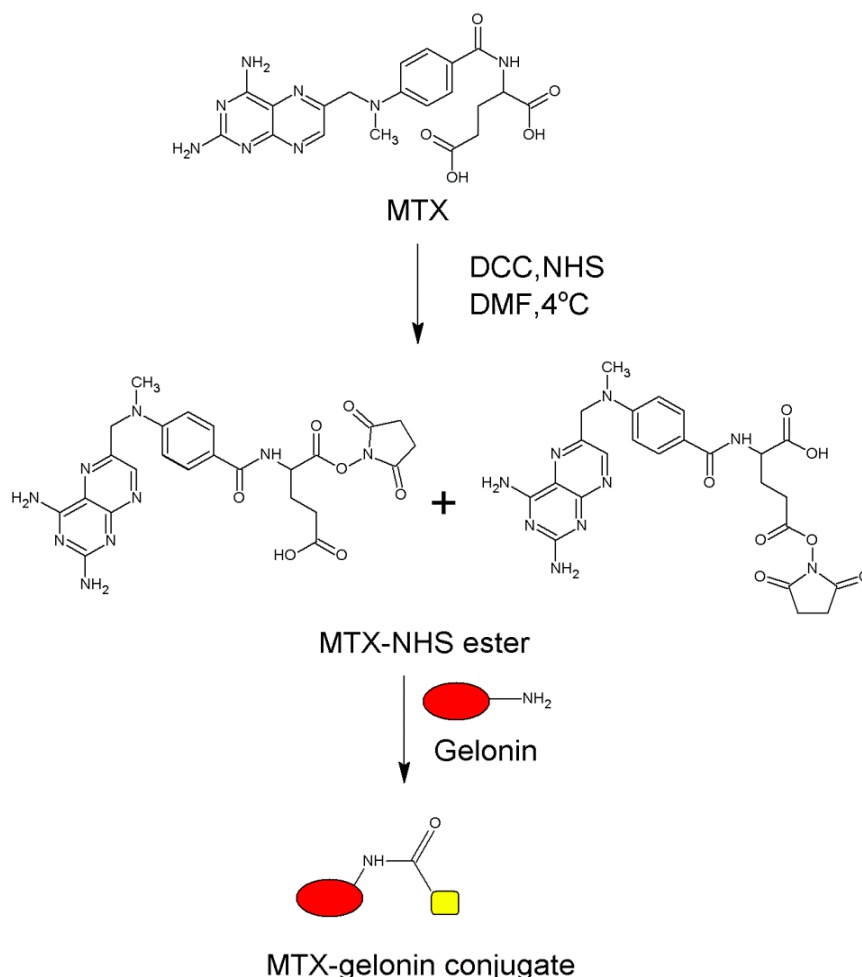


**Figure 29:** Synthesis of the MTX-gelonin conjugate.

#### 4.2.1.2. Synthesis and characterizations of MTX-gelonin conjugate

The MTX-gelonin conjugate was synthesized by reaction between gelonin and MTX-NHS ester in a molar ratio 1:6. Under conjugation conditions the active ester of MTX could react with amino groups of lysine residues forming an amide linkage between MTX and gelonin. The conjugate was dialyzed against PBS (pH 8.5) until the free MTX ester disappeared in PBS (pH 8.5). Molar ratio of MTX to gelonin in the conjugate was 5:1. Analysis of the final purified conjugate using SDS-PAGE shows a band (~32kda) that confirms the conjugation. It was found that all gelonin used for conjugate synthesis was bound to MTX as shown by the absence of additional bands in lane3 representing free protein. However, the broadness of the

conjugate bands compared with the free gelonin suggests that the synthesis product is a mixture of conjugates carrying a diverse number of MTX molecules (Fig. 31).

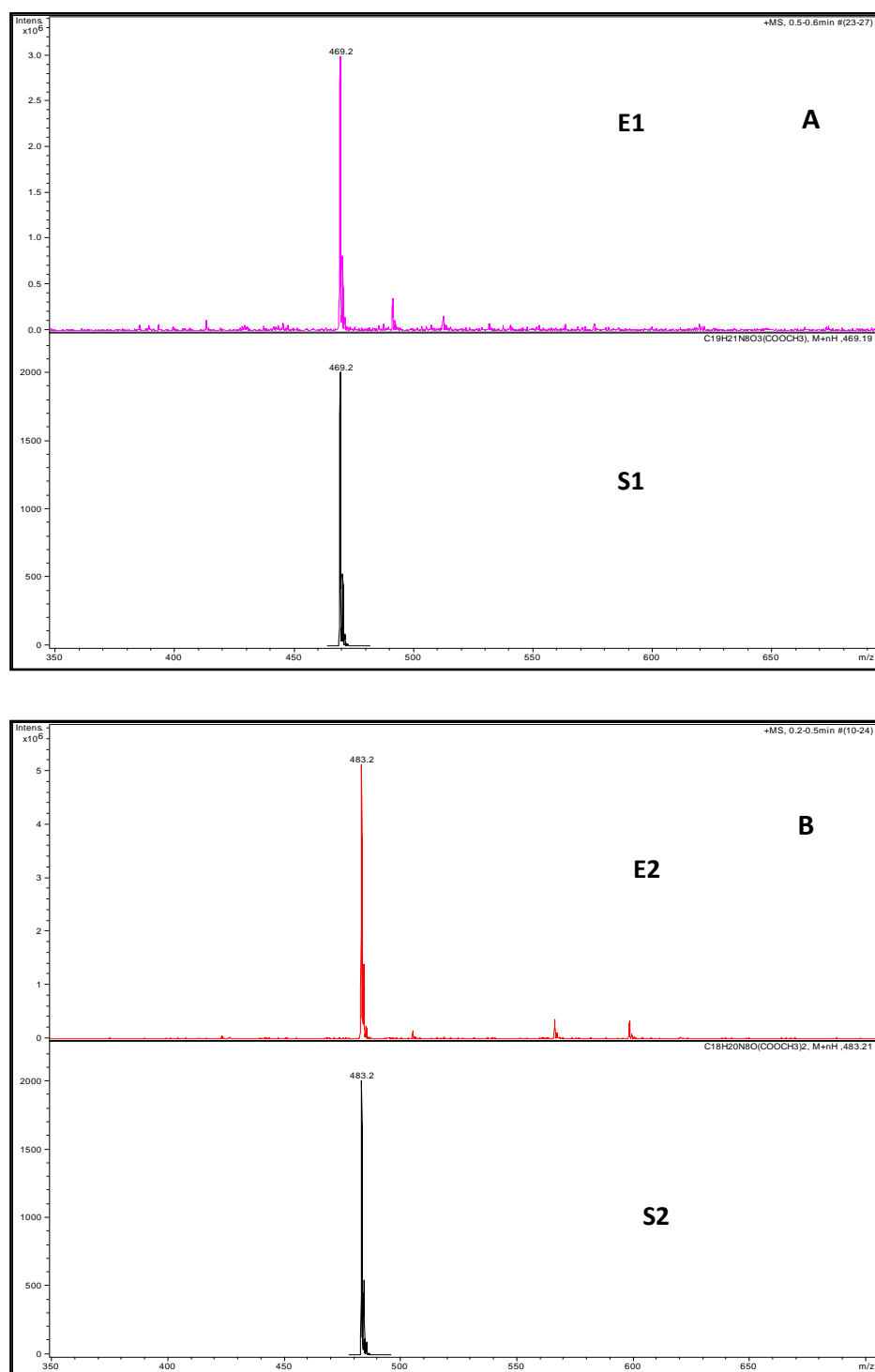


**Figure 30:** ESI-MS analysis spectra display molecular charge of A; MTX-mono-methyl ester (E1, experimental; S1, simulated) and B, MTX-dimethyl ester (E2, experimental; S2; simulated).

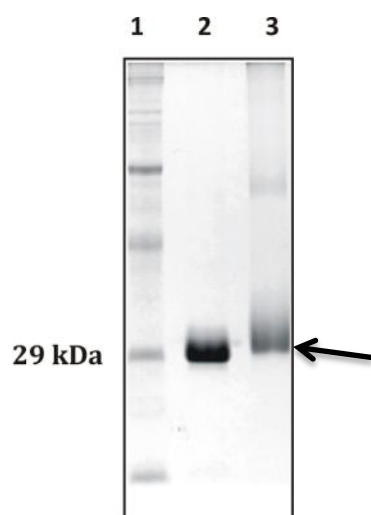


**Figure 31:** Characterization of gelonin and conjugate. SDS-PAGE showing lane 1: Marker; lane 2: gelonin (30kDa); lane 3: MTX-Gel (~32kda).

#### 4.2.1.3. Characterizations of MTX-binding sites by MALDI

To obtain a detailed structural analysis of the N-linked MTX we used in-gel tryptic digestion followed by MALDI-TOF analysis using DHB as a matrix. Data achieved by this analysis were compared with calculated values obtained from online digestion of gelonin “MS-digest”. Trypsin is a serine protease which cleaves proteins by hydrolyzing peptide bonds at the carboxyl side of lysyl (K) and arginyl (R) residues. The MTX- gelonin conjugate band of ~32 kDa (Fig.31, lane3) was excised and subjected to enzymatic digestion by trypsin as described in "Methods". The resulting peptide mixtures were analyzed by MALDI-TOF positive mode (Ultraflex MALDI-TOF-TOF, Bruker Daltonics).

It was found that the observed peptides in the MALDI-MS spectra (Fig. 32 and Table 3) cover more than 60% of the gelonin amino acid sequence. Interestingly, the peaks at  $m/z$  1054, 1134, 1758, 1949 and 1910 disappear and new peaks at  $m/z$  1491, 1571, 2195, 2348 and 2386 appear. However, these observed peptide signals do not correspond to any calculated values. So, we assumed that the practically measured mass of these fragments was increased due to modification with MTX (MW of 438 Da) linked to K or R residues of gelonin. Furthermore, we detected the exact lysine or arginine residue positions which bonded to MTX by comparison of modified and non-modified peptide sequences at approximately the same position (Table 4). Peptide sequence at position 1-10 carries only one amino acid, K<sub>10</sub>, which is capable of modification with MTX. So, we identified K<sub>10</sub>, K<sub>27</sub>, K<sub>207</sub>, K<sub>251</sub> and R<sub>130</sub> as possible modification sites (Table 4). Also, a glycosylation site at position 192-204 (Table 3) was detected. The peak appearing at  $m/z$  of 2495 was attributed to a peptide with  $m/z$  of 1470 carrying an additional 1023 Da sugar moiety.

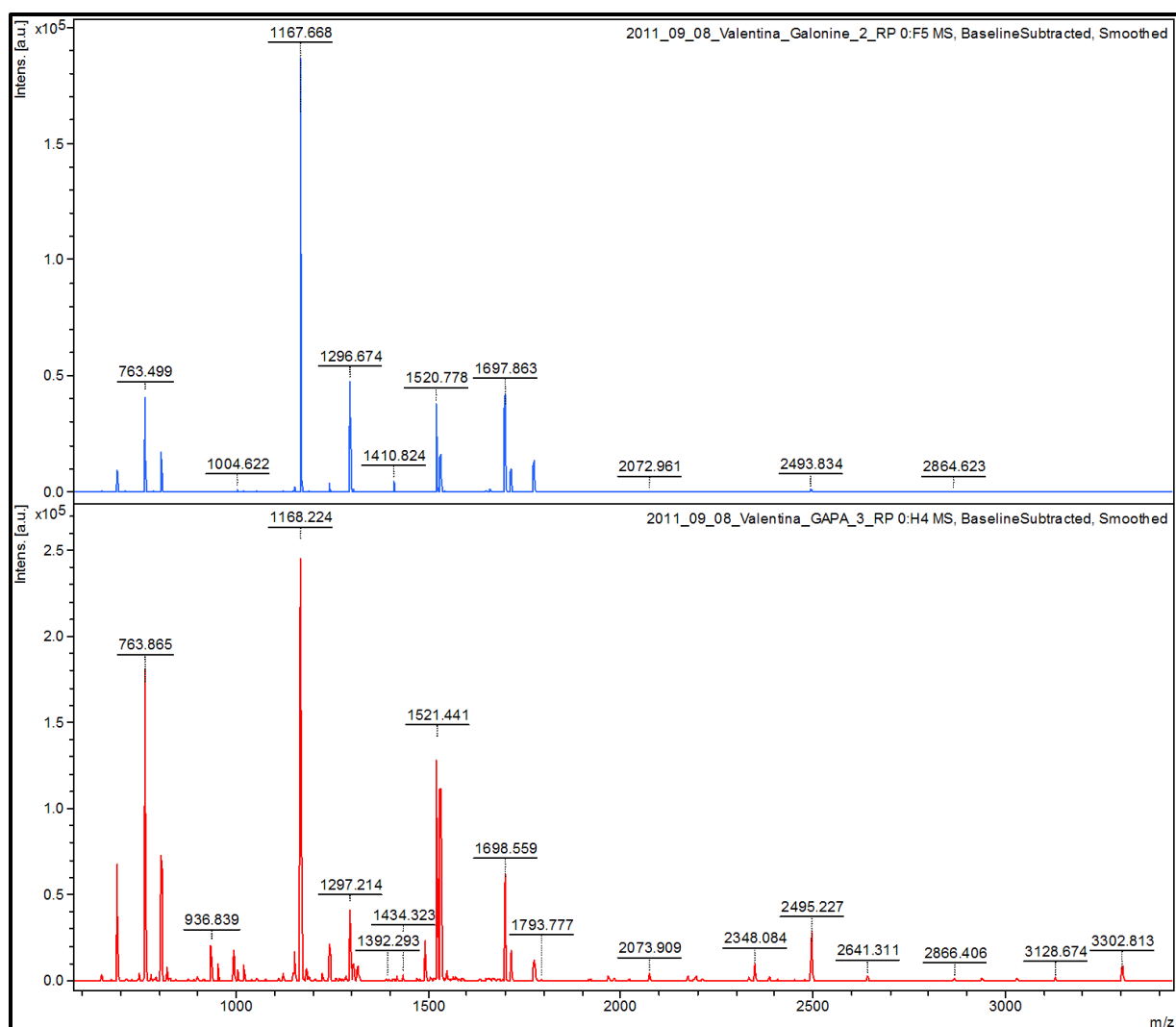


**Figure 32:** MALDI-MS TOF spectra display molecular ions of peptides obtained after in-gel trypsin digestion of gelonin (top) and MTX-gelonin conjugate (down).

**Table 3:** Assignment of peaks from Trypsin cleavage of MTX-gelonin conjugates (MALDI analysis).

Peptides	Position	Observed	Calculated
(R)SYFFK(D)	83-87	692.097	691.345
(R)KGDDPGK(C)	42-48	713.950	716.357
(K)LSFQIR(T)	208-213	763.865	763.446
(R)NNFQQR(I)	186-191	806.776	806.390
(R)FTFIENQIR(N)	177-185	1168.224	1167.615
(R)ETTDLGIPLR(I)	131-141	1244.249	1243.652
(K)DAPDAAYEGLFK(N)	88-99	1297.214	1296.610

(K)NTIKNPLLFGGK(T)	100-111	1304.234	1301.757
(K)YYVTAVDQVKPK(I)	235-246	1411.382	1410.762
<b>(-)GLDVSFSTK(G)</b>	<b>1-10</b>	<b>1491.358</b>	<b>1054.541</b>
(R)LHFGGSYPSLEGEK(A)	114-127	1521.441	1520.738
(K)LKPEGNSHGIPLLR(K)	28-41	1531.619	1530.875
<b>(K)WGKLSFQIR(T)</b>	<b>205-213</b>	<b>1571.570</b>	<b>1134.641</b>
(K)LKPEGNSHGIPLLRK(G)	28-42	1657.533	1654.937
(R)TSGANGMFSEAVELER(A)	214-229	1698.559	1697.779
(R)TSGANGM*FSEAVELER(A)	214-229	1714.581	1713.774
(K)GATYITYVNFNLNLR(V)	11-25	1774.763	1773.917
(K)TRLHFGGSYPSLEGEK(A)	112-127	1778.741	1777.886
<b>(R)VKLKPEGNSHGIPLLR(K)</b>	<b>26-41</b>	<b>2195.118</b>	<b>1758.038</b>
<b>(R)LHFGGSYPSLEGEKAYR(E)</b>	<b>114-130</b>	<b>2348.084</b>	<b>1910.939</b>
<b>(K)YYVTAVDQVKPKIALLK(F)</b>	<b>235-251</b>	<b>2386.284</b>	<b>1949.147</b>
<b>(R)IRPANNTISLENK(W)</b>	<b>192-204</b>	<b>2495.227</b>	<b>1469.807</b>

**Table 4:** Determination of sites modified with MTX.

MTX-modified		Modification position	Non-modified	
position	peptides		position	peptides
1-10	(-)GLDVSFSTK(G)	<b>K<sub>10</sub></b>	----	-----
26-41	(R)VKLKPEGNSHGIPLLR(K)	<b>K<sub>27</sub></b>	28-41	(K)LKPEGNSHGIPLLR(K)
114-130	(R)LHFGGSYPSLEGEKAYR(E)	<b>R<sub>130</sub></b>	114-127	(R)LHFGGSYPSLEGEK(A)
205-213	(K)WGKLSFQIR(T)	<b>K<sub>207</sub></b>	208-213	(K)LSFQIR(T)
235-251	(K)YYVTAVDQVKPKIALLK(F)	<b>K<sub>251</sub></b>	235-246	(K)YYVTAVDQVKPK(I)

## 4.2.2. Biology

### 4.2.2.1. Inhibitions of cell proliferation by MTX-gelonin conjugate

The toxicity of gelonin, MTX-gelonin, and MTX for MCF-7 cells was determined by an MTT assay. Cells were exposed to various concentrations (10 nM, 50 nM, and 100 nM) of gelonin, MTX-gelonin, and (6.6 nM, 33 nM, and 66 nM) MTX for 48 h in RPMI-1640 medium. The results of cytotoxic activity *in-vitro* were expressed as ID<sub>50</sub>— the dose which inhibits proliferation rate of the tumor cells by 50% compared with untreated cells. As shown in Fig. 33, gelonin itself did not cause any detectable inhibition of cell growth, simply as it could not enter the cells and MTX had no effect on cell viability at concentrations up to 66 nM. Treatment with MTX-gelonin reduced cell viability in a concentration-dependent fashion, resulting in 50%, 62%, or 70% cell death at 10 nM, 50nM or 100nM, respectively. These Results clearly demonstrated that MTX was able to successfully transduce an otherwise cell-impermeable protein toxin into cancer cells for possible therapeutic purposes.

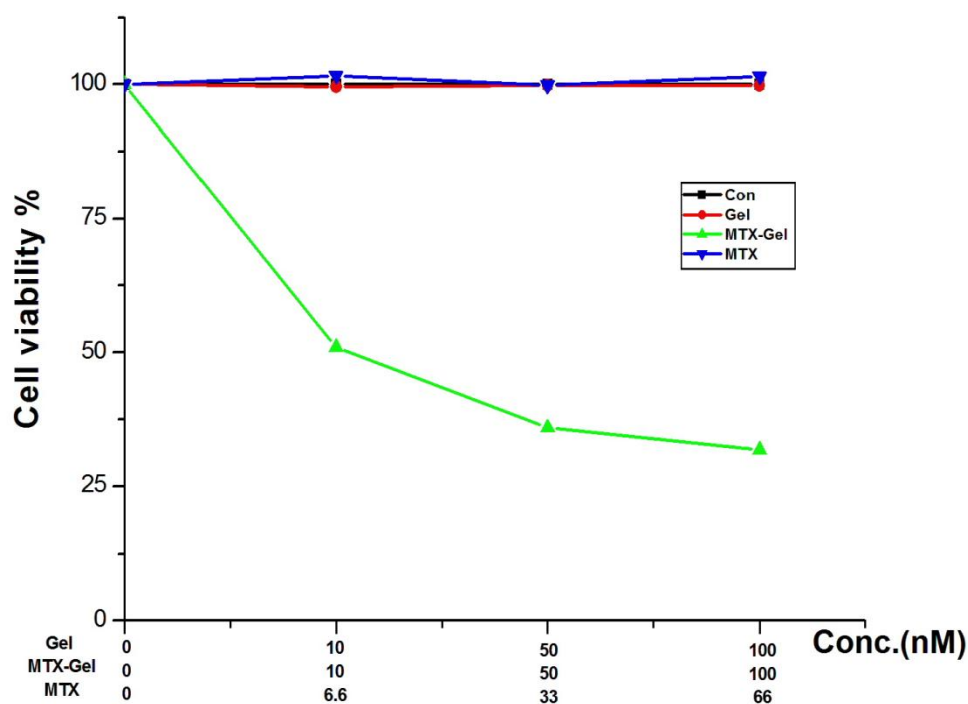


**Figure 33:** Cytotoxicity of native gelonin, MTX-gelonin, and MTX against MCF-7 cells. Various doses of each compound were added to the culture plates containing ~100 000 cells/plate. The plates were incubated for 48 h at 37°C under an atmosphere of 5% CO<sub>2</sub> in humidified air in an incubator. The amount of remaining cells in the wells was assessed by MTT assay and then compared with those of untreated cells in the control plates. Values were represented as mean ± SD. Each experiment was performed in triplicate.



#### 4.2.2.2. DNA Fragmentation Induced by MTX-gelonin

The comet assay, as generally used, detects strand breaks by virtue of their ability to relax supercoils of DNA and to allow DNA loops to extend to form a comet tail when an electric field is applied. The intensity of DNA in the tail reflects the DNA break frequency.

The MCF-7 cells were incubated with various concentrations (10nM, 50nM, and 100nM) of gelonin, MTX-gelonin, and (6.6 nM, 33 nM, and 66 nM) MTX for 24 h. DNA damage was not observed in MCF-7 cells treated with gelonin or MTX (Fig. 34) compared with controls. In addition, the extent of DNA damage was not enhanced in the presence of FPG glycosylase compared with controls. MTX-gelonin treatment caused a distinct direct DNA breakage (TI% > 20) in a dose-dependent manner. Additional oxidative DNA breakage (FPG-sensitive sites) was observed in the presence of FPG glycosylase.

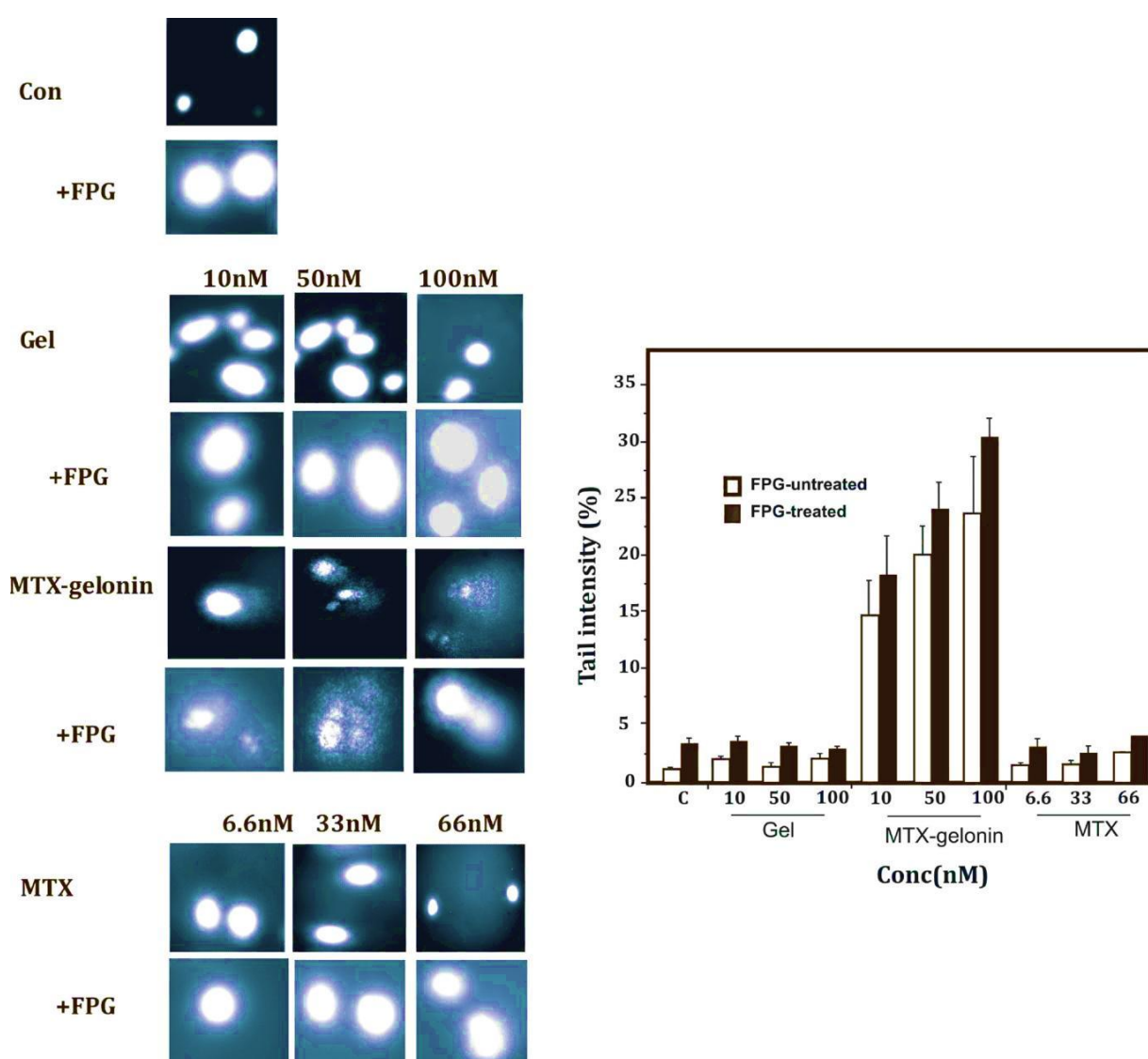


**Figure 34:** DNA damage (TI %) in MCF-7 cells exposed to gelonin, MTX-gelonin and MTX at different concentrations for 24 h in the absence or presence of FPG repair enzyme.

#### 4.2.2.3. *In-vitro* translation test

The ability of gelonin, MTX-gelonin or MTX to inhibit protein synthesis was tested in a rabbit reticulocyte lysate-based *in-vitro* translation assay. The decrease in the incorporation of [<sup>14</sup>C]-valine in nascent peptides was taken as a measure of protein synthesis inhibition by the toxin. Native gelonin inhibited translation by 50% at a concentration of 4.6 ng/ml, MTX-gelonin conjugate was less active, exhibiting a 50% inhibition of protein biosynthesis at 50.5 ng/ml whereas MTX alone has no inhibiting effect on protein synthesis in a reticulocyte *in-vitro* translation system (Fig. 35).

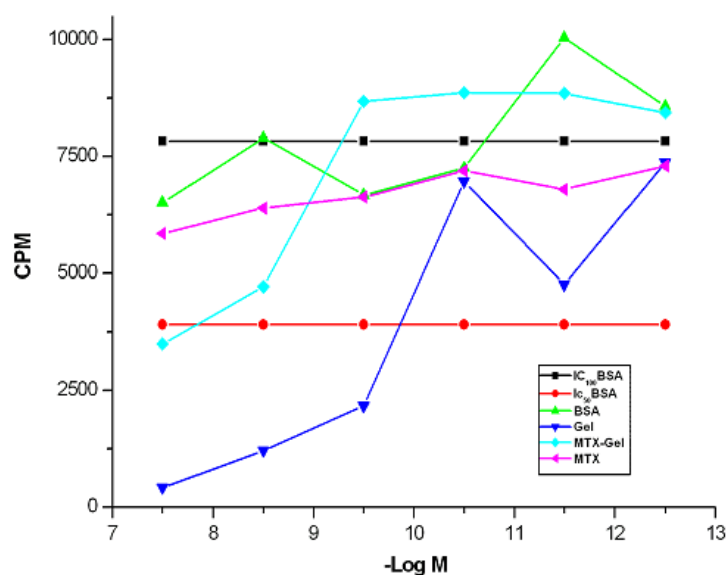


**Figure 35:** Inhibition of protein synthesis in the cell-free translational system from rabbit reticulocyte lysate assay by gelonin, MTX-gelonin and MTX.

#### 4.2.2.4. DNase-like activity assay

To investigate whether coupling of MTX to gelonin affected its DNase activity, a DNase activity assay was carried out, using pUC18 as a substrate. We found that gelonin degraded double-stranded DNA into fragments of different size as evidenced by the appearance of a smear, while no significant degradation was caused by MTX-gelonin and MTX (Fig. 36). These results indicate that the conjugation of gelonin to MTX is able to abolish *in-vitro* DNase activities of the native gelonin.

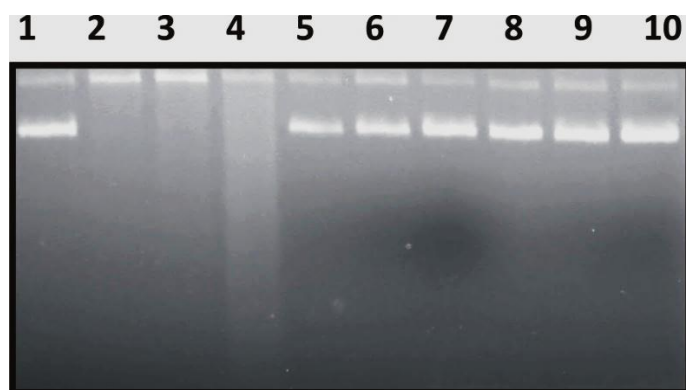


**Figure 36:** DNase activity of gelonin, MTX-gelonin, and MTX, Lane 1, control; lanes 2–4, gelonin; Lanes 5–7, MTX-gelonin; Lanes 8–10, MTX. A concentration series of proteins (100, 200, 400 ng) in the presence of 1000 ng dsDNA.

#### 4.2.2.5. DHFR Inhibition Activities of MTX and the Conjugates

The enzyme inhibition activities of free MTX and the conjugated MTX were evaluated in a cell-free assay (Fig. 37). This is based on the reduction of dihydrofolate to tetrahydrofolate by the enzyme DHFR in the presence of NADPH.

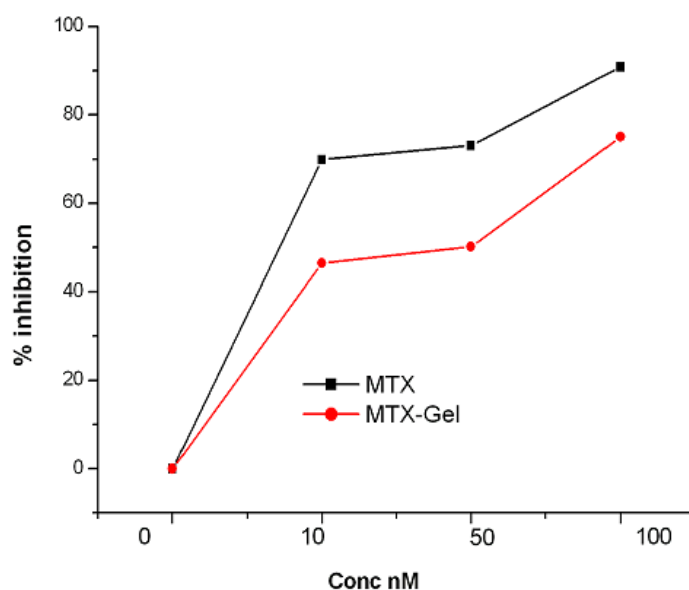


**Figure 37:** DHFR inhibition by free MTX and conjugates.

As can be seen from Fig. 37, free and the conjugate of the MTX showed concentration-dependent inhibitory activity against the target enzyme. Free MTX showed an  $IC_{50}$  value of 7 nM which agrees with previous work (Ma & Kovacs 2000; Pignatello et al., 2000). The conjugated MTX showed an  $IC_{50}$  value of 50 nM. Interestingly, the conjugate was less effective against DHFR by about 20% at higher concentration. This result suggested that

conjugation with gelonin might alter the binding affinity of MTX with dihydrofolate reductase, leading to the partial loss of its anti-folate activity.

### **4.2.3. Discussions**

To date, a lot of research is focusing on finding new systems to improve drug delivery and specificity, particularly in therapeutic areas such as cancer treatment. In order to reach this goal, tremendous efforts were undertaken to develop tumor-selective drugs by conjugating anti-cancer drugs to hormones, antibodies, and vitamins. Among them, folic acid and its analogs show a great deal of promise as a tumor-homing agent. Thus, the folate enhances the differential specificity of conjugated anti-cancer drugs by targeting the folate receptor.

The FR can actively internalize bound folates and folate conjugated compounds via receptor-mediated endocytosis (Kamen & Capdevila, 1986; Corona et al., 1998; Kamen & Smith, 2004). It has been found that FR is up-regulated in more than 90% of non-mucinous ovarian carcinomas. The FR density also appears to increase as the stage of the cancer increases (Elnakat et al., 2004).

MTX is an anti-metabolite and anti-folate drug that is used for chemotherapy either alone or in combination with other agents (Kulkarni et al., 1981; Pignatello et al., 2000). The uptake of MTX occurs via the folate receptor and reduced folate carrier on the cell surface which is highly expressed in rapidly dividing (cancer) cells (Elnakat et al., 2004; Parker et al. 2005).

Gelonin is a plant protein which can powerfully reduce the protein-synthetic capacity of eukaryotic ribosomes but is relatively non-toxic to intact cells because lack of a B-chain (Stirpe & Barbieri, 1986; Endo et al., 1988). One of the most important problems of effective anti-tumor gelonin activity is a selective transport of gelonin to cancer cells. One of the means to accomplish this goal is to use the carriers with a high affinity for target cells.

In this part, gelonin has been coupled to MTX to create a potent immunotoxic agent with specificity against cancer cells. In addition, we digested the synthesized product with trypsin and analyzed thus obtained peptide fragments by MALDI-TOF MS (Fig. 32). The peptides attributed to gelonin covered more than 60% of the amino acid sequence (Table 3). Five peptide sequences were identified carrying covalently bonded MTX. Thus, the exact bonding positions of MTX to the appropriate amino acids were K<sub>10</sub>, K<sub>27</sub>, K<sub>207</sub>, K<sub>251</sub> and R<sub>130</sub> (Table 4).

#### **4.2.3.1. MTX-conjugate is toxic to intact cells**

The MCF-7 cell growth inhibitory effect of MTX-gelonin was measured by the MTT assay (Fig. 33). We have demonstrated that a conjugate formed by covalently linking gelonin to MTX is a potent inhibitor of MCF-7 cell growth. It was found that ID<sub>50</sub> of conjugate in MCF-7 cells is 10 nM. In contrast, an unconjugated gelonin showed no detectable cell-growth inhibition when incubated with MCF-7 cells at 100 nM because the lack of toxicity of gelonin to intact cells. We infer that the lack of detectable cytotoxicity is due to lack of toxin cytosolic delivery.

In addition, MTX had also no detectable cell-growth inhibition when incubated with MCF-7 cells at 66 nM. This would be in line with another study (Vibet et al., 2007). However, Riebeseel et al., 2002 reported the ID<sub>50</sub> values for the MTX of 22 nM incubated for 7 days with MCF-7 cell lines. This can be explained by different incubation times. Our data suggest that the MCF-7 cell growth inhibitory effect of the conjugate is related to action of gelonin and not related to action of MTX.

The higher growth inhibition activity of MTX conjugate can be envisaged to be related to three different aspects: (a) cellular uptake, (b) intracellular gelonin release from the conjugate, and (c) the high ribosomal inhibitory effect of gelonin (Fig. 38).

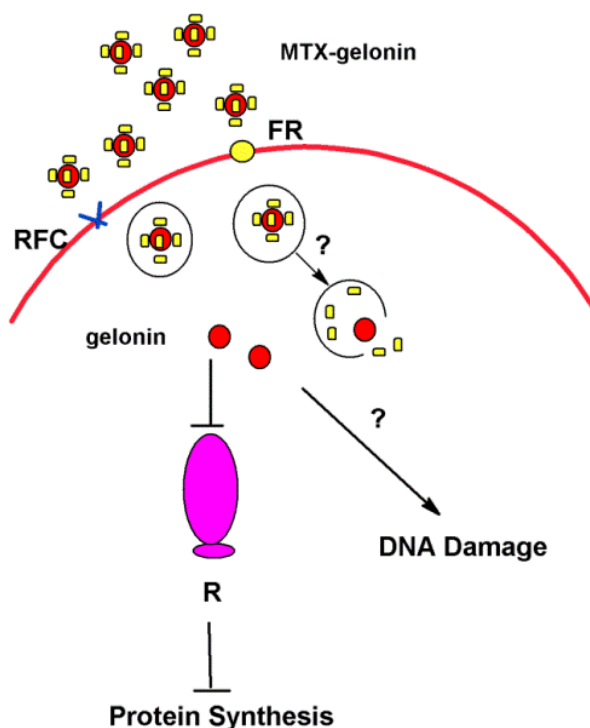


**Figure 38:** The expected mechanism of the growth inhibition activity of MTX-gelonin conjugate. FR, folate receptor; RFC, reduced folate carrier; R; ribosome.

Therefore, the folate receptor endocytosis is presumably responsible for cellular uptake of MTX-gelonin with subsequent lysosomal degradation to an active form of gelonin and MTX. The active form of gelonin exerts its action on the ribosome subunit, resulting in inhibition of protein synthesis, cell cycle alterations, and growth inhibition of tumor cells.

This hypothesis was supported by previous experimental results (Shen et al., 1981; Kralovec et al., 1989; Leamon et al., 1991; Atkinson et al., 2001; Kóczán et al., 2002) have shown that the mode of action of the MTX conjugates involves binding to the cell-surface, subsequent endocytic internalization, localization in the lysosomal system, and degradation by lysosomal enzymes to liberate the drug.

#### 4.2.3.2. Genotoxic effects of MTX-gelonin in MCF-7 cells

The comet assay is one of the most popular techniques for genotoxicity assessment. Moreover, it permits both qualitative and quantitative assessment of DNA damage at very low levels in any eukaryotic cell (Hartmann et al., 2003).

In the MCF-7 cell, MTX-gelonin induced distinct direct and oxidative DNA damage compared with the control or free gelonin (Fig. 34). Further, both gelonin and MTX do not have any effect on DNA, although the mechanism involved is not completely known. Gelonin has been shown to inhibit protein synthesis by specific irreversible damage to the 28S subunit of the ribosomal RNA. The damage to the protein synthesis pathway can subsequently cause mitochondrial stress by the loss of the mitochondrial membrane potential, oxidative stress and production of reactive oxygen species, finally leading to apoptosis (Narayanan et al., 2005). Previous reports (Narayanan et al., 2005) suggest that RIPs are also capable of inducing cell damage by apoptosis. Ricin has been shown to induce oxidative stress in mice (Kumar et al., 2003; Kumar et al., 2007; Muldoon et al., 1992), trichosanthin, a type I RIP, is able to generate high levels of ROS in human chorio-carcinoma cells (Zhang et al., 2001) and Shiga toxin has also be found to induce DNA lesions in human umbilical vein endothelial cells (Brigotti et al., 2002).

#### 4.2.3.3. Amino groups are involved in regulation of gelonin DNase and N-glycosidase activities

DNase activities of gelonin, MTX-gelonin, and MTX were determined using pUC18 as substrate (Fig.36). Experiments with gelonin indicated that it acts directly on DNA by introduction of selective cleavages into supercoiled covalently closed circular DNA molecules of pUC18 plasmid. These type I RIPs exhibit nuclease activity toward double-stranded DNA. Native plant gelonin exerts single- and double-stranded oligonucleotide degradation (Nicolas et al., 1997B; Nicolas et al., 1998; Nicolas et al., 2000). While, gelonin in the MTX-gelonin conjugate has no DNase activity. This study is in agreement with previous studies (Singh et al., 1989; Singh & Sairam, 1989; Singh et al., 2001) which reported that any modification of amino groups of gelonin leads to partial or complete loss of DNase activities compared to native gelonin.

In another experiment, we determined the biological activity of purified gelonin, MTX-gelonin, and MTX in the non-treated rabbit reticulocyte lysate system (Fig. 35). Conjugation of MTX to gelonin via amino modification results in an 11-fold decrease in activity of the toxin *in-vitro* translation assay. This study is in good agreement with previous studies (Brust et al., 1987) which reported that decrease of gelonin toxicity with increasing degree of modification by N-[4-(maleimidomethyl)-cyclohexylcarbonyoxy]succinimide and 2-iminotholane. The results in both experiments can be explained through binding of amino groups of gelonin with MTX resulting in loss of gelonin activity.

#### 4.2.3.4. The MTX $\alpha$ - and $\gamma$ -carboxyl groups are involved in MTX anti-folate activity

We also tested the effect of the conjugate on the DHFR activity. The conjugate was less effective against MTX target enzyme DHFR by about 20% (Fig. 37). Our result suggested that coupling of gelonin to  $\alpha$ - and  $\gamma$ -carboxyl groups of MTX could alter the binding affinity of MTX with DHFR, leading to partial loss of its anti-folate activity. Assessment of drug activity by the inhibition of dihydrofolate reductase showed some loss in the capacity of MTX to inhibit the enzyme when conjugated compared to an equi-molar amount of the free drug (Fig. 37). Such losses of dihydrofolate reductase inhibition have been reported previously when MTX was conjugated to several different macromolecules (Kulkarni et al., 1981; Deguchi et al., 1986; Fitzpatrick and Garnett et al., 1995), and is probably due to the interference of the MTX binding to the active site of the enzyme (Baker, 1969.) This result suggested that conjugation of a gelonin might alter the binding affinity of MTX with dihydrofolate reductase, leading to the partial loss of its anti-folate activity as compared to free MTX.

#### 4.2.4. Conclusion

An immunotoxin composed of gelonin, a basic protein of 30 kDa isolated from the Indian plant *Gelonium multiflorum* and the cytotoxic drug MTX has been studied as a potential tool of gelonin delivery into the cytoplasm of cells. Results of many experiments showed that, on the average, about 5 molecules of MTX were coupled to one molecule of gelonin. The MTX-gelonin conjugate is able to reduce the viability of MCF-7 cell in a dose-dependent manner ( $ID_{50}$ , 10 nM) as shown by MTT assay and significantly induce direct and oxidative DNA damage as shown by the alkaline comet assay. However, *in-vitro* translation toxicity MTX-gelonin conjugates have  $IC_{50}$ , 50.5 ng/ml which is less toxic than that of gelonin alone  $IC_{50}$ , 4.6 ng/ml. Also, the DNase activity test showed that gelonin loses of DNase activity compared to gelonin itself. It can be concluded that the positive charge plays an important role in the DNase activity as well as the N-glycosidase activity of gelonin. Furthermore, conjugation of MTX with gelonin through  $\alpha$ - and  $\gamma$ -carboxyl groups leads to the partial loss of its anti-folate activity compared to free MTX.

These results, taken together, indicate that conjugation of MTX to gelonin permits delivery of the gelonin into the cytoplasm of cancer cells and exerts a measurable toxic effect.

Finally, further experimental approaches are needed to

- Characterize the structural properties of MTX-gelonin conjugate in more details.
- Know how the MTX-gelonin conjugate exerts DNA damage inside the cell.
- Test anti-tumor properties of the MTX-gelonin conjugate *in vivo*.

### 4.3. Part C.

The SDS-PAGE analysis of *Gelonium* extract showed numerous bands which corresponded to different molecular weight proteins. Interestingly, two close bands appeared at 30 kDa and 31 kDa revealing two separate proteins (Fig. 40A). In order to identify these two proteins isolated from *Gelonium multiflorum* seeds, we needed to implement two steps: (1) peptide fragmentation by trypsin, and (2) peptide fragmentation by Arg-C.

The cleavage products were analyzed by MALDI-TOF and ESI ion-trap mass spectrometry (Esquire 3000<sup>+</sup>, Bruker Daltonics).

#### 4.3.1. Protein isolation and toxicity

##### 4.3.1.1. Gelonin isolation and purification

Gelonin (30 kDa) was isolated and purified from *Gelonium multiflorum* seeds by two methods as described in “Methods” (see 3.3.2).

For large scale, the first method by ion exchange chromatography was applied, where gelonin fractions were eluted, collected, dialyzed and concentrated. The gelonin purity was checked by means of SDS-PAGE (Fig. 40B) and its quantity estimated by means of the BCA assay. The total amount of gelonin isolated from 23 g seeds was about 56 mg. Upon concentrating the samples about 10% were lost.

Gelonin can also be isolated by gel filtration through a sephadex G75 column which was previously equilibrated with 10 mM Tris, 50 mM NaCl, pH 7.2. The gelonium extract was loaded on sephadex G75 column which resulted in two peaks (Fig. 39). The electrophoretic analysis of the first fraction on SDS-PAGE revealed two bands (31 kDa and 22 kDa) and the second fraction revealed a single band (30 kDa) (Fig. 40D). The fractions collected between 27-33 min contained pure gelonin.  $3.6 \pm 0.2$  mg of gelonin as isolated from 4 g of seed.

##### 4.3.1.2. GAP31 isolation and purification

The GAP31 was isolated and purified from *Gelonium multiflorum* seeds by the method as described in “Methods” (see 3.3.3). The purity of the sample was determined by means of SDS-PAGE (Fig. 40D) and the concentration by means of the BCA assay. The total amount of protein isolated from 4 g was 300  $\mu$ g.



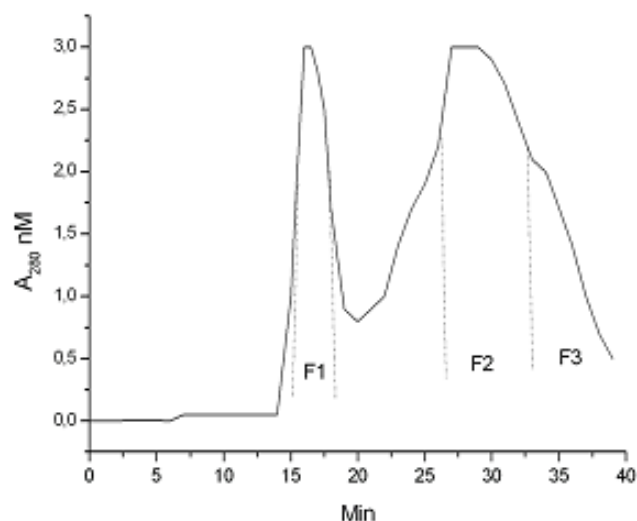


**Figure 39:** Sephadex G-75 column chromatography of *Gelonium* seed proteins. The homogenate (4 ml) was subjected to gel chromatography on a sephadex G-75 column (1.5 x 70 cm). The elution was performed with 10 mM Tris, 50 mM NaCl pH 7.2 at a flow rate of 2 ml/min. Three fractions were collected and checked by SDS-PAGE.

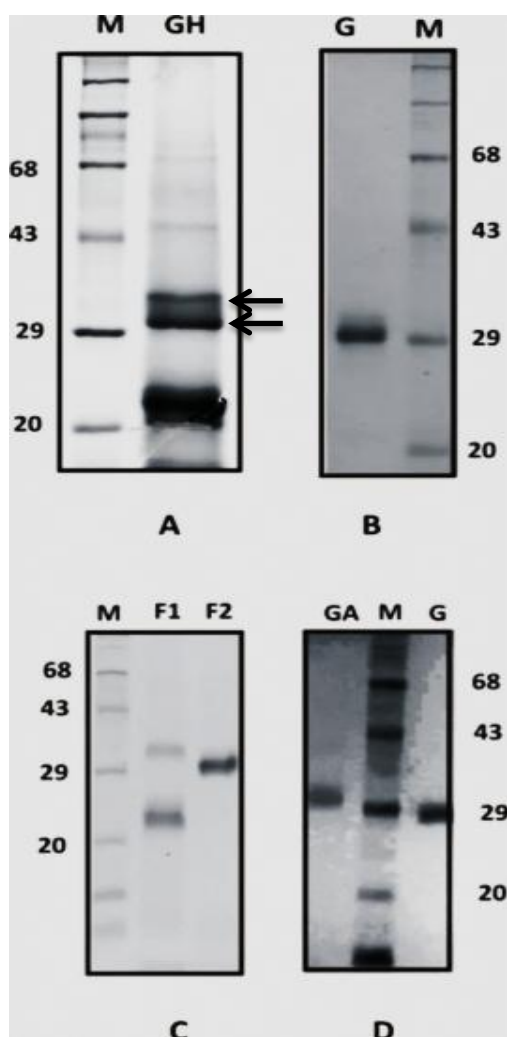


**Figure 40:** SDS-PAGE of (A) the *Gelonium multiflorum* homogenate. (B) Gelonin isolated by ion exchange column. (C) The fractions obtained by sephadex G-75 column. F1: GAP31 and 22kDa proteins, F2: gelonin. (D) Isolated proteins. GA: GAP31, M: marker, G: gelonin.

### 4.3.1.3. Protein synthesis inhibitory activity

To compare the N-glycosidase activity of the gelonin and GAP31 toxins, these materials were assayed by *in-vitro* protein translation in which [<sup>14</sup>C]-valine is incorporated into isolated rabbit reticulocytes. An inhibition curve for the GAP31 was compared to that of native gelonin. As shown in Fig. 41, the IC<sub>50</sub> values for the gelonin and GAP31 molecules were found to be 4.6 and 2 ng/ml, respectively.

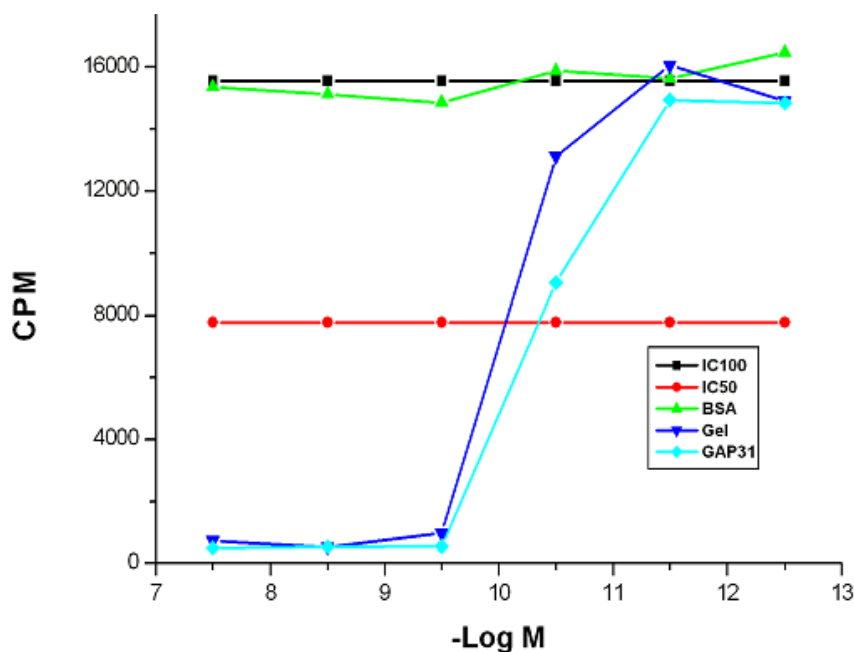


**Figure 41:** Inhibition of *in-vitro* translation by gelonin and GAP31. The incorporation of [<sup>14</sup>C]-valine into the nascent peptides was followed in a cell-free translation assay at various concentrations of gelonin and GAP31 with BSA as standard.

### 4.3.2. Peptide mapping

To determine the structural differences of gelonin and GAP31 amino acid compositions, 30 kDa and 31 kDa bands were enzymatically (trypsin and Arg-C) digested into peptides and subsequently compared with the Rosenblum and Huang primary structures, as reference peptide profile.

#### 4.3.2.1. In-gel tryptic gelonin digestion

The gelonin band of ~30 kDa (Fig. 40B) was excised and subjected to enzymatic digestion by trypsin as described in "Methods". The resulting peptide mixtures were analyzed by MALDI-TOF positive mode (Ultraflex MALDI-TOF-TOF, Bruker Daltonics). It was found that the observed peptides in the MALDI-MS spectra (Fig. 42 and Table 5) cover 78% of the gelonin

(Rosenblum sequence) amino acid sequence. Most notably, a signal at  $m/z$  1103.752 corresponding to the peptide sequence **N104-R113** (theoretical molecular mass, 1102.63 Da) was clearly detected in the spectrum of gelonin.

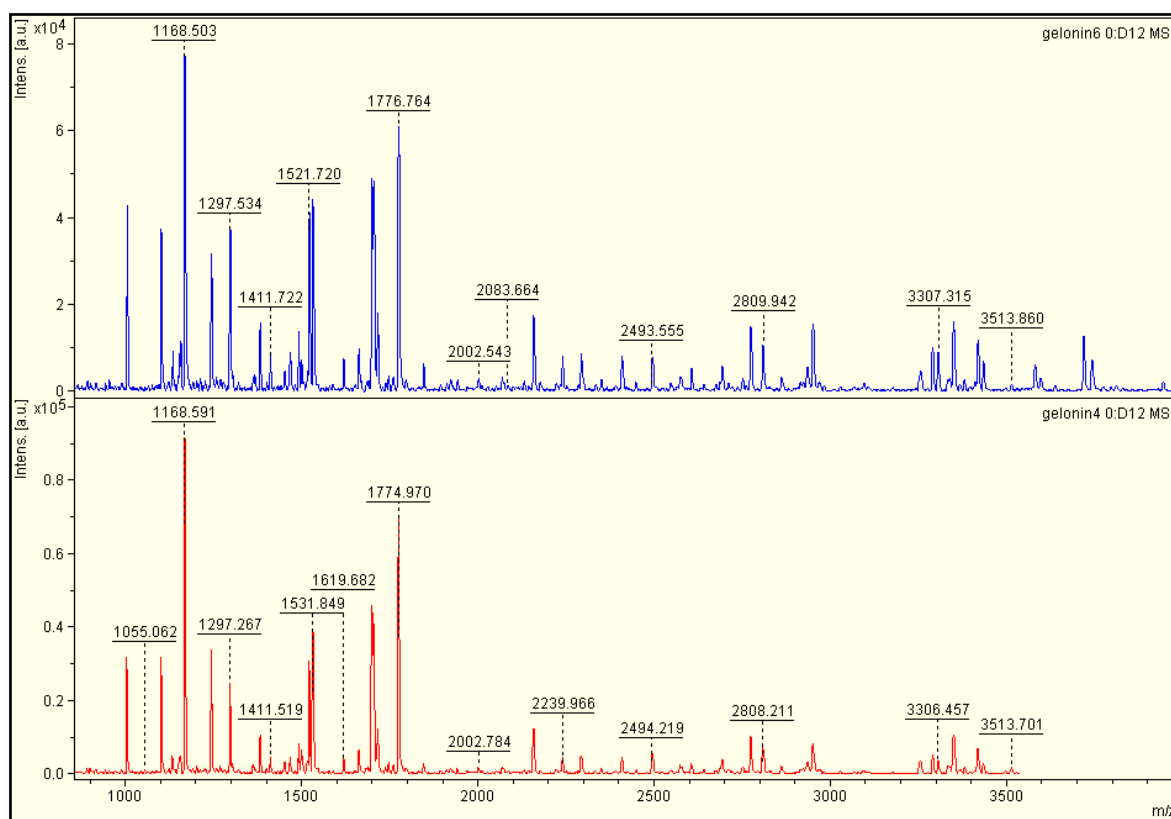


**Figure 42:** MALDI-MS TOF spectra display molecular ions  $[M + H]^+$  of peptides obtained after in-gel trypsin digestion of gelonin. An overall gelonin protein sequence coverage of 78% was obtained.

The characteristic ions (2170.1, 2493.55, 2659.1, and 2791.6) were recorded in the MALDI-MS mass spectrum. However, these observed peptide ions do not correspond to any theoretical (unmodified) tryptic peptides. So, we conclude that the measured mass of these fragments was increased due to modification with N-glycans (701, 1023, 1188, and 1351 Da) linked to N196 of  $^{192}\text{IRPAN}^{\text{Gly}}\text{NTISLENK}^{204}$  peptide. These ions were corresponding to the  $^{192}\text{IRPAN}^{\text{Gly}}\text{NTISLENK}^{204}$  peptide (theoretical molecular mass, 1469.8 Da) with sugar compositions  $\text{GlcNAc}_2\text{ManXyl}$ ,  $\text{GlcNAc}_2\text{Man}_3\text{Xyl}$ ,  $\text{GlcNAc}_2\text{Man}_4\text{Xyl}$ , and  $\text{GlcNAc}_2\text{Man}_5\text{Xyl}$ , respectively.

To confirm further the identity of the peptides, the gelonin (30 kDa) band was subjected to an in-gel tryptic digestion, and the resulting peptide mixtures were analyzed by ESI-MS positive mode. The peptides attributed to gelonin (Rosenblum sequence) covered 53% of the amino acid sequence (Fig. 43, Table 6). Interestingly, a signal at  $m/z$  1105 corresponding to peptide sequence **N104-R113** was observed in the spectrum of gelonin. As well as, the presence of an abundant doubly charged  $[M + 2H]^{+2}$  peptide ion at  $m/z$  1247.4 that does not match any

calculated values. So, we assumed that these signal matches perfectly with the glycosylated-peptide sequence  $^{192}\text{IRPAN}^{\text{Gly}}\text{NTISLENK}^{204}$ , where the theoretical mass of the peptide **I192-K204** is 1469.8 and the mass difference 1023 corresponds to the glycosylation motif GlcNAc<sub>2</sub>Man<sub>3</sub>Xyl linked to N196 of gelonin, respectively. A signal at  $m/z$  2681.3 was observed which indicated peptide **I192-K204** with a glycosylation motif GlcNAc<sub>2</sub>Man<sub>4</sub>Xyl + Na (1211 Da).

Although, the gelonin sequence has two potential sites for glycosylation N81 and N196, the ESI spectra showed the peak  $[M + 3H]$  at  $m/z$  964.7 which correspond to peptide sequence **N81-K87**. This peak has the theoretical  $m/z$  value of 961.4. This proves that the glycosylation modification is not located at N81.

**Table 5:** Assignment of peaks from Trypsin cleavage of gelonin (MALDI analysis)

Peptides	position	observed	calculated
NFQQR	186-191	806.637	806.3904
NPLLFGGKTR	104-113	1103.752	1102.636
FTFIENQIR	177-185	1168.503	1167.346
ETDLGIEPLR	131-141	1244.570	1243.395
YYVTAVDQVKPK	88-99	1297.534	1296.415
DAPDAAEGLFK	235 -246	1411.722	1410.651
LHFGGSYPSLEGEK	114-127	1521.720	1520.679
LKPEGNSHGIPLLR	28-41	1531.929	1530.875
KYYVTAVDQVKPK	234-246	1538.314	1538.857
TSGANGM(Oxidation)FSEAVELER	214-229	1714.429	1713.774
VKLPPEGNSHGIPLLR	26-41	1758.478	1758.038
GATYITYVNFLNELR	11-25	1774.721	1773.917
TRLHFGGSYPSLEGEK	112-127	1776.764	1777.886
LHFGGSYPSLEGEKAYR	114-130	1910.708	1910.939
GATYITYVNFLNELRVK	11-27	2002.543	2001.335
TSGANGM(Oxidation)FSEAVELERANGK	214-233	2083.664	2083.971
IRPANNTISLENK	192-204	2493.555	1470.678
GLDTSVFSTKGATYITYVNFLNELR	1-25	2809.942	2809.440
LDENAIIDNYKPTIEASSLLVVIQM(Oxidation)VSEAAR	147-176	3307.315	3305.767
CFVLVALSNDNGQLAEIAIDVTSVYVVGQYQVR	49-80	3513.860	3512.809
Carbamidomethyl			

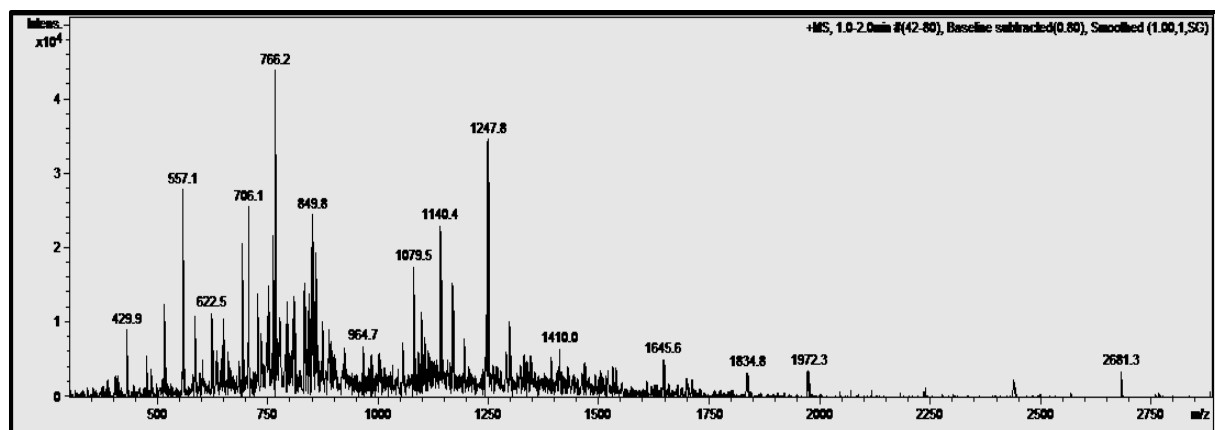


**Figure 43:** ESI-MS spectrum, in positive mode, of gelonin peptides obtained by in-gel tryptic digestion.

**Table 6:** Assignment of peaks from in-gel tryptic cleavage of gelonin (ESI analysis)

Sequence	Position (Rosenblum)	( <i>m/z</i> ) <sub>exp</sub>	charge	( <i>m/z</i> ) <sub>cal</sub>
IALLK	247-251	557.3	1+	557.4
FTFIENQIR	177-185	1167.3	1+	1167.4
YYVTAVDQVKPK	88-99	1296.3	1+	1296.6
SYFFK	83-87	691.2	1+	691.3
LKPEGNSHGIPLLR	28-41	765.8	2+	1530.6
NNFQQR	186-191	807.8	1+	806.3
FVDKDPE	252-258	849.3	1+	849.3
TSGANGM=OFSEAVELER	214-229	856.4	2+	1713.7
GATYITYVNFLNELR	11-25	887.7	2+	1773.9
LHFGGSYPSLEGEK	114-127	761.2	2+	1521.6
NRSYFFK	81-87	964.4	1+	962.2
IRPAN(Gly)NTISLENK	192-204	1247.7	2+	1470.6
NPLLFGGKTR	104-113	1105.5	1+	1103.3
YYVTAVDQVKPK	235-246	706.2	2+	1411.6

#### 4.3.2.2. In-gel tryptic GAP31 digestion

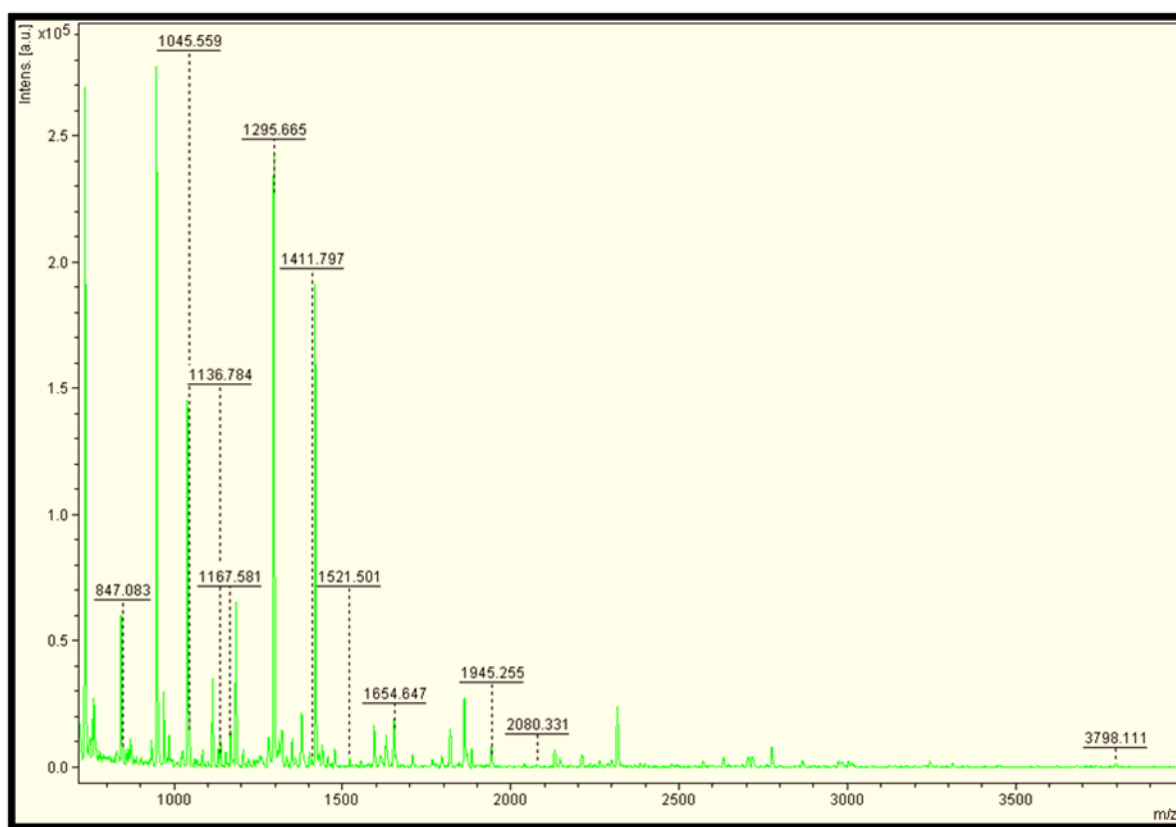
In a separate experiment, the 31 kDa band (Fig. 40D) was excised and subjected to enzymatic digestion by trypsin. The masses of the peptide fragments from each digest set were measured by MALDI as well as ESI mass spectrometry.

In a MALDI spectrum (Fig. 44) we were able to identify 20 different peptides derived from in-gel tryptic cleavage of 31 kDa (GAP31) which correspond to theoretical tryptic peptides of the GAP31 sequence (Huang et al. 1999) (Tab. 7). These peptides were attributed to cover 70% of the amino acid sequence (Fig. 46). Interestingly, a signal appeared at *m/z* 734.411 corresponding to the peptide sequence **N101-R106**. This peptide missed eight amino acids

(NPLLFGGK) which were observed in the MALDI spectra of gelonin. A signal at  $m/z$  3798.111 was observed. However, this observed peptide signal does not correspond to any calculated values. So, we assumed that the mass of this fragment peak corresponded to the peptide sequence **I185-K197**. The mass difference ( $m/z$  2329) indicates the mass of the glycosylation motif on N189.

ESI-MS spectra from GAP31 (trypsin-digest) are shown in Fig. 45, and the observed fragments are listed in Table 8. Ten peptides could be identified in the theoretical digest of the predicted 31 kDa protein. These peptides were found to cover 36% of the amino acid sequence (Fig. 46).

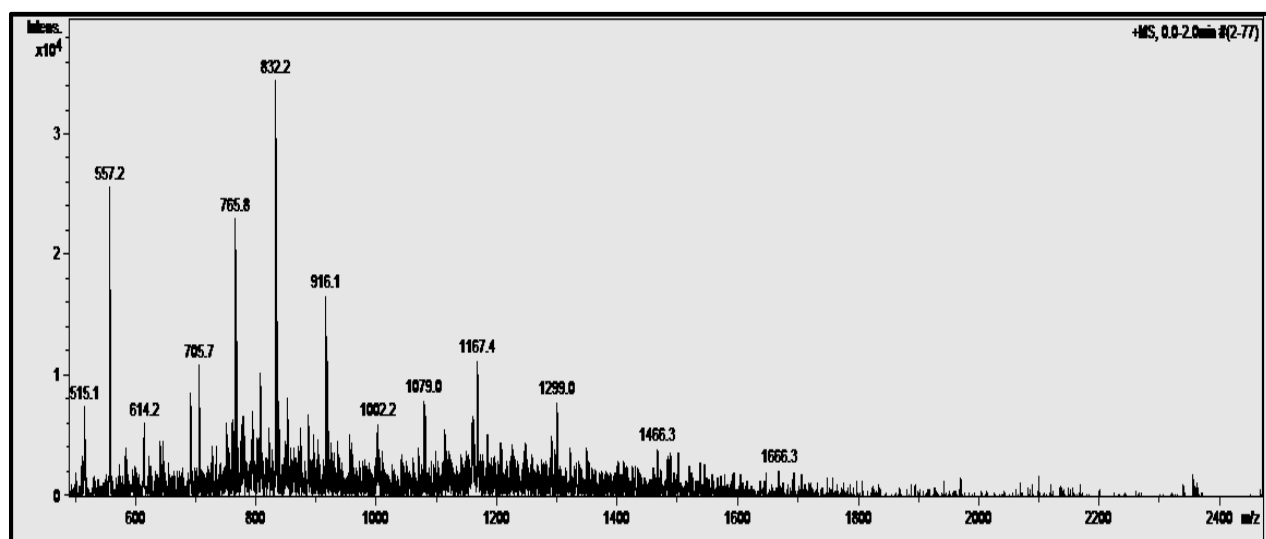
The GAP31 sequence has two potential sites for glycosylation N82 and N189. The MALDI spectra showed the peak  $[M + H]^+$  at  $m/z$  962.04 which is corresponding to peptide sequence **N82-K88**. This peak had a theoretical  $m/z$  value of 961.4. This proved that the glycosylation modification is not located at N82, and N-glycosylation is at N189.



**Figure 44:** MALDI-MS TOF spectra display molecular ions  $[MH]^+$  of peptides obtained after in-gel trypsin digestion of GAP31. Overall GAP31 protein sequence coverage of 70% was obtained.

**Table 7:** Assignment of peaks from trypsin cleavage of GAP3 (MALDI-MS analysis).

Peptides	Position	Observed	Calculated
NTIKTR	101-106	734.411	732.863
KCDDPGK	43-49	762.094	762.345
FVDKDPK	245-251	847.083	848.451
NRSYFFK	82-88	962.432	961.489
IALLKFVDK	240-248	1045.559	1046.660
GLDTSVFSFK	1-10	1055.419	1054.179
WGKLSFQIR	198-206	1136.784	1135.362
FTFIENQIR	170-178	1167.581	1166.615
IRPANNTISLENK	185-197	3798.111	1470.678
ETDLDGIEPLR	124-134	1244.666	1243.652
DAPDAAYEGLFK	89-100	1295.665	1296.610
YYVTAVDQVKPK	228-239	1411.797	1410.651
LHFGGSYPSLEGEK	107-120	1521.501	1520.679
LKPEGNSHGIPLLR	28-41	1531.654	1530.809
AYRETTDLGIEPLR	121-134	1633.464	1633.854
ETDLDGIEPLRIGIK	124-138	1654.647	1654.937
LKPEGNSHGIPLLRK	28-42	1659.306	1658.984
TSGANGM(Oxidation)FSEAVELER	207-222	1711.488	1713.774
GATYITYVNFNLNR	11-25	1773.370	1773.917
TRLHFGGSYPSLEGEK	105-120	1779.613	1777.974
YYVTAVDQVKPKIALLK	228-244	1945.255	1949.147
TSGANGM(Oxidation)FSEAVELERANGK	207-226	2080.331	2083.971

**Figure 45:** ESI-MS spectrum, in positive mode on an ESI ion-trap MS, of GAP31 peptide obtained by in-gel tryptic digestion.

**Table 8:** Assignment of peaks from in-gel tryptic cleavage of GAP31 (ESI analysis)

Sequence	Position	(m/z) <sub>exp</sub>	charge state
IALLK	240-244	557.2	1+
ETTDLGIEPLR	124-134	622.3	2+
YYVTAVDQVKPK	228-239	705.7	2+
NTIKTR	101-106	733.4	1+
LSFQIR	201-206	765.8	1+
NNFQQR	179-184	807.8	1+
GATYITYVNFNLNLR	11-25	887.2	2+
GLDTVSFSTK	1-10	1053.5	1-
FTFIENQIR	170-178	1167.4	1+
DAPDAAYEGLFK	89-100	1299.0	1+

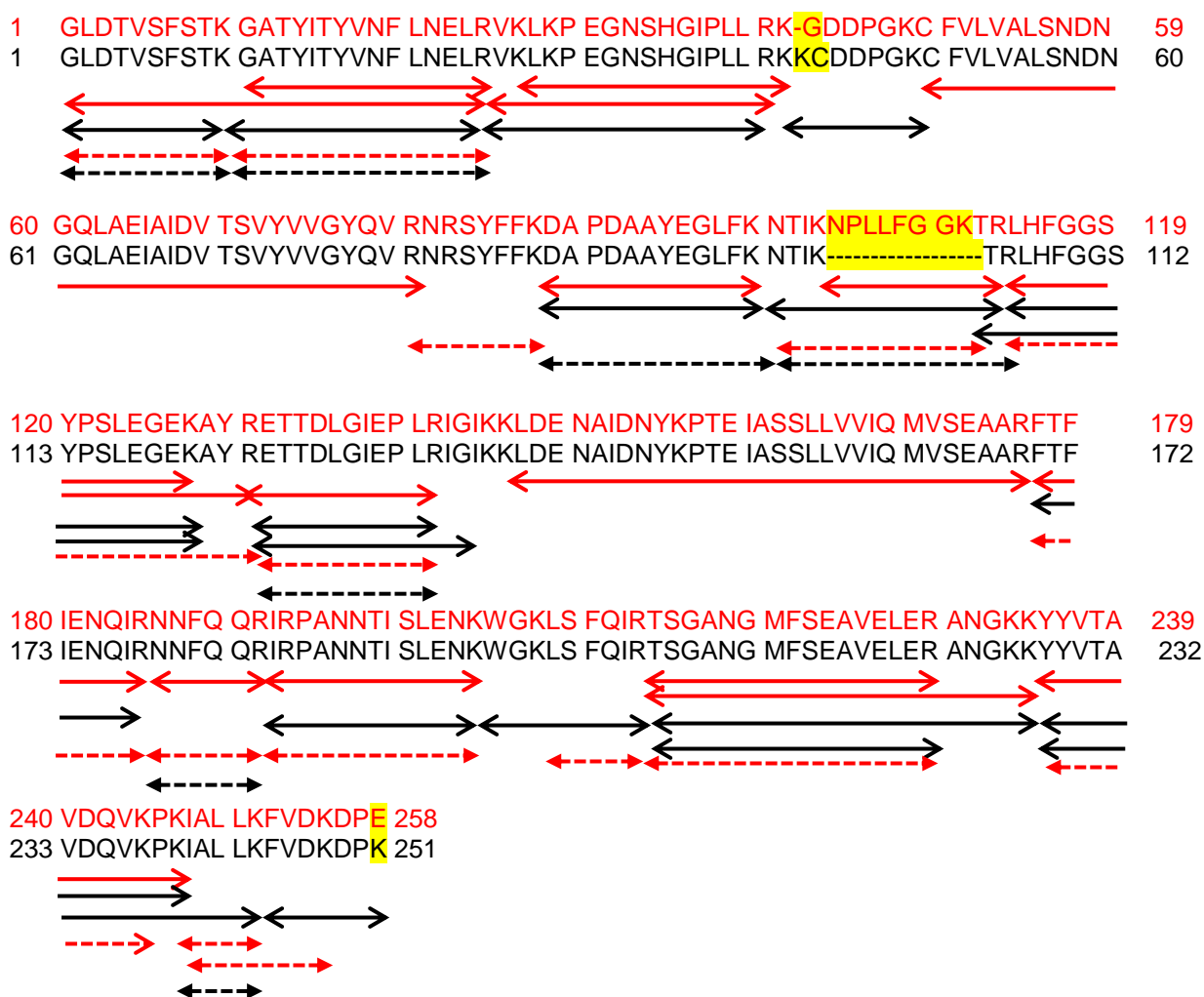


**Figure 46:** Overview of peptides generated by in-gel tryptic cleavage of gelonin (top) and GAP31 (bottom) and indicated beneath the sequences. Red arrows, peptides resulting from specific cleavage of gelonin with trypsin showed in MALDI spectra (  $\leftrightarrow$  ) and ESI spectra (  $\leftarrow\text{---}\rightarrow$  ). Black arrows, peptides resulting from specific cleavage of GAP31 with trypsin showed in MALDI spectra (  $\leftrightarrow$  ) and ESI spectra (  $\leftarrow\text{---}\rightarrow$  ).



### 4.3.2.3. In-gel Arg-C digestion of gelonin

Because the tryptic peptides are very short, we performed additional experiments with Arg-C before and after PNGase F treatment. Arg-C cleaves peptide bonds at the carboxyl side of arginine resulting in a limited number of fragments, while PNGase F is an amidase that hydrolyzes nearly all types of N-glycan chains from glycopeptides/proteins.

The 30 kDa band was excised, destained, digested with Arg-C and analyzed by MALDI-TOF. The resulting peptide mass spectra (Fig. 47A) matched the theoretical peak mass predicted by MS-digest software (Table 9) and provided 73% of total sequence coverage (Fig. 48). Interestingly, a signal at  $m/z$  3779 corresponding to peptide sequence **N81-R113** was observed only in the spectrum of gelonin. These data suggest that gelonin (Rosenblum) has 258 aa and is unglycosylated at N81. The molecular ions at  $m/z$  2741.14 and 3342.83 were observed. However, these observed peptide signals do not correspond to any calculated values. So, we assumed that the practically measured masses of these fragments were increased due to N-glycan modification at N196 and corresponded to the glycosylated-peptide sequence **P194-R213** (calculated  $m/z=2316.64$ ) plus, 425 and 1025.93, respectively.

In a second experiment, gelonin was treated with PNGase F, digested with Arg-C and analyzed by MALDI-TOF. MS spectra are shown in Fig. 47B, and the observed fragments are listed in Table 9. 66% of the amino acid sequence coverage was obtained (Fig. 48). The signals at  $m/z$  3318.11, 3610.36, and 3772.5 disappeared and were replaced by  $m/z$  2588.54 which corresponded to the peptide sequence **I192-R213**. The mass differences indicate the masses of the glycosylation motifs on N196.

**Table 9:** Assignment of peaks from Arg-C cleavage of gelonin (A) glycosylation (B) following deglycosylation by PNGase F

Peptide	Position	Observed A	Calculated	Observed B
NNFQQR	186-191	806.466	806.390	806.542
FTFIENQIR	177-185	1167.838	1167.615	1168.323
ETDLGIEPLR	131-141	1243.467	1243.652	1244.183
TSGANGM(=O)FSEAVELER	214-229	1714.078	1714.859	-----
VKLLKPEGNSHGIPLLR	26 -41	1758.280	1758.038	1759.128
LHFGGSYPSLEGEKAYR	114-130	1910.423	1910.939	1911.898
FTFIENQIRNNFQQR	177-191	1955.592	1954.988	-----
GLDTVSFSTKGATYITYVNFNLNLR	1 -25	2809.263	2809.440	2811.078
PAN(GLY)NTISLENKWKLSFQIR	192- 213	3318,11	2316.641	2318.651
NRSYFFKDAPDAAYEGLFKNTIKNPLLFGGKTR	81 -113	3779.357	3778.944	3779.842
IGIKKLDENAIIDNYKPTEIASSLLVVIQM(=O)VSEAAAR	142-176	3846.690	3845.072	3846.516

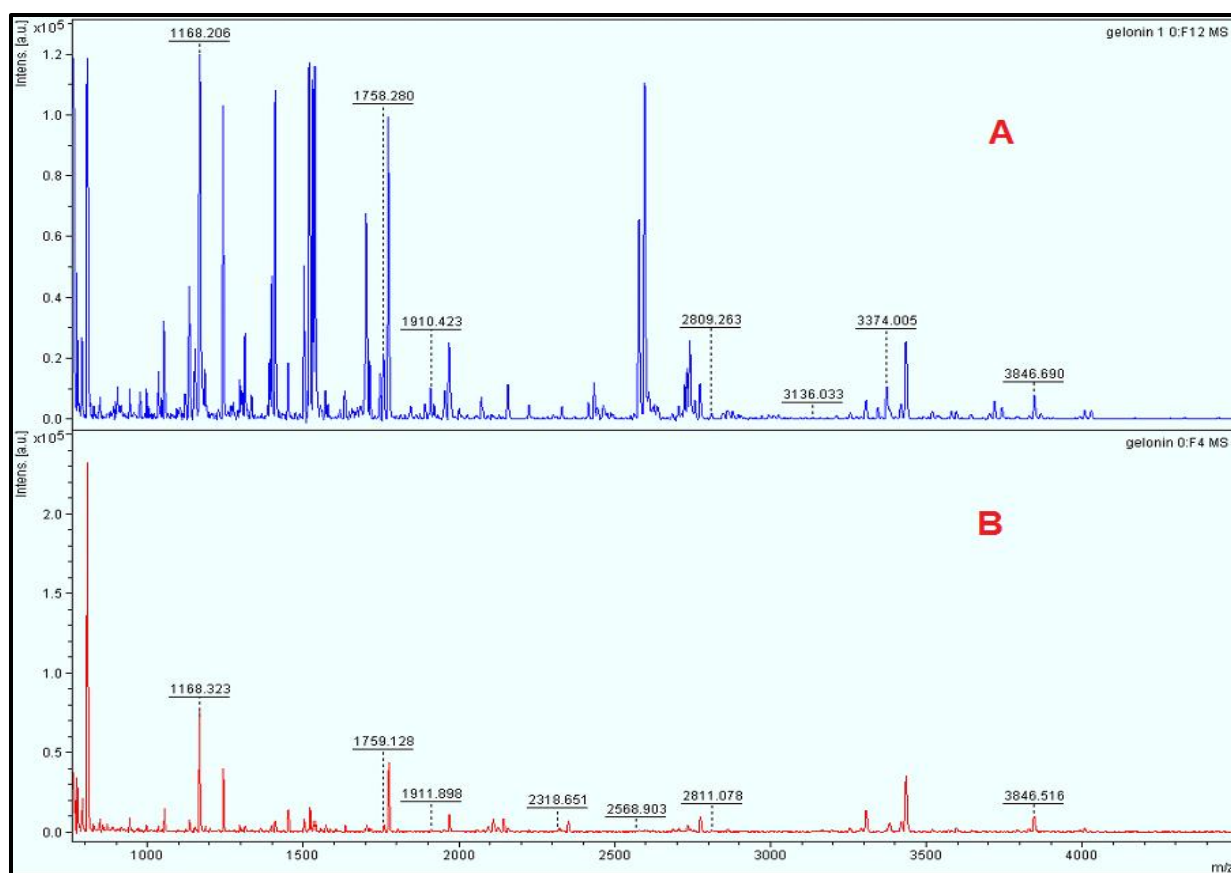


**Figure 47:** MALDI-MS TOF spectra display molecular ions [M<sup>+</sup>] of peptides obtained after in-gel Arg-C digestion of gelonin (A) glycosylation, and (B) following deglycosylation by PNGase F.

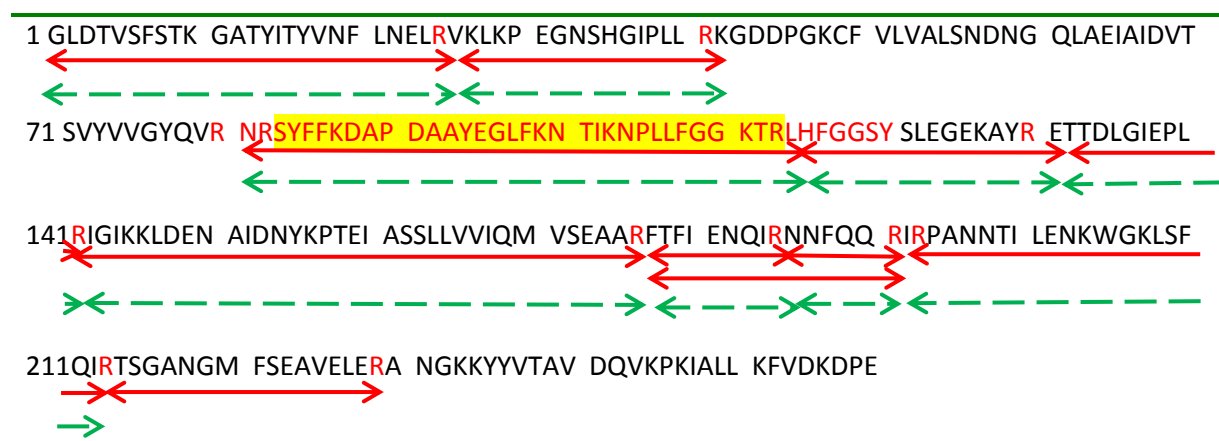


**Figure 48:** Overview of peptides generated by in-gel digestion of gelonin with Arg-C. (Red arrows, peptides resulting from specific cleavage of intact gelonin with Arg-C; and green arrows, peptides resulting from specific cleavage of gelonin with Arg-C following PNGase F deglycosylation).

#### 4.3.2.4. In-gel Arg-C digestion of GAP31

GAP31 (~31kDa) protein bands were excised, destained, digested with Arg-C and analyzed with MALDI. MS spectra are shown in Fig. 49A, and the observed fragments are listed in Table 10. 66% of the amino acid sequence coverage was obtained (Fig. 50). Interestingly, there was a single peak at  $m/z$  2683.168 corresponding to the peptide sequence **S84-R106**. This peptide is missing the eight-amino acid sequence (**NPLLFGGK**) that is present in the corresponding Arg-C peptide (**S83-R113**) which is observed in gelonin.

In a second experiment, GAP31 was treated with PNGase F, digested with Arg-C, and analyzed with MALDI. MS spectra are shown in Fig. 49B, and the observed fragments are listed in Table 10. 60% of the amino acid Sequence coverage was obtained (Fig. 50). The molecular ion at  $m/z$  2320.841, corresponding to the deglycosylated peptide **P187-R206** (theoretical molecular mass, 2320.841Da), was clearly detected.

**Table 10:** Assignment of peaks from Arg-C cleavage of GAP31 (A) glycosylation (B) following deglycosylation by PNGase F

Peptide	Position	Observed A	Calculated	Observed B
NNFQQR	179-184	806.869	806.390	806.686
FTFIENQIR	170-178	1167.895	1167.615	1167.884
ETDLGIEPLR	124-134	1243.616	1243.652	1243.954
TSGANGMFSEAVELER	207-222	1697.846	1697.779	1697.904
TSGANGM(=O)FSEAVELER	207-222	1713.392	1713.774	1713.990
VKLPPEGNSHGIPLLR	26-41	1758.431	1758.038	1758.259
LHFGGSYPSLEGEKAYR	107-123	1910.757	1910.939	1911.876
SYFFKDAPDAAYEGLFKNTIKTR	84-106	2683.168	2682.356	2683.261
GLDVSFSTKGATYITYVNFNLNLR	1-25	2809.414	2809.440	-----
IGIKLDENAIIDNYKPTIASSLLVVIQM(=O)VSEAAR	135-169	3845.665	3845.072	3845.379
PAN(Gly)NTISLENKWGKLSFQIR	185-206	4974.091	2316.641	2317.841

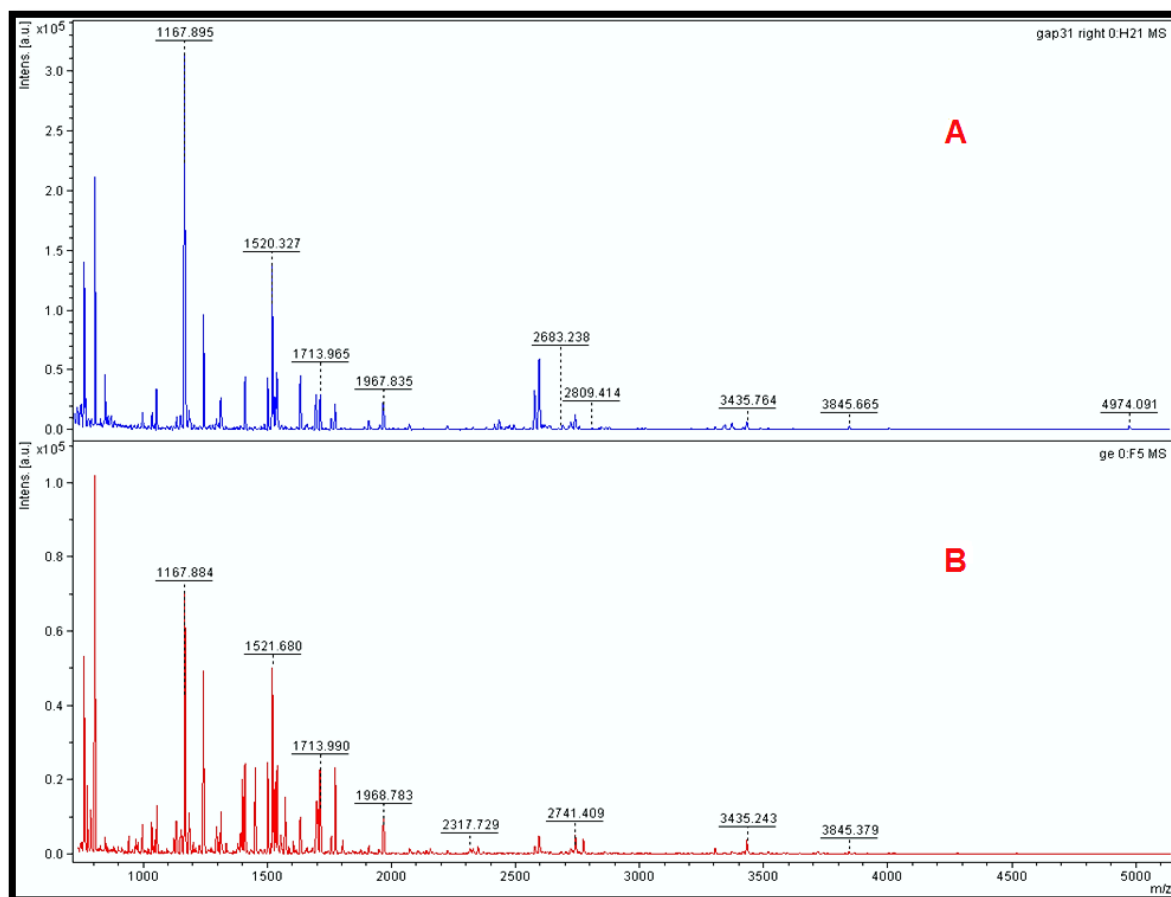


**Figure 49:** MALDI-MS TOF spectra display molecular ions [M] of peptides obtained after in-gel Arg-C digestion of GAP31 (A) glycosylation, and (B) following deglycosylation by PNGase F

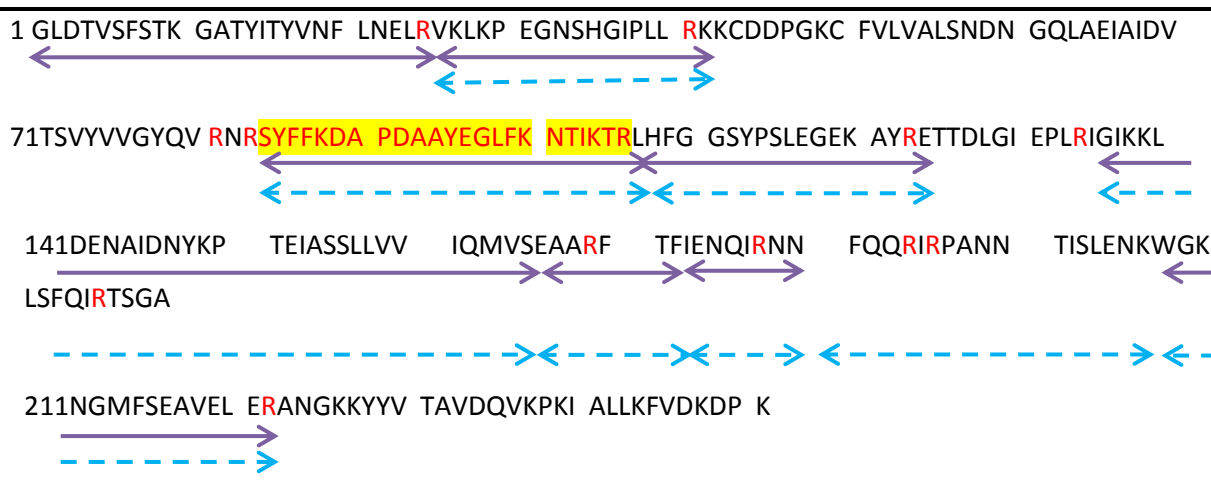


**Figure 50:** Overview of peptides generated by in-gel digestion of GAP31 with Arg-C. (Violet arrows, peptides resulting from specific cleavage of intact GAP31 with Arg-C; and blue arrows, peptides resulting from specific cleavage of GAP31 with Arg-C following PNGase F deglycosylation).

### 4.3.3. ESI-MS characterization of proteins

Gelonin was initially analyzed under acidic electrospray mass spectrometry conditions, in a 1:1 methanol:water solution with 1% acetic acid. The predominant mass spectrum of positive ions is shown in Figure 51A, where multiply charged protein ions were observed in the range 700-1600 upon ESI of gelonin. Whereas, the signals in the region  $m/z$  100-400 were observed (singly charged). They are most probably due to peptides that originate from the gelonin fragmentation process.

From the ESI-spectrum we can conclude that there are at least 3 different species (A, B, and C). These species are most likely different glycoforms of gelonin. The results for the three species are displayed below: Deconvolution (“de-charging”) of the spectrum gave a protein molecular weight (MW) of  $29850.79 \pm 0.45$ ,  $30013.41 \pm 0.67$  and  $30175.6 \pm 1.08$  Da, which is in good agreement with the theoretical MW of gelonin with different glycosylation patterns (Fig. 52). As shown in Tables. 11, 12 and 13, the masses are significantly higher than the most abundant mass calculated for gelonin amino acid sequences (Rosenblum = 28825.12 g/mol). This result implies that different post-translational modifications are attached to gelonin. These modifications are probably sugar residues since it was shown that gelonin contains mannose, glucosamine, and xylose (Daubenfeld et al., 2005). The mass difference between A and B or B and C of about 163 g/mol are probably due to one additional molecule of mannose attached to the protein.

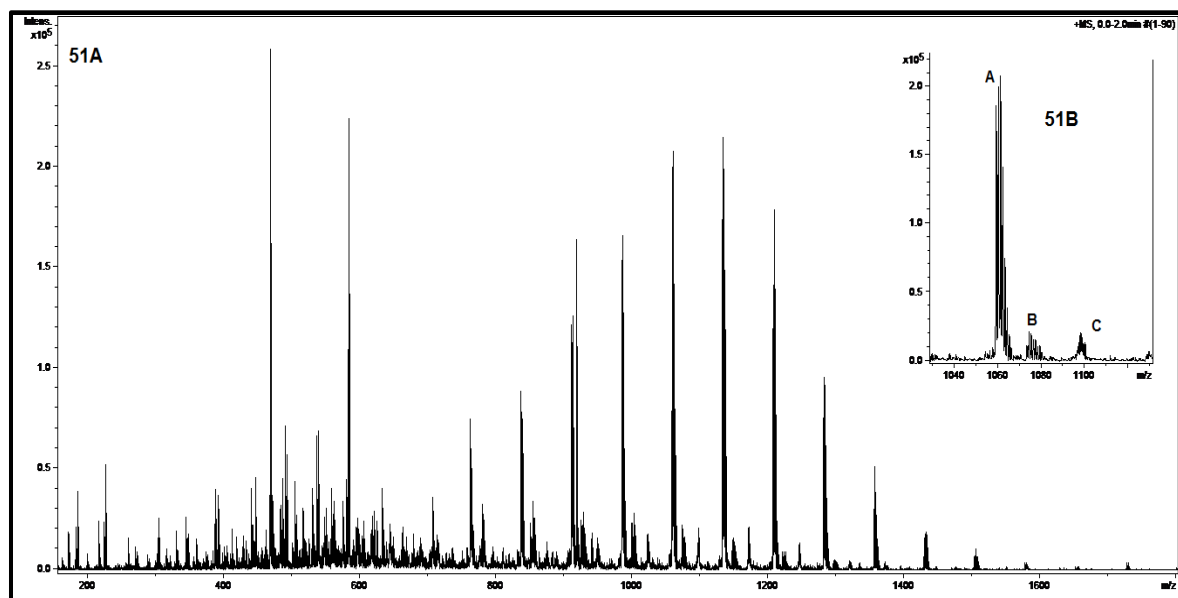


**Figure 51:** ESI-MS of gelonin (51A) and Enlargement of charge state  $28^+$  (51B).

**Table 11:** The most abundant masses of gelonin species A

<i>m/z</i>	<b>n<sub>1</sub> (calc.)</b>	<b>n<sub>1</sub></b>	<b>M / g mol<sup>-1</sup></b>
996.59	29.98	30	29850.77
1030.64	28.99	29	29851.32
1067.11	28.00	28	29851.08
1106.53	27.00	27	29849.31
1149.2	25.99	26	29850.9
1194.16	25.01	25	29852.86
1244.67	24.00	24	29848.08
1299.33	22.99	23	29851.2
1358.2	21.99	22	29851.61

**Table 12:** The most abundant masses of gelonin species B

<i>m/z</i>	<b>n<sub>1</sub> (calc.)</b>	<b>n<sub>1</sub></b>	<b>M / g mol<sup>-1</sup></b>
910.57	32.99	33	30013.08
938.18	32.02	32	30017.88
969.11	31.00	31	30011.41
1001.19	30.00	30	30012.7
1037.63	28.95	29	30013.55
1072.67	28.00	28	30013.19
1112.87	26.99	27	30009.37
1154.14	26.02	26	30016.23
1201.59	24.99	25	30014.75
1251.76	23.99	24	30011.99
1305.93	23.00	23	30013.39

**Table 13:** The most abundant masses of gelonin species C

<i>m/z</i>	<b>n<sub>1</sub> (calc.)</b>	<b>n<sub>1</sub></b>	<b>M / g mol<sup>-1</sup></b>
888.18	34.01	34	30172.99
915.21	33.00	33	30168.93
945.94	31.93	32	30181.38
974.66	30.99	31	30174.7
1007.14	29.99	30	30175.14
1041.76	28.99	29	30175.8
1079.24	27.98	28	30179.94
1118.78	26.99	27	30175.59
1162.09	25.98	26	30176.73
1208.19	24.99	25	30174.92

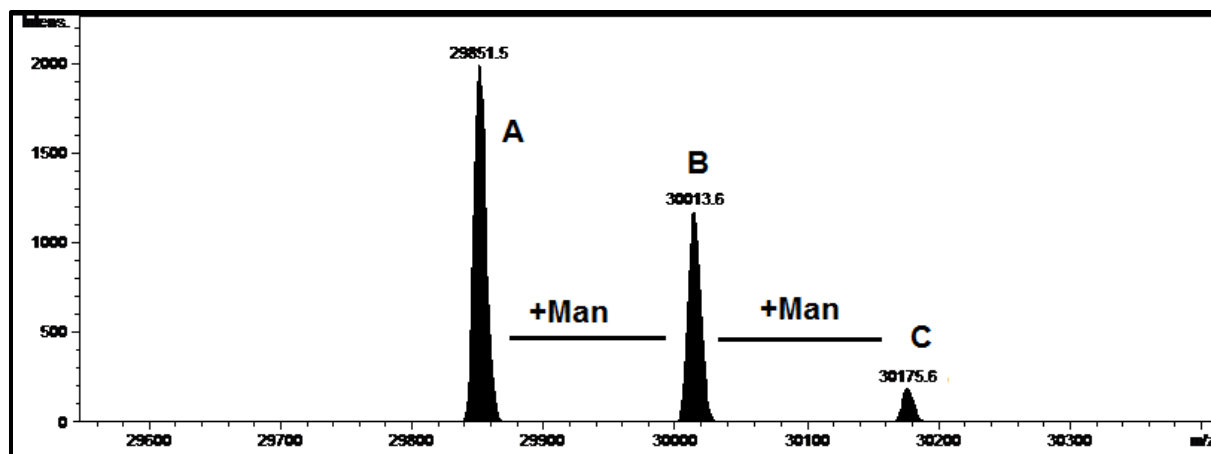
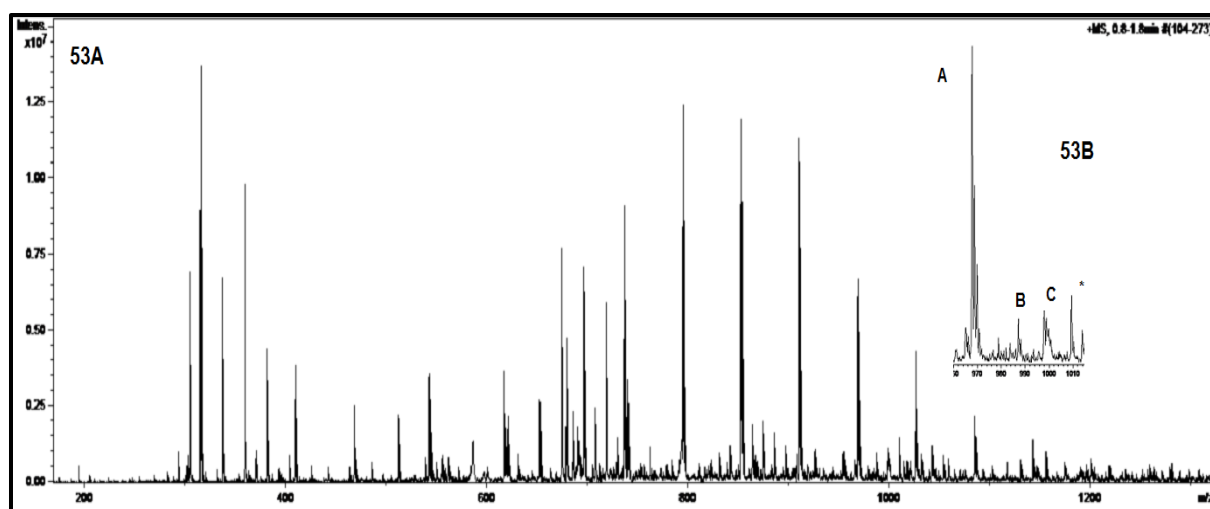


Figure 52: Deconvolution spectrum of Gelonin

Table 14: Composition and molecular masses of gelonin species as observed in the mass spectra

species	structure	Composition	MS <sub>exp</sub> /Da	MS <sub>calc</sub> /Da
A	Gel-GlcNAc <sub>2</sub> Man <sub>3</sub> Xyl	C <sub>1339</sub> H <sub>2116</sub> N <sub>351</sub> O <sub>414</sub> S <sub>3</sub>	29850.79±0.45	29851.4
B (A+Man)	Gel-GlcNAc <sub>2</sub> Man <sub>4</sub> Xyl	C <sub>1345</sub> H <sub>2126</sub> N <sub>351</sub> O <sub>419</sub> S <sub>3</sub>	30013.41±0.67	30013.6
C (A+2Man)	Gel-GlcNAc <sub>2</sub> Man <sub>5</sub> Xyl	C <sub>1351</sub> H <sub>2136</sub> N <sub>351</sub> O <sub>424</sub> S <sub>3</sub>	30175.60±1.08	30175.77

In another experiments, GAP31 was also analyzed under acidic electrospray mass spectrometry conditions, in a 1:1 methanol:water solution with 1% acetic acid. The ESI mass spectrum of positive ions is shown in Figure 53, where multiply charged protein ions were observed in the range 600-1200. From the ESI-spectrum we can conclude that there are at least 3 different species (A, B, and C). These species are most likely different glycoforms of GAP31. The deconvoluted mass obtained over several charge states was shown to be 29697.02±1.13, 30624.20±1.15, and 31083.40±1.9 Da, which is in excellent agreement with the theoretical MW of GAP31 with different glycosylation patterns (Fig. 54, Table 18). As shown in Tables. 15, 16 and 17, the masses are significantly higher than the most abundant masses calculated for the GAP31 amino acid sequence (Huang = 28173.4 g/mol).



**Figure 53:** ESI-MS of GAP31 (concentrated and dialyzed).

**Table 15:** The most abundant masses of GAP31 species A

$m/z$	$n_1$ (calc.)	$n_1$	$M / g \text{ mol}^{-1}$
849.8	34.98	35	29699.51
874.2	34.01	34	29697.53
901.1	32.99	33	29697.9
929.1	31.99	32	29697.34
959.1	30.99	31	29697.27
990.3	30.02	30	29698.79
1025.2	28.99	29	29701.8
1061.4	28.00	28	29691.2
1100.7	27.00	27	29691.9

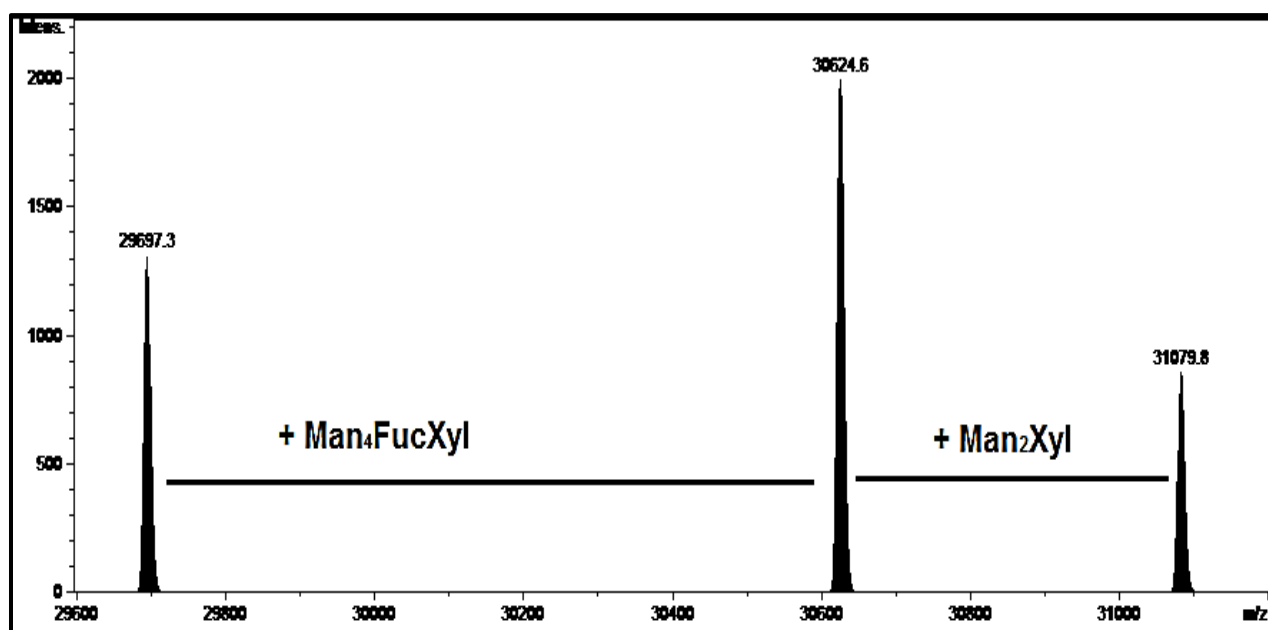
**Table 16:** The most abundant masses of GAP31 species B

$m/z$	$n_1$ (calc.)	$n_1$	$M / g \text{ mol}^{-1}$
766.6	40.00	40	30624
786.1	39.00	39	30618.9
807	37.99	38	30628
828.9	36.99	37	30632.3
851.9	35.99	36	30623.89
875.7	35.01	35	30623.25
901.1	34.02	34	30621.4
929.1	32.99	33	30627.3
958	32.00	32	30624
988.1	31.02	31	30619.84
1021.1	30.02	30	30623.4



**Table 17:** The most abundant masses of GAP31 species C

$m/z$	$n_1$ (calc.)	$n_1$	$M / \text{g mol}^{-1}$
798	38.99	39	31083
818.9	38.00	38	31080.2
841.4	36.98	37	31094.8
864.2	36.00	36	31075.2
889.1	34.99	35	31083.5
915	34.00	34	31076
943.1	32.99	33	31089.3
972.3	31.99	32	31081.6
1003.4	31.00	31	31074.4
1037.4	29.98	30	31092
1073.1	28.99	29	31090.9
1111	28.00	28	31080

**Figure 54:** Deconvoluted spectrum of GAP31**Table 18:** Composition and molecular masses of GAP31 species (ESI-MS spectra)

species	structure	Composition	$MS_{\text{exp}}/\text{Da}$	$MS_{\text{calc}}/\text{Da}$
A	GAP31-GlcNAc <sub>2</sub> Man <sub>6</sub> Fuc	C <sub>1326</sub> H <sub>2105</sub> N <sub>344</sub> O <sub>419</sub> S <sub>4</sub>	29697.02±1.13	29698.2
B	GAP31-GlcNAc <sub>2</sub> Man <sub>10</sub> Fuc <sub>2</sub> Xyl	C <sub>1361</sub> H <sub>2163</sub> N <sub>344</sub> O <sub>447</sub> S <sub>4</sub>	30624.20±1.15	30625.1
C	GAP31-GlcNAc <sub>2</sub> Man <sub>12</sub> Fuc <sub>2</sub> Xyl <sub>2</sub>	C <sub>1378</sub> H <sub>2191</sub> N <sub>344</sub> O <sub>461</sub> S <sub>4</sub>	31083.40±1.9	31080.5

#### 4.3.4. Enzymatic deglycosylation

In order to determine the composition and structures of the N-glycans of the gelonin and GAP31 proteins, the two proteins were treated with peptidyl-N-glycosidase F (PNGase F) before and after Endo H to release the N-linked carbohydrates. The N-glycans' masses obtained by ESI-MS were compared with molecular masses calculated from N-linked oligosaccharide structures commonly found in *Gelonium* seeds.

Enzymatic deglycosylation reduced the molecular mass of both proteins. SDS-PAGE shows that two bands were observed for both proteins (Fig. 55).

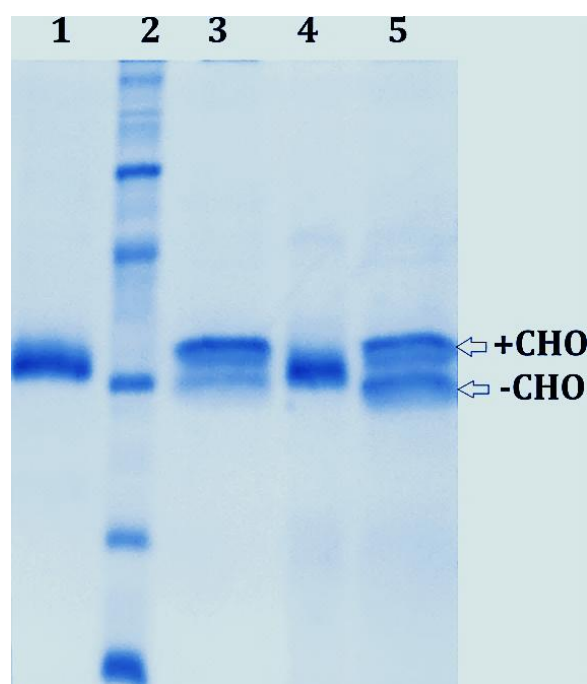


**Figure 55:** SDS-PAGE of purified and deglycosylated gelonin and GAP31. Lane 1, GAP31; lane 2, marker; lane 3, GAP31 after deglycosylation with PNGase F; lane 4, gelonin; and lane 5, gelonin after deglycosylation with PNGase F; +CHO, glycosylated; -CHO, deglycosylated protein.

#### 4.3.4.1. Enzymatic gelonin deglycosylation

- **N-glycan released by PNGase F**

Treatment of gelonin with the N-glycan-specific endoglycosidase peptide-N-glycosidase F (PNGase F) resulted in a discernible difference in apparent molecular weight on SDS-PAGE (Fig. 55), implying the presence of N-glycosylation. The released N-glycans were desalted and their mass determined by ESI-MS. The mass data revealed a range of singly charged species from approximately 769 to 1362 Da (Fig. 56A). This mass series corresponds with a high degree of accuracy to the mass of an N-linked, high-mannose composition series  $\text{GlcNAc}_2\text{Man}_{2-5}\text{Xyl}$ . Hence, the 768 ion was correlated with  $[\text{M} + \text{Na}]^+$  ions of  $\text{GlcNAc}_2\text{Man}_2$ . The next three most abundant ions (1083.5, 1203.9, and 1362.1) were correlated with  $[\text{M} + 2\text{Na}]^+$ ,  $[\text{M} + \text{H}]^+$ ,  $[\text{M}]$  ions of  $\text{GlcNAc}_2\text{Man}_3\text{Xyl}$  (calculated  $m/z$  1083),  $\text{GlcNAc}_2\text{Man}_4\text{Xyl}$  (calculated  $m/z$  1204), and  $\text{GlcNAc}_2\text{Man}_5\text{Xyl}$  (calculated  $m/z$  1362), respectively.

- **N-glycan released by Endo H and PNGase F**

The N-glycans were released from gelonin by treatment with Endo H. As shown in Figure 56B, the ESI-MS spectra showed three main ions (546.1, 856.7, and 1202.8), indicating the existence of oligomannose type N-glycans. Hence, the 546.1 ion was correlated with  $[\text{M} + \text{H}]^+$  ions of  $\text{GlcNAcMan}_2$  (calculated  $m/z$  545.4). The next two most abundant ions (856.7, and 1202.8) were correlated with  $[\text{M} + \text{H}_2\text{O}]^+$  ions of  $\text{GlcNAcMan}_3\text{Xyl}$  (calculated  $m/z$  855.7) and  $[\text{M} + \text{H}_2\text{O} + \text{Na}]^+$  ion of  $\text{GlcNAcMan}_5\text{Xyl}$  (calculated  $m/z$  1202), respectively.

Gelonin was found to be sensitive to Endo H deglycosylation, indicating the presence of complex and oligomannose N-glycans structures.

In the same experiments, the glycoprotein pellet - obtained after Endo H digestion - was treated with PNGase F and analyzed by ESI-MS. As shown in Figure 56C, the largest  $m/z$  measured was 205.1, which is in good agreement with the calculated  $m/z$  of the  $[\text{M} + \text{H}]^+$  ion of  $\text{GlcNAc}$  (calculated  $m/z$  204).

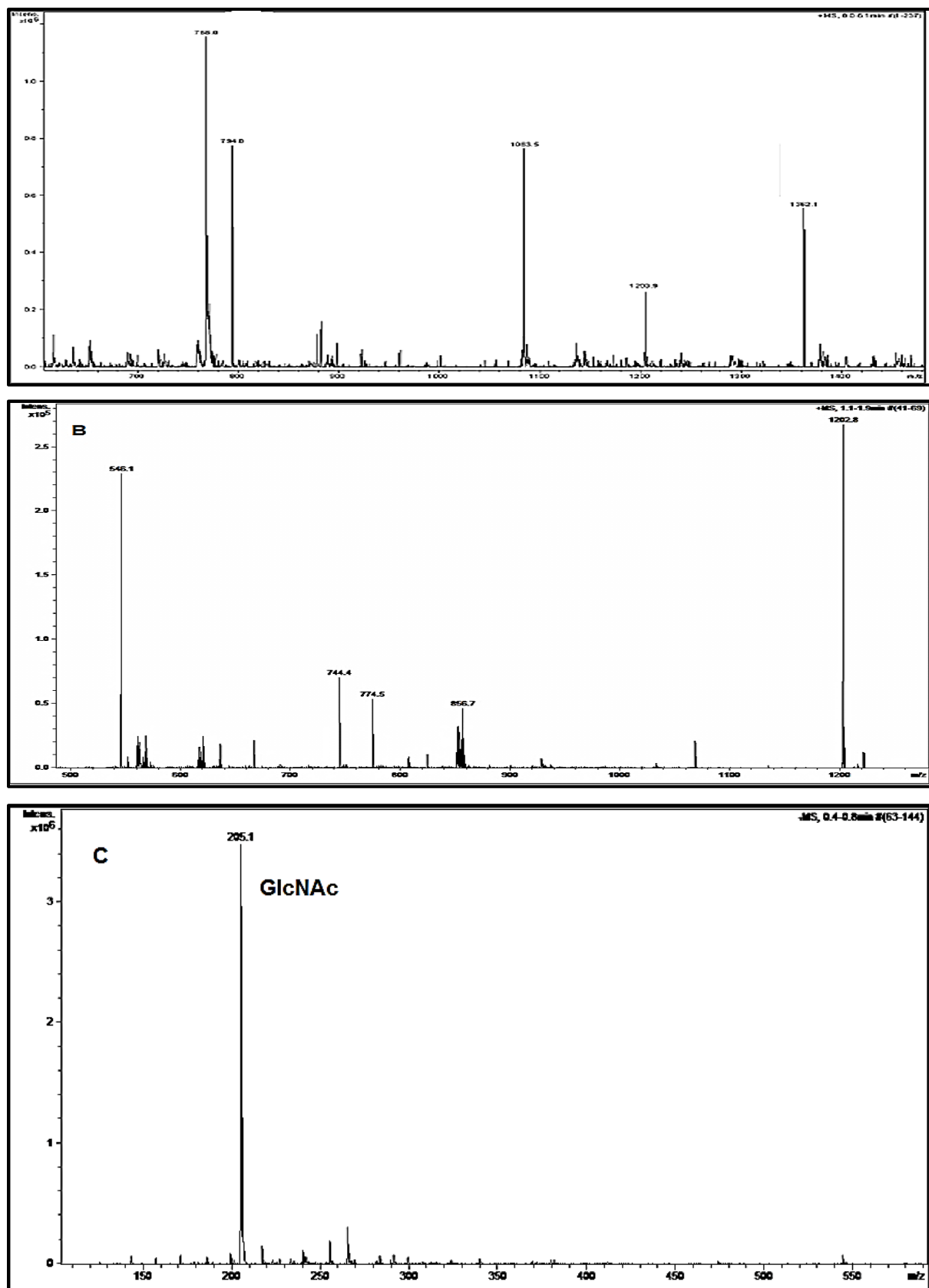


**Figure 56:** ESI-MS spectrum of released N-glycan from gelonin by (A) PNGase F treatment; (B) Endo H treatment; (C) PNGase F treatment after Endo H treatment.

#### 4.3.4.2. Enzymatic GAP31 deglycosylation

- **N-glycan released by PNGase F**

N-glycans were released from GAP31 by treatment with PNGase F alone according to the protocol described above and then analyzed directly by ESI-MS. As shown in Figure 57A, the N-glycan obtained after PNGase F digestion exhibited three main ions (1570.5, 2453.3, and 2933.2). Hence, the 2453.3 ion was correlated with  $[M + H]^+$  ions of  $\text{GlcNAc}_2\text{Man}_{10}\text{Fuc}_2\text{Xyl}$  (calculated  $m/z$  2452.18). The other ions (1570.5 and 2933.2) were correlated with  $[M + 2\text{Na}]^+$  and  $[M + \text{Na}]^+$  ions of  $\text{GlcNAc}_2\text{Man}_6\text{Fuc}$  (calculated  $m/z$  1570.3) and  $\text{GlcNAc}_2\text{Man}_{12}\text{Fuc}_2\text{Xyl}_2$  (calculated  $m/z$  2932.58), respectively.

- **N-glycan released by Endo H and PNGase F**

In another experiment, N-glycans were released from GAP31 by treatment with Endo H. As shown in Figure 57B, the ESI-MS spectra showed four main ions (1833.3, 2148, 2414 and 2576.3), indicating the existence of complex type *N*-glycan. Hence, the complex *N*-glycan with one pentose residue,  $\text{GlcNAcMan}_9\text{Xyl}$ , was detected at  $m/z$  1833.3 as a singly charged anion, containing one sodium adduct (calculated  $m/z$  1832.5). The complex oligosaccharides containing both fucose and pentose,  $\text{GlcNAcMan}_{11}\text{FucXyl}_2$  and  $\text{GlcNAcMan}_{12}\text{FucXyl}_2$ , were detected as singly charged ions at  $m/z$  2414 and 2576.3 (calculated  $m/z$  2413.9 and 2575.2), respectively. The other ion 2148 was correlated with  $[M]^+$  ion of  $\text{GlcNAcMan}_{11}\text{Fuc}$  (calculated  $m/z$  2148). The mass difference of 162 Da between singly charged ions at  $m/z$  of 2414 and 2576.3 indicate the presence of a mannose residue.

In the same experiments, the glycoprotein pellet - obtained after Endo H digestion - was treated with PNGase F and analyzed by ESI-MS. As shown in Figure 57C, the largest  $m/z$  measured was 368.9, which is in good agreement with the calculated  $m/z$  of the  $[M + \text{H}_2\text{O}]^+$  ion of  $\text{GlcNAcFuc}$  (calculated  $m/z$  368.3). The other peaks observed in the ESI-MS spectra may probably be attributed to noise derived from the fragmentation of N-glycan patterns.

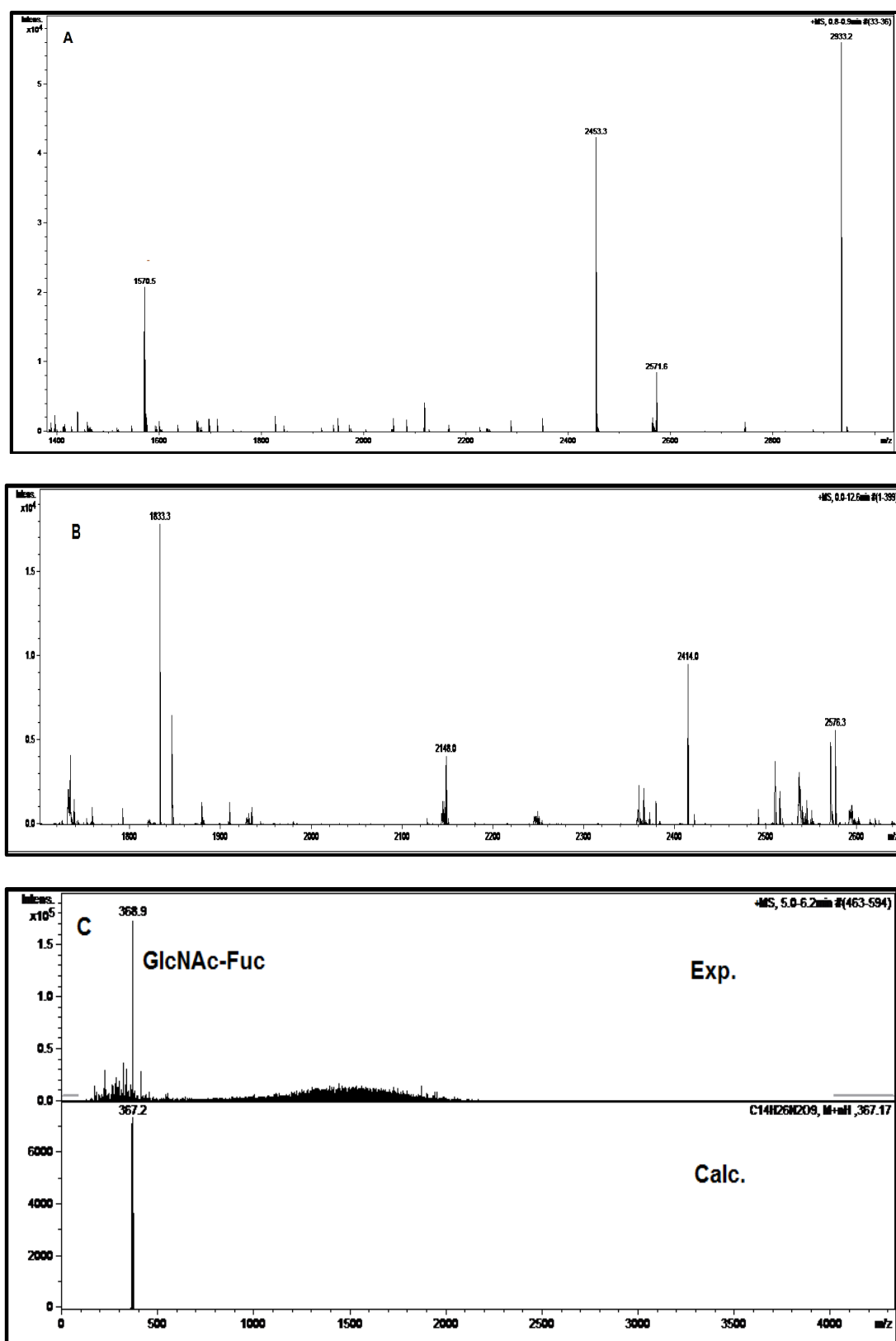


**Figure 57:** ESI-MS spectrum, in positive mode, of N-glycan from GAP31 obtained by (A) PNGase F treatment; (B) Endo H treatment; (C) PNGase F treatment after Endo H treatment.

### 4.3.5. Discussion

We have isolated and characterized two RIP proteins (gelonin and GAP31) that constitute about 40 % of the total soluble proteins from the seeds of *Gelonium multiflorum*. Gelonin and GAP31 were extracted and purified by means of a size-exclusion chromatographic procedure (Fig. 40) and ion exchange chromatography. However, the isolation of GAP31 demanded more effort due to its lower yield upon purification. Both gelonin and GAP31 exert N-glycosidase activity as shown in a cell-free *in-vitro* translation system of non-treated rabbit reticulocyte lysate (Fig. 42). The IC<sub>50</sub> of gelonin and GAP31 were found to be 4.6 (Hossann et al., 2006) and 2 ng/ml, respectively.

The ESI-MS analysis of gelonin and GAP31 exhibited at least three different species that are both modified by post-translational N-glycosylation patterns (Tables 14 and 18).

In the trypsin digest, a peptide corresponding to the **N104-R113** was clearly detected in the spectrum of the 30 kDa protein (Fig. 43). In the Arg-C digest, a peptide corresponding to the **N81-R113** was clearly observed only in the spectrum of the 30 kDa (Fig. 48). These results confirm the Rosenblum sequence to be the correct sequence for the 30 kDa protein. The eight amino acid insert was not detected in the tryptic and Arg-C digest of the 31 kDa protein (Fig. 50). These results prove that the 31 kDa protein corresponds to the Huang sequence (GAP31).

#### 4.3.5.1. Characterization of the glycosylation sites

There are two possible glycosylation sites in gelonin (N81 and N196). The peptides containing unglycosylated N81 were identified in both trypsin and Arg-C digests. A mass of 964.7 Da was obtained for the tryptic peptide, in agreement with the theoretical value of the **N81-K87** peptide (Fig. 43, Table 6). The molecular ion at  $m/z$  3779 corresponding to peptide sequence **N81-R113** was obtained for the Arg-C peptide (Fig. 48A, Table 9). This proves that the glycosylation modification is not located at N81 which is in line with previous studies (Barbieri et al., 1993; Daubenfeld et al., 2005).

The GAP31 sequence has also two potential sites for glycosylation N82 and N189. In trypsin digest the peptides containing unglycosylated N82 were identified. The MALDI spectra showed the peak  $[M + H]^+$  at  $m/z$  962.04 which is corresponding to peptide sequence **N82-K88**. This peak has a theoretical  $m/z$  value of 961.4. This proves that the glycosylation modification is not located at N82 which is in line with previous studies (Li et al., 2010).

#### 4.3.5.2. Structures of N-linked glycan

ESI-MS analysis of N-glycans released with PNGase F from gelonin revealed mixtures of oligosaccharides. In addition, a certain low amount of high-mannose N-glycans was detected. Most of the structures could be assigned by calculation to paucimannosidic-type (small complex-type) N-glycans, expected to contain Xyl residues. The highly abundant

polysaccharides released from gelonin are high-mannose and paucimannosidic-type N-glycan series containing pentose (GlcNAc<sub>2</sub>Man<sub>2-5</sub>Xyl<sub>0-1</sub>) which are known as typical vacuole-type N-glycans (Lerouge et al. 1998).

The N-glycan released with PNGase F from the 30 kDa glycoprotein after Endo H revealed an intense ion which can be observed at  $m/z$  205.1 and corresponds to the calculated  $m/z$  of the  $[M + H]^+$  ion of GlcNAc (calculated  $m/z$  204). Our result leads to the conclusion that, the N-glycan core of gelonin is N-acetyl-D-glucosamine. The total sugar composition of the glycan chains of gelonin amounts to a 4.5% neutral sugar content which agrees with previous work (Falasca et al., 1982; Daubenfeld et al., 2005). Figure 53A shows the ESI-MS spectrum of GAP31 N-glycans. Hence, two complex-type structures, GlcNAc<sub>2</sub>Man<sub>6</sub>Fuc and GlcNAc<sub>2</sub>Man<sub>12</sub>Fuc<sub>2</sub>Xyl<sub>2</sub>, were detected as singly charged sodium adducts at  $m/z$  1570.5 and 2933.2, respectively. In addition, the complex-type N-glycan containing both pentose and deoxyhexose residues (GlcNAc<sub>2</sub>Man<sub>10</sub>Fuc<sub>2</sub>Xyl) were detected as singly charged ions at  $m/z$  2453.3. Thus, the proposed glycosylation pattern for GAP31, GlcNAc<sub>2</sub>Man<sub>6-12</sub>Fuc<sub>1-2</sub>Xyl<sub>0-2</sub>, constitutes a mixture of paucimannosidic-type and complex-type. Our result leads to the conclusion that, the sugar residues of GAP31 amount to 9.4% of the total molecular mass. Further, the N-glycan released with PNGase F from the 31 kDa glycoprotein after Endo H revealed an intense ion which can be observed at  $m/z$  368.9 and corresponds to the calculated  $m/z$  of the  $[M + H_2O]^+$  ion of GlcNAcFuc. Our result leads to the conclusion that, the N-glycan core of GAP31 is  $\alpha$ (1-6) fucose residue linked to the reducing terminal N-acetyl-D-glucosamine.

#### 4.3.6. Conclusion

We have isolated and characterized two ribosome-inactivating proteins (RIPs) type I, gelonin and GAP31, from seeds of *Gelonium multiflorum*. Both proteins exhibit RNA-N-glycosidase activity. The amino acid sequences of gelonin and GAP31 were identified by MALDI and ESI mass spectrometry. Gelonin and GAP31 peptides - obtained by proteolytic digestion (trypsin and Arg-C) - are consistent with the amino acid sequence published by Rosenblum and Huang, respectively. Further structural characterization of gelonin and GAP31 (tryptic and Arg-C peptide mapping) showed that the two RIPs have 96% similarity in their sequence. Thus, these two proteins are most probably isoforms arisen from the same gene by alternative splicing. The ESI-MS analysis of gelonin and GAP31 exhibited at least three different post-translationally modified forms. A standard plant paucidomannosidic N-glycosylation pattern (GlcNAc<sub>2</sub>Man<sub>2-5</sub>Xyl<sub>0-1</sub> and GlcNAc<sub>2</sub>Man<sub>6-12</sub>Fuc<sub>1-2</sub>Xyl<sub>0-2</sub>) was identified using electrospray ionization MS for gelonin on N196 and GAP31 on N189, respectively. Based on these results, both proteins are located in the vacuoles of *Gelonium multiflorum* seeds.



## 5. References

- Aggarwal, P., S. Naik, K. P. Mishra, A. Aggarwal, and R. Misra. 2006. Correlation between methotrexate efficacy & toxicity with C677T polymorphism of the methylenetetrahydrofolate gene in rheumatoid arthritis patients on folate supplementation. *Indian J Med Res* **124**:521-526.
- Arazi, T., H. P. Lee, P. L. Huang, L. Zhang, S. Y. Moshe, A. Gal-On, and S. Lee-Huang. 2002. Production of antiviral and antitumor proteins MAP30 and GAP31 in cucurbits using the plant virus vector ZYMV-AGII. *Biochem Biophys Res Commun* **292**:441-448.
- Atkinson, S. F., T. Bettinger, L. W. Seymour, J. P. Behr, and C. M. Ward. 2001. Conjugation of folate via gelonin carbohydrate residues retains ribosomal-inactivating properties of the toxin and permits targeting to folate receptor positive cells. *J Biol Chem* **276**:27930-27935.
- Barbieri, L., M. G. Battelli, and F. Stirpe. 1993. Ribosome-inactivating proteins from plants. *Biochim Biophys Acta* **1154**:237-282.
- Barbieri, L., M. Ciani, T. Girbes, W. Y. Liu, E. J. Van Damme, W. J. Peumans, and F. Stirpe. 2004. Enzymatic activity of toxic and non-toxic type 2 ribosome-inactivating proteins. *Febs Lett* **563**:219-222.
- Barbieri, L., P. Valbonesi, E. Bonora, P. Gorini, A. Bolognesi, and F. Stirpe. 1997. Polynucleotide:adenosine glycosidase activity of ribosome-inactivating proteins: effect on DNA, RNA and poly(A). *Nucleic Acids Res* **25**:518-522.
- Barlow, D. J., and J. M. Thornton. 1988. Helix geometry in proteins. *J Mol Biol* **201**:601-619.
- Battelli, M. G., L. Barbieri, A. Bolognesi, L. Buonamici, P. Valbonesi, L. Polito, E. J. Van Damme, W. J. Peumans, and F. Stirpe. 1997. Ribosome-inactivating lectins with polynucleotide:adenosine glycosidase activity. *Febs Lett* **408**:355-359.
- Begam, M., S. Kumar, S. Roy, J. J. Campanella, and H. C. Kapoor. 2006. Molecular cloning and functional identification of a ribosome inactivating/antiviral protein from leaves of post-flowering stage of *Celosia cristata* and its expression in *E. coli*. *Phytochemistry* **67**:2441-2449.
- Bourinbaiar, A. S., and S. Lee-Huang. 1996. The activity of plant-derived antiretroviral proteins MAP30 and GAP31 against herpes simplex virus in vitro. *Biochem Biophys Res Commun* **219**:923-929.
- Bradford, M. M. 1976. A rapid and sensitive method for the quantitation of microgram quantities of protein utilizing the principle of protein-dye binding. *Anal Biochem* **72**:248-254.
- Brigotti, M., R. Alfieri, P. Sestili, M. Bonelli, P. G. Petronini, A. Guidarelli, L. Barbieri, F. Stirpe, and S. Sperti. 2002. Damage to nuclear DNA induced by Shiga toxin 1 and ricin in human endothelial cells. *Faseb J* **16**:365-372.

- Brigotti, M., D. Carnicelli, P. Alvergnà, A. Pallanca, R. Lorenzetti, M. Denaro, S. Sperti, and L. Montanaro. 1995.** 3'-immature tRNA(Trp) is required for ribosome inactivation by gelonin, a plant RNA N-glycosidase. *Biochem J* **310** ( Pt 1):249-253.
- Brust, S., G. Filipp, U. Hofmann, I. Kalies, K. Peper, K. Rajki, R. K. Sterz, and W. E. Trommer. 1987.** Antigen-gelonin conjugates. Preparation and application in experimental myasthenia gravis. *Biol Chem Hoppe Seyler* **368**:991-999.
- Bueno, R., K. Appasani, H. Mercer, S. Lester, and D. Sugarbaker. 2001.** The alpha folate receptor is highly activated in malignant pleural mesothelioma. *J Thorac Cardiovasc Surg* **121**:225-233.
- Cavallaro, U., A. Nykjaer, M. Nielsen, and M. R. Soria. 1995.** Alpha 2-macroglobulin receptor mediates binding and cytotoxicity of plant ribosome-inactivating proteins. *Eur J Biochem* **232**:165-171.
- Chabner, B. A., and T. J. Roberts. 2005.** Timeline: Chemotherapy and the war on cancer. *Nat Rev Cancer* **5**:65-72.
- Cheenpracha, S., O. Yodsauoe, C. Karalai, C. Ponglimanont, S. Subhadhirasakul, S. Tewtrakul, and A. Kanjana-opas. 2006.** Potential anti-allergic ent-kaurene diterpenes from the bark of *Suregada multiflora*. *Phytochemistry* **67**:2630-2634.
- Colaco, M., M. M. Bapat, S. Misquith, M. Jadot, C. S. Wattiaux-De, and R. Wattiaux. 2002.** Uptake and intracellular fate of gelonin, a ribosome-inactivating protein, in rat liver. *Biochem Biophys Res Commun* **296**:1180-1185.
- Collins, A. R., M. Dusinska, C. M. Gedik, and R. Stetina. 1996.** Oxidative damage to DNA: do we have a reliable biomarker?. *Environ Health Perspect* **104 Suppl 3**:465-469.
- Corona, G., F. Giannini, M. Fabris, G. Toffoli, and M. Boiocchi. 1998.** Role of folate receptor and reduced folate carrier in the transport of 5-methyltetrahydrofolic acid in human ovarian carcinoma cells. *Int J Cancer* **75**:125-133.
- Cronstein, B. N. 2005.** Low-dose methotrexate: a mainstay in the treatment of rheumatoid arthritis. *Pharmacol Rev* **57**:163-172.
- Da, C. M., and S. P. Rothenberg. 1996.** Purification and characterization of folate binding proteins from rat placenta. *Biochim Biophys Acta* **1292**:23-30.
- Das, B., and K. Chakravarty. 1993.** Three flavone glycosides from *Gelonium multiflorum*. *Phytochemistry* **33**:493-496.
- Delius, M., and G. Adams. 1999.** Shock wave permeabilization with ribosome inactivating proteins: a new approach to tumor therapy. *Cancer Res* **59**:5227-5232.
- Elnakat, H., and M. Ratnam. 2004.** Distribution, functionality and gene regulation of folate receptor isoforms: implications in targeted therapy. *Adv Drug Deliv Rev* **56**:1067-1084.
- Endo, Y., K. Mitsui, M. Motizuki, and K. Tsurugi. 1987.** The mechanism of action of ricin and related toxic lectins on eukaryotic ribosomes. The site and the characteristics of the modification in 28 S ribosomal RNA caused by the toxins. *J Biol Chem* **262**:5908-5912.

- Endo, Y., and K. Tsurugi. 1988.** The RNA N-glycosidase activity of ricin A-chain. The characteristics of the enzymatic activity of ricin A-chain with ribosomes and with rRNA. *J Biol Chem* **263**:8735-8739.
- Falasca, A., A. Gasperi-Campani, A. Abbondanza, L. Barbieri, and F. Stirpe. 1982.** Properties of the ribosome-inactivating proteins gelonin, Momordica charantia inhibitor, and dianthins. *Biochem J* **207**:505-509.
- Fitzpatrick, J. J., and M. C. Garnett. 1995.** Studies on the mechanism of action of an MTX-HSA-MoAb conjugate. *Anticancer Drug Des* **10**:11-24.
- Foa-Tomasi, L., G. Campadelli-Fiume, L. Barbieri, and F. Stirpe. 1982.** Effect of ribosome-inactivating proteins on virus-infected cells. Inhibition of virus multiplication and of protein synthesis. *Arch Virol* **71**:323-332.
- Frei, E. R. 1985.** Curative cancer chemotherapy. *Cancer Res* **45**:6523-6537.
- Garnett, M. C., M. J. Embleton, E. Jacobs, and R. W. Baldwin. 1985.** Studies on the mechanism of action of an antibody-targeted drug-carrier conjugate. *Anticancer Drug Des* **1**:3-12.
- Gruner, B. A., and S. D. Weitman. 1998.** The folate receptor as a potential therapeutic anticancer target. *Invest New Drugs* **16**:205-219.
- Gurdag, S., J. Khandare, S. Stapels, L. H. Matherly, and R. M. Kannan. 2006.** Activity of dendrimer-methotrexate conjugates on methotrexate-sensitive and -resistant cell lines. *Bioconjug Chem* **17**:275-283.
- Hartmann, L. C., G. L. Keeney, W. L. Lingle, T. J. Christianson, B. Varghese, D. Hillman, A. L. Oberg, and P. S. Low. 2007.** Folate receptor overexpression is associated with poor outcome in breast cancer. *Int J Cancer* **121**:938-942.
- Hossann, M., Z. Li, Y. Shi, U. Kreilinger, J. Buttner, P. D. Vogel, J. Yuan, J. G. Wise, and W. E. Trommer. 2006.** Novel immunotoxin: a fusion protein consisting of gelonin and an acetylcholine receptor fragment as a potential immunotherapeutic agent for the treatment of Myasthenia gravis. *Protein Expr Purif* **46**:73-84.
- Hosur, M. V., B. Nair, P. Satyamurthy, S. Misquith, A. Surolia, and K. K. Kannan. 1995.** X-ray structure of gelonin at 1.8 Å resolution. *J Mol Biol* **250**:368-380.
- Huang, P. L., Y. Sun, H. C. Chen, H. F. Kung, and S. Lee-Huang. 1999.** Proteolytic fragments of anti-HIV and anti-tumor proteins MAP30 and GAP31 are biologically active. *Biochem Biophys Res Commun* **262**:615-623.
- Kamen, B. A., and A. Capdevila. 1986.** Receptor-mediated folate accumulation is regulated by the cellular folate content. *Proc Natl Acad Sci U S A* **83**:5983-5987.
- Kamen, B. A., and A. K. Smith. 2004.** A review of folate receptor alpha cycling and 5-methyltetrahydrofolate accumulation with an emphasis on cell models in vitro. *Adv Drug Deliv Rev* **56**:1085-1097.
- Katiyar, S. P., D. Bakkiyaraj, and P. S. Karutha. 2011.** Role of aromatic stack pairing at the catalytic site of gelonin protein. *Biochem Biophys Res Commun* **410**:75-80.

- Kaufman, Y., S. Drori, P. D. Cole, B. A. Kamen, J. Sirota, I. Ifergan, M. W. Arush, R. Elhasid, D. Sahar, G. J. Kaspers, G. Jansen, L. H. Matherly, G. Rechavi, A. Toren, and Y. G. Assaraf. 2004.** Reduced folate carrier mutations are not the mechanism underlying methotrexate resistance in childhood acute lymphoblastic leukemia. *Cancer* **100**:773-782.
- Kim, Y., and J. D. Robertus. 1992.** Analysis of several key active site residues of ricin A chain by mutagenesis and X-ray crystallography. *Protein Eng* **5**:775-779.
- Kobayashi, K., C. Terada, and I. Tsukamoto. 2002.** Methotrexate-induced apoptosis in hepatocytes after partial hepatectomy. *Eur J Pharmacol* **438**:19-24.
- Kodama, T., A. G. Doukas, and M. R. Hamblin. 2003.** Delivery of ribosome-inactivating protein toxin into cancer cells with shock waves. *Cancer Lett* **189**:69-75.
- Kralovec, J., M. Singh, M. Mammen, A. H. Blair, and T. Ghose. 1989.** Synthesis of site-specific methotrexate-IgG conjugates. Comparison of stability and antitumor activity with active-ester-based conjugates. *Cancer Immunol Immunother* **29**:293-302.
- Kreitman, R. J. 2006.** Immunotoxins for targeted cancer therapy. *AAPS J* **8**:E532-E551.
- Kulkarni, P. N., A. H. Blair, and T. I. Ghose. 1981.** Covalent binding of methotrexate to immunoglobulins and the effect of antibody-linked drug on tumor growth in vivo. *Cancer Res* **41**:2700-2706.
- Leamon, C. P., and P. S. Low. 1991.** Delivery of macromolecules into living cells: a method that exploits folate receptor endocytosis. *Proc Natl Acad Sci U S A* **88**:5572-5576.
- Lee, C. L., F. R. Chang, P. W. Hsieh, M. Y. Chiang, C. C. Wu, Z. Y. Huang, Y. H. Lan, M. Chen, K. H. Lee, H. F. Yen, W. C. Hung, and Y. C. Wu. 2008.** Cytotoxic ent-abietane diterpenes from *Gelonium aequoreum*. *Phytochemistry* **69**:276-287.
- Lee-Huang, S., P. L. Huang, P. L. Huang, A. S. Bourinbaiar, H. C. Chen, and H. F. Kung. 1995.** Inhibition of the integrase of human immunodeficiency virus (HIV) type 1 by anti-HIV plant proteins MAP30 and GAP31. *Proc Natl Acad Sci U S A* **92**:8818-8822.
- Lee-Huang, S., P. L. Huang, Y. Sun, H. C. Chen, H. F. Kung, P. L. Huang, and W. J. Murphy. 2000.** Inhibition of MDA-MB-231 human breast tumor xenografts and HER2 expression by anti-tumor agents GAP31 and MAP30. *Anticancer Res* **20**:653-659.
- Lee-Huang, S., H. F. Kung, P. L. Huang, A. S. Bourinbaiar, J. L. Morell, J. H. Brown, P. L. Huang, W. P. Tsai, A. Y. Chen, H. I. Huang, and A. Et. 1994.** Human immunodeficiency virus type 1 (HIV-1) inhibition, DNA-binding, RNA-binding, and ribosome inactivation activities in the N-terminal segments of the plant anti-HIV protein GAP31. *Proc Natl Acad Sci U S A* **91**:12208-12212.
- Lee-Huang, S., H. F. Kung, P. L. Huang, P. L. Huang, B. Q. Li, P. Huang, H. I. Huang, and H. C. Chen. 1991.** A new class of anti-HIV agents: GAP31, DAPs 30 and 32. *Febs Lett* **291**:139-144.
- Lee-Huang, S., L. Zhang, P. L. Huang, Y. T. Chang, and P. L. Huang. 2003.** Anti-HIV activity of olive leaf extract (OLE) and modulation of host cell gene expression by HIV-1 infection and OLE treatment. *Biochem Biophys Res Commun* **307**:1029-1037.

- Lerouge, P., M. Cabanes-Macheteau, C. Rayon, A. C. Fischette-Laine, V. Gomord, and L. Faye. 1998.** N-glycoprotein biosynthesis in plants: recent developments and future trends. *Plant Mol Biol* **38**:31-48.
- Levitt, M., and C. Chothia. 1976.** Structural patterns in globular proteins. *Nature* **261**:552-558.
- Li, H. G., P. L. Huang, D. Zhang, Y. Sun, H. C. Chen, J. Zhang, P. L. Huang, X. P. Kong, and S. Lee-Huang. 2010.** A new activity of anti-HIV and anti-tumor protein GAP31: DNA adenosine glycosidase--structural and modeling insight into its functions. *Biochem Biophys Res Commun* **391**:340-345.
- Li, H. G., S. Z. Xu, S. Wu, L. Yan, J. H. Li, R. N. Wong, Q. L. Shi, and Y. C. Dong. 1999.** Role of Arg163 in the N-glycosidase activity of neo-trichosanthin. *Protein Eng* **12**:999-1004.
- Li, Z., Y. Qu, H. Li, and J. Yuan. 2007.** Truncations of gelonin lead to a reduction in its cytotoxicity. *Toxicology* **231**:129-136.
- Ma, L., and J. A. Kovacs. 2000.** Expression and characterization of recombinant human-derived *Pneumocystis carinii* dihydrofolate reductase. *Antimicrob Agents Chemother* **44**:3092-3096.
- Madan, S., and P. C. Ghosh. 1992.** Interaction of gelonin with macrophages: effect of lysosomotropic amines. *Exp Cell Res* **198**:52-58.
- Mir, L. M., H. Banoun, and C. Paoletti. 1988.** Introduction of definite amounts of nonpermeant molecules into living cells after electroporation: direct access to the cytosol. *Exp Cell Res* **175**:15-25.
- Mir, O., S. Ropert, and F. Goldwasser. 2008.** Neoadjuvant chemotherapy with high-dose methotrexate in osteosarcoma. *Lancet Oncol* **9**:1198.
- Mol, F., B. W. Mol, W. M. Ankum, F. van der Veen, and P. J. Hajenius. 2008.** Current evidence on surgery, systemic methotrexate and expectant management in the treatment of tubal ectopic pregnancy: a systematic review and meta-analysis. *Hum Reprod Update* **14**:309-319.
- Montanaro, L., S. Sperti, A. Mattioli, G. Testoni, and F. Stirpe. 1975.** Inhibition by ricin of protein synthesis in vitro. Inhibition of the binding of elongation factor 2 and of adenosine diphosphate-ribosylated elongation factor 2 to ribosomes. *Biochem J* **146**:127-131.
- Mosmann, T. 1983.** Rapid colorimetric assay for cellular growth and survival: application to proliferation and cytotoxicity assays. *J Immunol Methods* **65**:55-63.
- Narayanan, S., K. Surendranath, N. Bora, A. Surolia, and A. A. Karande. 2005.** Ribosome inactivating proteins and apoptosis. *Febs Lett* **579**:1324-1331.
- Nicolas, E., J. M. Beggs, B. M. Haltiwanger, and T. F. Taraschi. 1998.** A new class of DNA glycosylase/apurinic/aprimidinic lyases that act on specific adenines in single-stranded DNA. *J Biol Chem* **273**:17216-17220.

- Nicolas, E., J. M. Beggs, B. M. Haltiwanger, and T. F. Taraschi. 1997A.** Direct evidence for the deoxyribonuclease activity of the plant ribosome inactivating protein gelonin. *Febs Lett* **406**:162-164.
- Nicolas, E., J. M. Beggs, and T. F. Taraschi. 2000.** Gelonin is an unusual DNA glycosylase that removes adenine from single-stranded DNA, normal base pairs and mismatches. *J Biol Chem* **275**:31399-31406.
- Nicolas, E., I. D. Goodyer, and T. F. Taraschi. 1997B.** An additional mechanism of ribosome-inactivating protein cytotoxicity: degradation of extrachromosomal DNA. *Biochem J* **327 ( Pt 2)**:413-417.
- Nolan, P. A., D. A. Garrison, and M. Better. 1993.** Cloning and expression of a gene encoding gelonin, a ribosome-inactivating protein from *Gelonium multiflorum*. *Gene* **134**:223-227.
- Olsnes, S., and A. Pihl. 1973.** Isolation and properties of abrin: a toxic protein inhibiting protein synthesis. Evidence for different biological functions of its two constituent-peptide chains. *Eur J Biochem* **35**:179-185.
- Olsnes, S., and K. Sandvig. 1988.** How protein toxins enter and kill cells. *Cancer Treat Res* **37**:39-73.
- Palmer, D. C., J. S. Skotnicki, and E. C. Taylor. 1988.** Synthesis of analogues of folic acid, aminopterin and methotrexate as antitumour agents. *Prog Med Chem* **25**:85-231.
- Parker, N., M. J. Turk, E. Westrick, J. D. Lewis, P. S. Low, and C. P. Leamon. 2005.** Folate receptor expression in carcinomas and normal tissues determined by a quantitative radioligand binding assay. *Anal Biochem* **338**:284-293.
- Peumans, W. J., Q. Hao, and E. J. Van Damme. 2001.** Ribosome-inactivating proteins from plants: more than RNA N-glycosidases?. *Faseb J* **15**:1493-1506.
- Pignatello, R., G. Spampinato, V. Sorrenti, C. Di Giacomo, L. Vicari, J. J. McGuire, C. A. Russell, G. Puglisi, and I. Toth. 2000.** Lipophilic methotrexate conjugates with antitumor activity. *Eur J Pharm Sci* **10**:237-245.
- Richardson, J. S. 1981.** The anatomy and taxonomy of protein structure. *Adv Protein Chem* **34**:167-339.
- Riebeseel, K., E. Biedermann, R. Loser, N. Breiter, R. Hanselmann, R. Mulhaupt, C. Unger, and F. Kratz. 2002.** Polyethylene glycol conjugates of methotrexate varying in their molecular weight from MW 750 to MW 40000: synthesis, characterization, and structure-activity relationships in vitro and in vivo. *Bioconjug Chem* **13**:773-785.
- Roncuzzi, L., and A. Gasperi-Campani. 1996.** DNA-nuclease activity of the single-chain ribosome-inactivating proteins dianthin 30, saporin 6 and gelonin. *Febs Lett* **392**:16-20.
- Rosenblum, M. G., W. A. Kohr, K. L. Beattie, W. G. Beattie, W. Marks, P. D. Toman, and L. Cheung. 1995.** Amino acid sequence analysis, gene construction, cloning, and expression of gelonin, a toxin derived from *Gelonium multiflorum*. *J Interferon Cytokine Res* **15**:547-555.

- Rosenblum, M. G., J. W. Marks, and L. H. Cheung. 1999.** Comparative cytotoxicity and pharmacokinetics of antimelanoma immunotoxins containing either natural or recombinant gelonin. *Cancer Chemother Pharmacol* **44**:343-348.
- Rosenblum, M. G., J. L. Murray, L. Cheung, R. Rifkin, S. Salmon, and R. Bartholomew. 1991.** A specific and potent immunotoxin composed of antibody ZME-018 and the plant toxin gelonin. *Mol Biother* **3**:6-13.
- Rosenblum, M. G., J. E. Zuckerman, J. W. Marks, J. Rotbein, and W. R. Allen. 1992.** A gelonin-containing immunotoxin directed against human breast carcinoma. *Mol Biother* **4**:122-129.
- Rosowsky, A., and C. S. Yu. 1978.** Methotrexate analogues. 10. Direct coupling of methotrexate and diethyl L-glutamate in the presence of peptide bond-forming reagents. *J Med Chem* **21**:170-175.
- Ross, J. F., P. K. Chaudhuri, and M. Ratnam. 1994.** Differential regulation of folate receptor isoforms in normal and malignant tissues in vivo and in established cell lines. Physiologic and clinical implications. *Cancer* **73**:2432-2443.
- Rybak, S., J. Lin, D. Newton, H. Kung, A. Monks, H. Chen, P. Huang, and S. Leehuang. 1994.** In-vitro antitumor-activity of the plant ribosome-inactivating proteins map-30 and gap-31. *Int J Oncol* **5**:1171-1176.
- Sandvig, K., and B. van Deurs. 2000.** Entry of ricin and Shiga toxin into cells: molecular mechanisms and medical perspectives. *Embo J* **19**:5943-5950.
- Sandvig, K., and B. van Deurs. 2002.** Transport of protein toxins into cells: pathways used by ricin, cholera toxin and Shiga toxin. *Febs Lett* **529**:49-53.
- Schaefer, S., M. Baum, G. Eisenbrand, and C. Janzowski. 2006.** Modulation of oxidative cell damage by reconstituted mixtures of phenolic apple juice extracts in human colon cell lines. *Mol Nutr Food Res* **50**:413-417.
- Schreiber, C. A., L. Wan, Y. Sun, L. Lu, L. C. Krey, and S. Lee-Huang. 1999.** The antiviral agents, MAP30 and GAP31, are not toxic to human spermatozoa and may be useful in preventing the sexual transmission of human immunodeficiency virus type 1. *Fertil Steril* **72**:686-690.
- Scudiero, D. A., R. H. Shoemaker, K. D. Paull, A. Monks, S. Tierney, T. H. Nofziger, M. J. Currens, D. Seniff, and M. R. Boyd. 1988.** Evaluation of a soluble tetrazolium/formazan assay for cell growth and drug sensitivity in culture using human and other tumor cell lines. *Cancer Res* **48**:4827-4833.
- Selbo, P. K., A. Hogset, L. Prasmickaite, and K. Berg. 2002.** Photochemical internalisation: a novel drug delivery system. *Tumour Biol* **23**:103-112.
- Singh, N. P., M. T. McCoy, R. R. Tice, and E. L. Schneider. 1988.** A simple technique for quantitation of low levels of DNA damage in individual cells. *Exp Cell Res* **175**:184-191.
- Singh, R. C., A. Alam, and V. Singh. 2001.** Role of positive charge of lysine residue on ribosome-inactivating property of gelonin. *Indian J Biochem Biophys* **38**:309-312.

- Singh, V. 1991.** Hormonotoxins: synthesis, characterization and bioefficacy of some defined disulfide linked conjugates of ovine LH with a ribosome inactivating protein, gelonin. *Indian J Exp Biol* **29**:916-925.
- Singh, V., and R. R. Curtiss. 1994.** Hormonotoxins: the role of positive charge of lysine residue on the immunological, biological and cytotoxic properties of ovine lutropin-S-S-gelonin conjugates. *Mol Cell Biochem* **130**:91-101.
- Singh, V., and R. R. Curtiss. 1993.** Disulfide linked alpha oLH-gelonin conjugate failed to recombine with beta oLH subunit to generate bioeffective hormonotoxin. *Mol Cell Biochem* **120**:95-102.
- Singh, V., and M. R. Sairam. 1989.** Effects of thiolation on the immunoreactivity of the ribosome-inactivating protein gelonin. *Biochem J* **263**:417-423.
- Singh, V., M. R. Sairam, G. N. Bhargavi, and R. G. Akhras. 1989.** Hormonotoxins. Preparation and characterization of ovine luteinizing hormone-gelonin conjugate. *J Biol Chem* **264**:3089-3095.
- Steeves, R. M., M. E. Denton, F. C. Barnard, A. Henry, and J. M. Lambert. 1999.** Identification of three oligosaccharide binding sites in ricin. *Biochemistry-US* **38**:11677-11685.
- Stehle, G., H. Sinn, A. Wunder, H. H. Schrenk, S. Schutt, W. Maier-Borst, and D. L. Heene. 1997.** The loading rate determines tumor targeting properties of methotrexate-albumin conjugates in rats. *Anticancer Drugs* **8**:677-685.
- Stirpe, F., and L. Barbieri. 1986.** Ribosome-inactivating proteins up to date. *Febs Lett* **195**:1-8.
- Stirpe, F., L. Barbieri, M. G. Battelli, M. Soria, and D. A. Lappi. 1992.** Ribosome-inactivating proteins from plants: present status and future prospects. *Biotechnology (N Y)* **10**:405-412.
- Stirpe, F., S. Olsnes, and A. Pihl. 1980.** Gelonin, a new inhibitor of protein synthesis, nontoxic to intact cells. Isolation, characterization, and preparation of cytotoxic complexes with concanavalin A. *J Biol Chem* **255**:6947-6953.
- Sun, Y., P. L. Huang, J. J. Li, Y. Q. Huang, L. Zhang, P. L. Huang, and S. Lee-Huang. 2001.** Anti-HIV agent MAP30 modulates the expression profile of viral and cellular genes for proliferation and apoptosis in AIDS-related lymphoma cells infected with Kaposi's sarcoma-associated virus. *Biochem Biophys Res Commun* **287**:983-994.
- Surolia, N., and S. Misquith. 1996.** Cell surface receptor directed targeting of toxin to human malaria parasite, Plasmodium falciparum. *Febs Lett* **396**:57-61.
- Tewtrakul, S., S. Subhadhirasakul, S. Cheenpracha, O. Yodsaoue, C. Ponglimanont, and C. Karalai. 2011.** Anti-inflammatory principles of Suregada multiflora against nitric oxide and prostaglandin E2 releases. *J Ethnopharmacol* **133**:63-66.
- Tian, H., and B. N. Cronstein. 2007.** Understanding the mechanisms of action of methotrexate: implications for the treatment of rheumatoid arthritis. *Bull NYU Hosp Jt Dis* **65**:168-173.



- Toffoli, G., C. Cernigoi, A. Russo, A. Gallo, M. Bagnoli, and M. Boiocchi. 1997.** Overexpression of folate binding protein in ovarian cancers. *Int J Cancer* **74**:193-198.
- Urbatsch, I. L., R. K. Sterz, K. Peper, and W. E. Trommer. 1993.** Antigen-specific therapy of experimental myasthenia gravis with acetylcholine receptor-gelonin conjugates in vivo. *Eur J Immunol* **23**:776-779.
- Valentin-Severin, I., L. Le Hegarat, J. C. Lhuguenot, A. M. Le Bon, and M. C. Chagnon. 2003.** Use of HepG2 cell line for direct or indirect mutagens screening: comparative investigation between comet and micronucleus assays. *Mutat Res* **536**:79-90.
- Vibet, S., K. Maheo, J. Gore, P. Dubois, P. Bougnoux, and I. Chourpa. 2007.** Differential subcellular distribution of mitoxantrone in relation to chemosensitization in two human breast cancer cell lines. *Drug Metab Dispos* **35**:822-828.
- Walsh, T. A., A. E. Morgan, and T. D. Hey. 1991.** Characterization and molecular cloning of a proenzyme form of a ribosome-inactivating protein from maize. Novel mechanism of proenzyme activation by proteolytic removal of a 2.8-kilodalton internal peptide segment. *J Biol Chem* **266**:23422-23427.
- Weitman, S. D., K. M. Frazier, and B. A. Kamen. 1994.** The folate receptor in central nervous system malignancies of childhood. *J Neurooncol* **21**:107-112.
- Weitman, S. D., R. H. Lark, L. R. Coney, D. W. Fort, V. Frasca, V. J. Zurawski, and B. A. Kamen. 1992.** Distribution of the folate receptor GP38 in normal and malignant cell lines and tissues. *Cancer Res* **52**:3396-3401.
- Wu, M., W. Gunning, and M. Ratnam. 1999.** Expression of folate receptor type alpha in relation to cell type, malignancy, and differentiation in ovary, uterus, and cervix. *Cancer Epidemiol Biomarkers Prev* **8**:775-782.
- Zarling, J. M., P. A. Moran, O. Haffar, J. Sias, D. D. Richman, C. A. Spina, D. E. Myers, V. Kuebelbeck, J. A. Ledbetter, and F. M. Uckun. 1990.** Inhibition of HIV replication by pokeweed antiviral protein targeted to CD4+ cells by monoclonal antibodies. *Nature* **347**:92-95.
- Zuo, C., Y. T. Chen, and Z. M. Wang. 2009.** [Clinical efficacy of Corydalis composite combined with methotrexate in treating rheumatoid arthritis]. *Zhongguo Zhong Xi Yi Jie He Za Zhi* **29**:1023-1025.







## 7. Acknowledgements

First of all, I would like to take this opportunity to express my deepest sense of gratitude and admiration to my supervisor, Prof. Dr. Wolfgang E. Trommer for providing me with the opportunity to work in his research group and for providing patient guidance, numerous and excellent ideas, and continuous efforts to revise my thesis.

I would like to thank Dr. R. Philipp for solving all types of computer problems and for the unforgettable time.

I would like to give my best wishes to all colleagues in our group, i.e. Christian, Doreen, Elke, Jessica, Michaela, Mohammed Chakour, Sandra and Valentina for their assistance and for providing a pleasant team atmosphere.

I would like to thank Jennifer Meyer for MALDI analysis. Special thanks go to Fabian Menges who spared his precious time to perform ESI.

My special thanks go to Frau Carolin Fluck and their consistent support and particularly for their friendship.

I would like to thank Mohamed Lisfi and Abdel-Rahim Madhour for their assistance and particularly for their friendship.

Finally, I would like to dedicate this work to my family (my father, my mother, my wife and my children Fatma, Sohaila, and Salma).

## 8. Curriculum Vitae

### Personal data

Name Mohamed Mohamed Mohamed Abd El Fattah Badr  
Date of birth 16/02/1977  
Place of birth El Menofyia, Egypt.  
Nationality Egyptian  
Marital status Married  
Address Ashma, El Shouhada, El Menofyia, Egypt  
E-mail *Mohamed\_badr180@yahoo.com*

### Education

83-88 Ashma Primary School, El Menofyia, Egypt  
88-91 Al-azhar Middle School, El Shouhada, El Menofyia, Egypt  
91-95 Al-azhar high school, El Shouhada, El Menofyia, Egypt  
95-2000 Faculty of Pharmacy, Al-azhar University, Cairo, Egypt.  
(B. Sc. in pharmaceutical sciences)  
2003-2005 Diploma, postgraduate courses in biochemistry, Al-azhar University, Cairo, Egypt.  
3/2008-5/2009 Department of Chemistry/Biochemistry, Technical University of Kaiserslautern, Germany.  
Master Thesis: The influence of endoplasmic reticulum stress on hypoxia-inducible factor-1-dependent plasminogen activator inhibitor-1 expression  
Supervisor: Prof. Dr. T. Kietzmann  
6/2009- till now Department of Chemistry/Biochemistry, Technical University of Kaiserslautern, Germany.  
Thesis: The ribosome-inactivating protein gelonin and parts thereof to be employed for a potential treatment of cancer  
Supervisor: Prof. Dr. Wolfgang E. Trommer

## **Eidesstattliche Erklärung**

Hiermit erkläre ich, dass ich die vorliegende Arbeit selbstständig angefertigt und keine anderen als die von mir angegebenen Quellen und Hilfsmittel benutzt habe.

Ich versichere außerdem, dass diese Dissertation weder in gleicher noch in anderer Form bereits in einem anderen Prüfverfahren vorgelegen hat.

Kaiserslautern, den 26/04/2012

( \_\_\_\_\_ )

Mohamed Badr